

NEA NUCLEAR SCIENCE COMMITTEE

# **CALCULATIONS OF DIFFERENT TRANSMUTATION CONCEPTS**

*An International Benchmark Exercise*

*February 2000*

NUCLEAR ENERGY AGENCY  
ORGANISATION FOR ECONOMIC AND CO-OPERATION DEVELOPMENT

## **ORGANISATION FOR ECONOMIC CO-OPERATION AND DEVELOPMENT**

Pursuant to Article 1 of the Convention signed in Paris on 14th December 1960, and which came into force on 30th September 1961, the Organisation for Economic Co-operation and Development (OECD) shall promote policies designed:

- to achieve the highest sustainable economic growth and employment and a rising standard of living in Member countries, while maintaining financial stability, and thus to contribute to the development of the world economy;
- to contribute to sound economic expansion in Member as well as non-member countries in the process of economic development; and
- to contribute to the expansion of world trade on a multilateral, non-discriminatory basis in accordance with international obligations.

The original Member countries of the OECD are Austria, Belgium, Canada, Denmark, France, Germany, Greece, Iceland, Ireland, Italy, Luxembourg, the Netherlands, Norway, Portugal, Spain, Sweden, Switzerland, Turkey, the United Kingdom and the United States. The following countries became Members subsequently through accession at the dates indicated hereafter: Japan (28th April 1964), Finland (28th January 1969), Australia (7th June 1971), New Zealand (29th May 1973), Mexico (18th May 1994), the Czech Republic (21st December 1995), Hungary (7th May 1996), Poland (22nd November 1996) and the Republic of Korea (12th December 1996). The Commission of the European Communities takes part in the work of the OECD (Article 13 of the OECD Convention).

## **NUCLEAR ENERGY AGENCY**

The OECD Nuclear Energy Agency (NEA) was established on 1st February 1958 under the name of the OEEC European Nuclear Energy Agency. It received its present designation on 20th April 1972, when Japan became its first non-European full Member. NEA membership today consists of 27 OECD Member countries: Australia, Austria, Belgium, Canada, Czech Republic, Denmark, Finland, France, Germany, Greece, Hungary, Iceland, Ireland, Italy, Japan, Luxembourg, Mexico, the Netherlands, Norway, Portugal, Republic of Korea, Spain, Sweden, Switzerland, Turkey, the United Kingdom and the United States. The Commission of the European Communities also takes part in the work of the Agency.

The mission of the NEA is:

- to assist its Member countries in maintaining and further developing, through international co-operation, the scientific, technological and legal bases required for a safe, environmentally friendly and economical use of nuclear energy for peaceful purposes, as well as
- to provide authoritative assessments and to forge common understandings on key issues, as input to government decisions on nuclear energy policy and to broader OECD policy analyses in areas such as energy and sustainable development.

Specific areas of competence of the NEA include safety and regulation of nuclear activities, radioactive waste management, radiological protection, nuclear science, economic and technical analyses of the nuclear fuel cycle, nuclear law and liability, and public information. The NEA Data Bank provides nuclear data and computer program services for participating countries.

In these and related tasks, the NEA works in close collaboration with the International Atomic Energy Agency in Vienna, with which it has a Co-operation Agreement, as well as with other international organisations in the nuclear field.

### **© OECD 2000**

Permission to reproduce a portion of this work for non-commercial purposes or classroom use should be obtained through the Centre français d'exploitation du droit de copie (CCF), 20, rue des Grands-Augustins, 75006 Paris, France, Tel. (33-1) 44 07 47 70, Fax (33-1) 46 34 67 19, for every country except the United States. In the United States permission should be obtained through the Copyright Clearance Center, Customer Service, (508)750-8400, 222 Rosewood Drive, Danvers, MA 01923, USA, or CCC Online: <http://www.copyright.com/>. All other applications for permission to reproduce or translate all or part of this book should be made to OECD Publications, 2, rue André-Pascal, 75775 Paris Cedex 16, France.

## FOREWORD

In April 1996, the NEA Nuclear Science Committee (NSC) Expert Group on Physics Aspects of Different Transmutation Concepts launched a benchmark exercise to compare different transmutation concepts based on pressurised water reactors (PWRs), fast reactors, and an accelerator-driven system (ADS). The aim was to investigate the physics of complex fuel cycles involving reprocessing of spent PWR reactor fuel and its subsequent reuse in different reactor types. The objective was also to compare the calculated activities for individual isotopes as a function of time for different plutonium and minor actinide (MA) transmutation scenarios in different reactor systems.

This report gives the analysis of results of the 15 solutions provided by the participants: six for the PWRs, six for the fast reactor and three for the accelerator case. Various computer codes and nuclear data libraries were applied.

For the PWR benchmark, the results show consistency well within the limits on multiple plutonium recycling established by the NEA Working Party on Plutonium Fuels and Innovative Fuel Cycles (WPPR). For the fast reactor benchmark, the computer code systems used by the participants show a good general agreement in the prediction of the nuclear characteristics of the minor actinide loaded fast reactor core. For the ADS benchmark, large discrepancies are observed in main neutronic characteristics such as initial  $k_{\text{eff}}$  and burn-up behaviour.

The analysis of the current ADS benchmark results indicates a need for refining the benchmark specification and continuing the exercise with a wider participation to resolve the discrepancies observed before proceeding to more complex problems.

### *Acknowledgements*

The Secretariat wishes to express its special thanks to all participants who devoted their time and effort to this endeavour.



## TABLE OF CONTENTS

<b>Executive Summary</b> .....	11
<b>Chapter 1. INTRODUCTION</b> .....	13
<b>Chapter 2. SUMMARY OF THE PRESSURISED WATER REACTOR BENCHMARK</b> .....	15
2.1 Problem specification.....	15
2.2 Requested results.....	15
2.3 Participants .....	16
2.4 Results and discussions .....	16
2.5 Conclusions .....	17
<b>Chapter 3. SUMMARY OF THE FAST REACTOR BENCHMARK</b> .....	19
3.1 Problem specification.....	19
3.2 Requested results.....	19
3.3 Participants .....	19
3.4 Results and discussions .....	19
3.5 Conclusions .....	21
<b>Chapter 4. SUMMARY OF THE ACCELERATOR-DRIVEN SYSTEM BENCHMARK</b> .....	23
4.1 Problem specification.....	23
4.2 Required cross-section library and code description.....	23
4.3 Spallation neutron source spectrum .....	24
4.4 Requested results.....	24
4.5 Participants .....	25
4.6 Results and discussions .....	25
4.7 Conclusions .....	26

<b>Chapter 5. CONCLUSIONS AND RECOMMENDATIONS</b> .....	29
<b>REFERENCES</b> .....	31
<b>TABLES</b> .....	33
<b>FIGURES</b> .....	61
<b>Appendix A. BENCHMARK SPECIFICATIONS</b> .....	83
A.1 NEA/NSC benchmark on physics aspects of different transmutation concepts – specifications for PWRs .....	85
A.2 Proposal for a benchmark calculation of MA transmutation in fast reactors (1 000 MWe).....	99
A.3 JAERI proposal of benchmark problem on method and data to calculate the nuclear characteristics in accelerator-based transmutation system with fast neutron flux.....	111
<b>Appendix B. CALCULATION DETAILS SUPPLIED BY PARTICIPANTS</b> .....	119
B.1 Pressurised water reactor benchmark .....	121
B.2 Fast reactor benchmark.....	135
B.3 Accelerator-driven system benchmark .....	151
<b>LIST OF CONTRIBUTORS</b> .....	157

*List of tables*

Table 2.1.	Benchmark cell specifications for PWR .....	35
Table 2.2.	Number densities of PWR UO <sub>2</sub> cell at BOL .....	35
Table 2.3.	Actinide atom per cent fraction .....	36
Table 2.4.	Number densities of the normal PWR lattice .....	36
Table 2.5.	Number densities of the wider PWR lattice .....	37
Table 2.6.	Proposed macro steps for depletion calculations.....	37
Table 2.7.	Fission products weight (kg) of <sup>99</sup> Tc, <sup>129</sup> I and <sup>135</sup> Cs generated at the burn-up 33 GWd/tHM and normalised to 1 t fuel.....	38
Table 2.8.	Index of MA transmutation which means negative or positive sign corresponding to decrease or increase from initial loading MA .....	38
Table 2.9.	Comparison of Doppler and void reactivities, Part I – MOX12.....	39
	Comparison of Doppler and void reactivities, Part II – MOX22 .....	41
	Comparison of Doppler and void reactivities, Part III – MOX22 (wide).....	43
Table 3.1.	Plutonium isotopic composition (PWR UO <sub>2</sub> fuel 50 GWd/tHM, seven years cooling) .....	44
Table 3.2.	Homogenised atomic density .....	45
Table 3.3.1.	k <sub>eff</sub> at 0, 365, 1 460, 1 825 EFPD (reference core) .....	46
Table 3.3.2.	k <sub>eff</sub> at 0, 365, 1 460, 1 825 EFPD (2.5% MA core) .....	46
Table 3.3.3.	k <sub>eff</sub> at 0, 365, 1 460, 1 825 EFPD (5% MA core) .....	46
Table 3.4.1.	Spectral indices at 0 EFPD (reference core).....	46
Table 3.4.2.	Spectral indices at 0 EFPD (2.5% MA core).....	46
Table 3.4.3.	Spectral indices at 0 EFPD (5% MA core).....	47
Table 3.5.1.	Reactivity losses over five cycles (reference core) .....	47
Table 3.5.2.	Reactivity losses over five cycles (2.5% MA core) .....	47
Table 3.5.3.	Reactivity losses over five cycles (5% MA core) .....	47
Table 3.6.1.	Isotopic composition variation (EOC-BOC) (reference core, inner core).....	48
Table 3.6.2.	Isotopic composition variation (EOC-BOC) (2.5% MA core, inner core).....	48
Table 3.6.3.	Isotopic composition variation (EOC-BOC) (5% MA core, inner core).....	49
Table 3.7.1.	Sodium reactivity worth at the beginning of the fourth cycle (BOC) (reference core, sodium void whole core) .....	49
Table 3.7.2.	Sodium reactivity worth at the beginning of the fourth cycle (BOC) (2.5% MA core, sodium void whole core) .....	49
Table 3.7.3.	Sodium reactivity worth at the beginning of the fourth cycle (BOC) (5% MA core, sodium void whole core) .....	50
Table 3.8.1.	Doppler reactivity worth at the fourth cycle (reference core) .....	50

Table 3.8.2.	Doppler reactivity worth at the fourth cycle (2.5% MA core) .....	50
Table 3.8.3.	Doppler reactivity worth at the fourth cycle (5% MA core) .....	50
Table 3.9.1.	Decay heat at different cooling times (reference core, inner core) .....	50
Table 3.9.2.	Decay heat at different cooling times (2.5% MA core, inner core).....	50
Table 3.9.3.	Decay heat at different cooling times (5% MA core, inner core).....	51
Table 3.10.1.	Neutron source at different cooling times (reference core, inner core).....	51
Table 3.10.2.	Neutron source at different cooling times (2.5% MA core, inner core).....	51
Table 3.10.3.	Neutron source at different cooling times (5% MA core, inner core).....	51
Table 3.11.	Transmutation rate of MA.....	51
Table 4.1.	Specification of target/core transmutation system .....	52
Table 4.2.	Actinide atom per cent fraction .....	52
Table 4.3.	Homogenised atomic number densities ( $\times 10^{24}/\text{cm}^3$ ).....	53
Table 4.4.	Normalised spallation neutron spectrum from the target .....	54
Table 4.5.	Number of spallation neutrons per incident proton (n/p) .....	54
Table 4.6.	Maximum and average heat power densities in target region .....	54
Table 4.7.	Nuclear characteristics results .....	55
Table 4.8.	Fission and capture rate (initial core) .....	55
Table 4.9.	Fission and capture rate (200 GWd/tHM burn-up) .....	56
Table 4.10.	PSI results (MOX11).....	56
Table 4.11.	PSI results (MOX12).....	57
Table 4.12.	JAERI results (MOX11).....	58
Table 4.13.	JAERI results (MOX12).....	59
Table 4.14.	IPPE results (MOX11) .....	60
Table 4.15.	IPPE results (MOX12) .....	60

*List of figures*

Figure 1.1.	Schematic fuel cycle scenario for the benchmark proposal .....	63
Figure 2.1.	Benchmark cell geometry .....	64
Figure 2.2.	$k_{\infty}$ as a function of burn-up for MOX12 (33 GWd/tHM) and MA 0.0% .....	64
Figure 2.3.	$k_{\infty}$ as a function of burn-up for MOX12 (33 GWd/tHM) and MA 1.0% .....	65
Figure 2.4.	$k_{\infty}$ as a function of burn-up for MOX12 (33 GWd/tHM) and MA 2.5% .....	65
Figure 2.5.	$k_{\infty}$ as a function of burn-up for MOX22 (50 GWd/tHM) and MA 0.0% .....	66
Figure 2.6.	$k_{\infty}$ as a function of burn-up for MOX22 (50 GWd/tHM) and MA 1.0% .....	66
Figure 2.7.	$k_{\infty}$ as a function of burn-up for MOX22 (50 GWd/tHM) and MA 2.5% .....	67



Figure 2.8. $k_{\infty}$ as a function of burn-up for MOX22 (50 GWd/tHM) wide lattice and MA 0.0% .....	67
Figure 2.9. $k_{\infty}$ as a function of burn-up for MOX22 (50 GWd/tHM) wide lattice and MA 1.0% .....	68
Figure 2.10. $k_{\infty}$ as a function of burn-up for MOX22 (50 GWd/tHM) wide lattice and MA 2.5% .....	68
Figure 2.11. Atomic number density of $^{237}\text{Np}$ as a function of burn-up for MOX22 (50 GWd/tHM) and MA 2.5% .....	69
Figure 2.12. Atomic number density of $^{241}\text{Pu}$ as a function of burn-up for MOX22 (50 GWd/tHM) and MA 2.5% .....	69
Figure 2.13. Atomic number density of $^{242}\text{Pu}$ as a function of burn-up for MOX22 (50 GWd/tHM) and MA 2.5% .....	70
Figure 2.14. Atomic number density of $^{242\text{m}}\text{Am}$ as a function of burn-up for MOX22 (50 GWd/tHM) and MA 2.5% .....	70
Figure 2.15. Radioactivity of $^{239}\text{Pu}$ (Bq) as a function of decay time (years) for MOX22 (50 GWd/tHM) and MA 2.5% .....	71
Figure 2.16. Radioactivity of $^{241}\text{Pu}$ (Bq) as a function of decay time (years) for MOX22 (50 GWd/tHM) and MA 2.5% .....	71
Figure 2.17. Radioactivity of $^{242\text{m}}\text{Am}$ (Bq) as a function of decay time (years) for MOX22 (50 GWd/tHM) and MA 2.5% .....	72
Figure 2.18. Radioactivity of $^{243}\text{Cm}$ (Bq) as a function of decay time (years) for MOX22 (50 GWd/tHM) and MA 2.5% .....	72
Figure 3.1. Reference core (1 000 MWe class FBR) .....	73
Figure 3.2. Dependence of $k_{\text{eff}}$ on burn-up (reference core).....	74
Figure 3.3. Dependence of $k_{\text{eff}}$ on burn-up (2.5% MA core).....	74
Figure 3.4. Dependence of $k_{\text{eff}}$ on burn-up (5% MA core).....	75
Figure 3.5. Number density of $^{237}\text{Np}$ at various cooling times (2.5% MA core) .....	75
Figure 4.1. Calculational model .....	76
Figure 4.2. Target and fuel configurations .....	77
Figure 4.3. Axial distribution of neutrons (> 15 MeV) leaking from target at $r = 150$ mm .....	78
Figure 4.4. Average neutron spectrum in-core (MOX11).....	78
Figure 4.5. Time evolution of $k_{\text{eff}}$ (MOX11).....	79
Figure 4.6. Time evolution of $k_{\text{eff}}$ (MOX12).....	79
Figure 4.7. Time evolution of $^{237}\text{Np}$ number density (MOX11) .....	80
Figure 4.8. Time evolution of $^{237}\text{Np}$ number density (MOX12) .....	80
Figure 4.9. Time evolution of $^{241}\text{Am}$ number density (MOX11) .....	81
Figure 4.10. Time evolution of $^{241}\text{Am}$ number density (MOX12) .....	81



## EXECUTIVE SUMMARY

During the past decade, the transmutation of plutonium and minor actinides (MAs) in existing reactors and/or innovative systems has gained interest and become one of the attractive options to reduce the inventories of actinides and long-lived fission products in nuclear waste.

However, the state of the art in minor actinide transmutation calculations is not as well established as that of the conventional uranium and plutonium fuelled reactor systems, because nuclear data for minor actinides are less accurate and burn-up decay chains are not completely modelled in current computations.

In this context, a benchmark has been launched in order to evaluate the actual status of MA transmutation calculations for different reactor systems. The focus of the benchmark is on the physics of minor actinide transmutation in MOX fuel in pressurised water reactors (PWR), fast reactors (FR), and fast flux accelerator-driven systems (ADS). The emphasis is on long-term activities of the final wastes and to optimise the transmutation scheme involving complex but realistic fuel cycle scenarios.

Concerning the PWR benchmark geometry, a standard PWR cell (volume ratio of moderator to fuel  $V_m/V_f = 1.929$ ) and a wide lattice cell ( $V_m/V_f = 3.0$ ) for the highly moderated PWR were considered and two target burn-ups, 33 GWd/tHM and 50 GWd/tHM, were investigated. Six institutions have contributed results: FZK (Germany), IKE (Germany), JAERI (Japan), Tohoku University (Japan) ITEP (Russian Federation) and IPPE (Russian Federation). Overall, the results submitted show consistency, and are well within the limits on multiple plutonium recycling established by the NEA Working Party on Plutonium Fuels and Innovative Fuel Cycles (WPPR).

The fast reactor (FR) benchmark was for a 1 000 MWe fast breeder reactor with a breeding ratio near 1.25. The core consists of two fuel zones with different enrichments. The fuel comprises mixed oxide pins of depleted uranium and once-through PWR plutonium. Three kinds of fuels, containing different quantities of minor actinides (0%, 2.5% and 5%), were selected. Contributions have been provided by JAERI (Japan), CEA (France), JNC (Japan), Mitsubishi (Japan), Toshiba (Japan) and IPPE (Russian Federation). Excellent agreement is observed with regard to the main neutronic characteristics, but discrepancies in burn-up composition variations for some isotopes are relatively large. In general, it is found that the calculation code systems used have a very good general agreement in the predictions of the nuclear characteristics of the minor actinide loaded FR core.

For the accelerator-driven system (ADS) benchmark, a sodium cooled sub-critical system ( $k_{eff} = 0.9$ ) driven by a proton beam of 1 GeV and 10 mA was considered. The sub-critical system consists of a beam duct with void, a two-region tungsten target, a minor actinide dominant nitride fuelled core and a surrounding reflector region. This system was analysed by the following three contributors: JAERI (Japan), PSI (Switzerland) and IPPE (Russian Federation). Satisfactory agreements are observed in the number of spallation neutrons per incident proton and the axial distribution of leakage neutrons from the spallation target ( $> 15$  MeV), but large discrepancies are found in the maximum and average heat power densities in the target. Significant discrepancies are also found in the  $k_{eff}$  and burn-up characteristics. This is probably due to differences in capture and

fission cross-sections used for minor actinides in different nuclear data libraries and also due to different treatment of fission products in burn-up calculations. These results require a thorough investigation into differences in nuclear data libraries and into different calculation procedures and approximations. A wider participation is needed in order to draw further conclusions from these ADS results.

## *Chapter 1*

### INTRODUCTION

Various systems for plutonium and minor actinide (MA) transmutation have been considered to optimise the transmutation scheme. The state-of-the-art MA transmutation calculations are not as well established as those of the conventional uranium and plutonium burn-up reactor systems, because nuclear data for MAs are less reliable and the burn-up chains for decay and generation are not completely modelled in the computation.

A benchmark of the OECD/NEA Task Force on Physics Aspects of Different Transmutation Concepts was launched in April 1996 [1]. It was done so in order to investigate the physics of complex fuel cycles involving reprocessing of spent PWR reactor fuel and its subsequent reuse in different reactor types, and to compare the calculated activities for individual isotopes as a function of time for different stages of plutonium and MA transmutation scenarios in different reactor systems.

The focus of the benchmark is on the physics of recovered MA transmutations in MOX fuel in pressurised water reactors (PWR), fast reactors (FR), and fast flux accelerator-driven systems (ADS) with emphasis on the long-term activities of the final wastes.

The benchmark consists of three stages (Figure 1.1). The first stage – the input stage – considers the UO<sub>2</sub> fuelled PWR reactor. A representative pin cell is used to perform the burn-up calculations to a target burn-up of 50 GWd/tHM. The PWR benchmark also considers the 33 GWd/tHM burn-up to provide insight into the effects of burn-up extension on the long-term radiological characteristics of PWR wastes. The spent PWR fuel is then reprocessed after seven years of cooling, and the plutonium and MAs are recovered. Plutonium and MAs are then used to specify the MOX fuel composition for the second stage of the benchmark – the recycling stage. A three-year MOX fuel fabrication time is assumed, allowing for build-up of <sup>241</sup>Am in the MOX fuel.

In the recycling stage, two different possibilities are considered: the MOX fuel defined in the input stage is fed either into a PWR pin cell or into a full core model of a FR. Burn-up calculations are then performed to obtain exit fuel compositions of MOX fuel from a PWR and a FR. The spent MOX fuel from the second stage of the benchmark is subject to reprocessing and then used for defining fuel compositions for the third stage of the benchmark – the partitioning and transmutation stage.

In the third stage of the benchmark, three possibilities are considered: another MOX fuelled PWR, another FR and an ADS. At this stage the MAs from the first input stage are admixed to the second recycling stage reprocessed fuel or several admix combinations of the MAs from stages one and two are considered.

The fuel specifications of the four accelerator cases considered are based on the MA and plutonium vectors following from the PWR benchmark but are MA dominated (unlike the PWR and FR benchmarks). This reflects the design constraints of JAERI's accelerator-driven system, which is

dedicated to MA transmutation and is not intended to generate electricity. Its core remains sub-critical when using MA dominated fuel and becomes super-critical for low MA content fuel typical of PWRs and FRs.

At the end of the benchmark, a total of 15 solutions (six for the PWR, six for the FR and three for the accelerator case) was received. The summary of the benchmark was presented at the Long Island conference in the late summer of 1998 [2]. For the PWR benchmark, the results show consistency with limits of multiple plutonium recycling established by the NEA Working Party on Plutonium Fuels and Innovative Fuel Cycles. For the FR benchmark, calculational code systems of participants have a good general agreement in the predictions of the nuclear characteristics of the MA loaded FR core. For the ADS benchmark, very good agreements are observed for spallation neutron number/proton, axial neutron distribution from the target and so on. Large discrepancies are, however, observed in  $k_{eff}$  and burn-up characteristics.

## *Chapter 2*

### **SUMMARY OF THE PRESSURISED WATER REACTOR BENCHMARK**

#### **2.1 Problem specification**

The full benchmark specification for PWRs can be found in Appendix A.1. The benchmark cell specifications for PWR are summarised in Tables 2.1 and 2.2. The geometry of the benchmark cell is specified in Figure 2.1. The pitch and the equivalent outer cell radius are given for two cells: the smaller one (normal lattice) for the standard PWR and the larger one (wide lattice) for the highly moderated PWR. The volume ratios of moderator relative to fuel,  $V_m/V_f$ , are 1.929 and 3.0 for the normal and wide lattices, respectively. For the sake of simplicity, the influences of water boration and of the fuel assembly structures are neglected in this benchmark.

The very comprehensive PWR proposal covers many possibilities for plutonium utilisation in the PWRs. Two target burn-ups are considered: 33 GWd/tHM and 50 GWd/tHM for both the initial  $UO_2$  and MOX fuels. As the input specifications to PWR or accelerator benchmark calculations, four desirable plutonium and MA compositions were originally considered. These are denoted as MOX11, MOX21, MOX12 and MOX22 as shown in Table 2.3.

- MOX11 refers to plutonium and MA compositions resulting from reprocessing of 3.25%  $UO_2$  fuel from PWR burned to 33 GWd/tHM.
- MOX21 is plutonium and MA compositions from 50 GWd/tHM burned results of 4.65%  $UO_2$  fuel PWR.
- MOX12 is the compositions from 33 GWd/tHM burn-up using the MOX11 compositions.
- MOX22 is the compositions obtained from 50 GWd/tHM burn-up for MOX21.

In all cases, seven years cooling time before reprocessing plus three years of MOX manufacturing time is considered. In addition, the total MA contents specified are 0.0, 1.0 and 2.5 wt.%, respectively.

Finally, in the present benchmark calculations, the MOX12 and MOX22 cases were selected for the standard PWR lattice. For the highly moderated PWR lattices, only the MOX22 case was adopted. The actinide atom per cent fraction and atomic number densities are shown in Tables 2.4 and 2.5.

#### **2.2 Requested results**

The edited data to be required for the burn-up calculation are as follows:

- $k_\infty$  as a function of burn-up.

- Atomic number densities (atom/cm<sup>3</sup>) and weight (kg) normalised to one tonne of initial heavy metal at each burn-up step in Table 2.6 for the following isotopes: <sup>234</sup>U, <sup>235</sup>U, <sup>236</sup>U, <sup>238</sup>U, <sup>237</sup>Np, <sup>239</sup>Np, <sup>238</sup>Pu, <sup>239</sup>Pu, <sup>240</sup>Pu, <sup>241</sup>Pu, <sup>242</sup>Pu, <sup>241</sup>Am, <sup>242</sup>Am, <sup>242m</sup>Am, <sup>243</sup>Am, <sup>242</sup>Cm, <sup>243</sup>Cm, <sup>244</sup>Cm and <sup>245</sup>Cm, and the long-lived fission products (LLFPs) Tc<sup>99</sup>, <sup>129</sup>I and <sup>135</sup>Cs.
- Radioactivities at reactor shutdown time and cooling times of 7, 10, 20, 50, 100, 200, 500, 1 000, 2 000, 5 000, 10 000, 20 000, 50 000 and 100 000 years.
- Void reactivities for the void fractions of 40, 70 and 95%.
- Doppler reactivity for temperature change from 660 to 960°C.

### 2.3 Participants

There were six participants for the PWR benchmark. The list of participants, their basic data and codes used are given in the following table.

Institution (country)	Participants	Basic data	Codes
FZK (Germany)	C. Broeders	KEDAK4 ENDF/B-5 and 6 JEF-2.2	KAPROS/ KARBUS
IKE (Germany)	D. Lutz	JEF-2.2	RESMOD/ RSYST
JAERI (Japan)	H. Takano H. Akie K. Kaneko	JENDL-3.2	SRAC95
Tohoku University (Japan)	T. Iwasaki D. Fujiwara	JENDL-3.2	SWAT
ITEP (Russian Federation)	B. Kochurov A. Kwaratzheli N. Selivanova	BNAB-26	TRIFON
IPPE (Russian Federation)	A. Tsiboulia	FOND-2	WIMS

### 2.4 Results and discussions

The six participants reported a remarkably large number of results. The results obtained are summarised as follows.

The variations of  $k_{\infty}$  as a function of burn-up are shown in Figures 2.2-2.4 for the MOX12 (33 GWd/tHM), Figures 2.5-2.7 for the MOX22 (50 GWd/tHM) with the normal lattice, and Figures 2.8-2.10 for the MOX22 (50 GWd/tHM) with the wide lattice.



The discrepancies in  $k_{\infty}$  values are about 3% between the ITEP and IPPE results and about 2% between ITEP and Tohoku for MOX22 (wide), though a good agreement can be observed between the Japanese and German results, including MA contents of 1.0 and 2.5%. Burn-up reactivity swing is moderated by increasing the MA contents. This tendency is more strongly observed in the case of MOX12 than in that of MOX22, due to  $^{237}\text{Np}$  in MA compositions. Furthermore, this is observed in the MOX22 (standard) case rather than the MOX22 (wide) case.

In the comparison of the atomic number densities, a good agreement is seen among the six results as a function of burn-up with the exception of a few cases:  $^{237}\text{Np}$  of FZK becomes much larger than the other results with increasing burn-up (Figure 2.11). Atomic number densities of  $^{241}\text{Pu}$ ,  $^{242}\text{Pu}$  and  $^{242\text{m}}\text{Am}$  become more discrepant with burn-up among all participants (Figures 2.12-2.14). There are seven zero values for  $^{239}\text{Np}$  and  $^{242}\text{Cm}$  of JAERI,  $^{242}\text{Am}$  of IKE,  $^{243}\text{Cm}$  and  $^{245}\text{Cm}$  of FZK, and FPs of IPPE, because these results were not reported.

The fission products  $^{99}\text{Tc}$ ,  $^{129}\text{I}$  and  $^{135}\text{Cs}$  are in good agreement with each other, with the exception of  $^{129}\text{I}$  of FZK. Table 2.7 shows the FP production (kg) at the 33 GWd/tHM burn-up in the cases of MOX12, MOX22 (standard) and MOX22 (wide). The production of  $^{99}\text{Tc}$  and  $^{129}\text{I}$  do not change in all cases and with different MA contents. However,  $^{135}\text{Cs}$  depends considerably on the MA content for all types of fuels, i.e. MOX12 and MOX22. This is probably due to the differences in neutron spectra between  $\text{UO}_2$  and MOX fuels, standard and wide lattice cell, and MA contents. That is,  $^{135}\text{Xe}$  are transmuted to  $^{136}\text{Xe}$  before decay to  $^{135}\text{Cs}$ .

Table 2.8 shows an index for MA transmutation of  $^{237}\text{Np}$ ,  $^{241}\text{Am}$ ,  $^{243}\text{Am}$  and  $^{244}\text{Cm}$  by PWR. Though  $^{237}\text{Np}$  and  $^{241}\text{Am}$  are transmuted and initial loading quantities are reduced,  $^{243}\text{Am}$  and  $^{244}\text{Cm}$  increase by larger generation than transmutation rates, except for the Japanese results in the MOX22 (wide) case with 2.5% MA.

The activities are calculated by four participants for the 0.0% MA and six participants for the 1.0% and 2.5% MA. For uranium and plutonium isotopes, they are in good agreement with each other (Figure 2.15 for  $^{239}\text{Pu}$ ).  $^{241}\text{Pu}$  of JAERI stops at 500 years (Figure 2.16 for  $^{241}\text{Pu}$ ), as they did not consider the decay chain of  $^{245}\text{Cm}$ . In several isotopes of americium and curium, significant discrepancies are observed ( $^{242\text{m}}\text{Am}$ , Figure 2.17). Particularly,  $^{243}\text{Cm}$  and  $^{245}\text{Cm}$  of FZK show different variations from the others ( $^{243}\text{Cm}$ , Figure 2.18).

Void and Doppler reactivities are compared in Table 2.9. The Doppler reactivities are in a good agreement with each other, with the exception of the results for wider lattice by ITEP. In the void reactivities, the discrepancies among the calculated results expand as the void fraction increases. This becomes particularly remarkable for a void fraction of 95%. The void reactivity becomes positive as the MA content increases. In the MOX 12 and MOX 22 standard lattice, the reactivities become positive at the 70% void fraction when MA content is 2.5%. In the wider lattice, the reactivities are expressed with more negative values than for the results of standard lattice. The JAERI values are more positive than those of the others.

## 2.5 Conclusions

In general, good agreement was observed among results submitted. Overall, the results show consistency with limits of multiple plutonium recycling established by the NEA Working Party on Plutonium Fuels and Innovative Fuel Cycles.



## *Chapter 3*

### **SUMMARY OF THE FAST REACTOR BENCHMARK**

#### **3.1 Problem specification**

The detailed benchmark specification for FRs can be found in Appendix A.2; only its main features are described here. The FR benchmark is for a 1 000 MWe (2 600 MWth) fast breeder reactor which operates on a 365 EFPD cycle at 80% capacity factor; one-third of the core is refuelled per cycle. As shown in Figure 3.1, the core is of a homogeneous layout with two radial enrichment zones and a radial blanket zone. Axially, the core is one meter high and has axial blankets of 30 cm. The breeding ratio is near 1.25. The fuel comprises mixed oxide pins of depleted uranium and once-through PWR plutonium, as shown in Table 3.1. Three kinds of fuel containing minor actinides (0%, 2.5% and 5%) are selected in the FR benchmark. The beginning of life compositions are specified as shown in Table 3.2.

#### **3.2 Requested results**

Participants were requested to provide the following results:

- Eigenvalues ( $k_{\text{eff}}$ ) and critical balance (absorption and leakage) as a function of burn-up.
- Neutron balance (neutron production and absorption).
- Spectral indices.
- Reactivity loss as a function of burn-up.
- Inner and outer core isotopic composition variation (including MA build-up).
- Safety coefficients such as sodium void coefficient and fuel Doppler reactivity.
- Decay heat, neutron sources and radiotoxicity of wastes at various cooling times.

#### **3.3 Participants**

Six solutions were submitted for the fast reactor benchmark. The table appearing on the following page shows a synopsis of contributors, basic data and codes used in the solution of the problem. Some of the contributions were only partial.

#### **3.4 Results and discussions**

In the following paragraphs, some major features of the exercise are analysed.

In Table 3.3 and Figures 3.2, 3.3 and 3.4,  $k_{eff}$  is shown. For the reference core with 0% MA, a good overall agreement within 0.3%  $\Delta k/k'$  can be observed in  $k_{eff}$ . For the 2.5% MA core, three results (JNC, CEA, JAERI) are very close; Toshiba and Mitsubishi results are slightly lower (within 0.5%  $\Delta k/k'$ ) in comparison with the first three results. The IPPE result is a bit higher at the beginning of cycle (about 0.6%  $\Delta k/k'$ ). For the 5.0% MA core, the CEA, JAERI and JNC results are very similar, the Toshiba and Mitsubishi results show small deviations, and the IPPE results are quite different. The shape of the  $k_{eff}$  curve calculated by IPPE shows a different trend in comparison with the other results.

#### List of contributors, basic data and codes

Organisation (Country)	Contributors	Basic data	Number of energy groups	Codes
JAERI (Japan)	K. Tsujimoto H. Oigawa T. Mukaiyama	JENDL-3.2	70 1 (burn-up calc.)	ABC-SC code system • SLAROM • CITATION-FBR • ORILIB • ORIGEN-2 • F-CHANGE • PERKY • RADAMES
CEA (France)	J. Tommasi	CARNAVAL-IV + JEF-1	25	• ERANOS
JNC (Japan)	T. Wakabayashi	JENDL-3.2	70 7 (burn-up calc.)	• SLAROM • CITATION-FBR • ORIGEN-2 • PERKY
MITSUBISHI (Japan)	M. Yano	JENDL-3.2	18 7 (burn-up calc.)	• ODDBURN • 2DBURN • HANYO
TOSHIBA (Japan)	M. Kawashima M. Yamaoka	JENDL-3.2	70 7 (burn-up calc.)	• STANBRE-V3
IPPE (Russian Federation)	M. Semenov A. Tsiboulia	FOND-2	26	• CONSYST2 • TRIGEX • CARE

Spectral indices at the core centre are shown in Table 3.4. Very good agreements can be observed in spectral indices for all participants.

Table 3.5 shows reactivity losses due to burn-up. Reactivity losses are in very good agreement with maximum difference of 0.3% in  $\Delta k/k'$  for all three (0%, 2.5%, 5% MA) cores.

Table 3.6 shows some results for the isotopic composition variation due to burn-up. Of the 23 isotopes considered, a good agreement is found between isotopic composition variations as a function of burn-up for all isotopes except  $^{238}\text{Pu}$ ,  $^{240}\text{Pu}$ ,  $^{242}\text{Pu}$ ,  $^{241}\text{Am}$ ,  $^{243}\text{Am}$ ,  $^{244}\text{Cm}$  and  $^{237}\text{Np}$ . The CEA results present a high value for the build-up of  $^{243}\text{Am}$  and curium isotopes. A perturbation analysis would be very valuable to help understand the differences.

Reactivity worths for sodium void and Doppler coefficient are shown in Tables 3.7 and 3.8.

Excellent agreements for five results (within 8%) can be observed for sodium void reactivity, with the exception of the IPPE result. For IPPE, a discrepancy of about 20% is found for all three cores considered (0%, 2.5%, 5% MA).

The Doppler coefficient of reactivity (total for the core) is in very good agreement, within 10% for all results (the discrepancy for this parameter is usually of the order of 20% for calculations versus measurements). Doppler components nuclide-by-nuclide are also in good agreement for all cases.

Some results of decay heat and neutron sources are shown in Tables 3.9 and 3.10. Decay heat results appear to be in good agreement between JAERI and CEA, while JNC has decidedly lower values for the reference core with 0% MA. A good overall agreement can be observed in neutron sources.

Transmutation rates for the 2.5% and 5% MA cores are shown in Table 3.11. A good overall agreement within 4% can be observed for the transmutation rate.

Typical results of number densities of wastes at various cooling times are shown in Figure 3.5. The CEA, JAERI and JNC results for number densities and activities of waste are similar.

### 3.5 Conclusions

Six solutions were submitted for the FR benchmark. The following conclusions can be derived from the benchmark calculations:

1. Particularly satisfactory agreements are observed in  $k_{\text{eff}}$ , spectral indices, reactivity losses, sodium void reactivity, Doppler reactivity, neutron sources and transmutation rate.
2. The main discrepancies are observed in  $^{238}\text{Pu}$ ,  $^{240}\text{Pu}$ ,  $^{242}\text{Pu}$ ,  $^{241}\text{Am}$ ,  $^{243}\text{Am}$ ,  $^{244}\text{Cm}$  and  $^{237}\text{Np}$  isotopic composition variations. They are due to cross-section differences.
3. The lesser discrepancies are noticed in decay heat and activities of waste.

It is found that the calculational code systems of participants have a very good general agreement in the predictions of the nuclear characteristics of the MA-loaded FR core.



## *Chapter 4*

### **SUMMARY OF THE ACCELERATOR-DRIVEN SYSTEM BENCHMARK**

#### **4.1 Problem specification**

A benchmark problem was provided for code and data validation in a proton accelerator-driven transmutation system (ADS) which is based on a conceptual design study by JAERI. The detailed benchmark specification for ADS is given in Appendix A.3. The main characteristics of the benchmark system are summarised in Table 4.1. The dirty plutonium from HLW is mixed into MA fuel to suppress the reactivity swing at the first burn-up stage. Here, plutonium and MA in HLW (obtained through partitioning after seven years cooling of the fuel burned up to 33 GWd/tHM, plus three years of manufacturing time) have compositions as shown in Table 4.2 (this fuel is denoted as MOX11).

Three more fuel compositions based on plutonium and MA vectors are denoted as MOX21, MOX12 and MOX22; they have been added to this benchmark as presented in Table 4.2. These extra cases are considered by FZK, Germany as part of a proposal regarding the investigation of physics of different transmutation concepts in PWRs. Hence, MOX21 refers to plutonium and MA compositions resulting from the reprocessing of 4.65% UO<sub>2</sub> fuel from Stage 1 PWR burned to 50 MWd/tHM, MOX12 refers to plutonium and MA compositions resulting from reprocessing of 4.1% MOX11 burned to 33 MWd/tHM in a Stage 2 PWR and then admixed with depleted uranium, and MOX22 refers to plutonium and MA compositions resulting from reprocessing of 6.0% MOX21 burned to 50 MWd/tHM in a Stage 2 PWR and then admixed with natural uranium. In all cases seven years of cooling time of spent fuel before reprocessing plus three years of MOX manufacturing time is considered. The resulting accelerator fuel compositions are heavily MA dominated as required by the design constraints of the accelerator considered (sub-critical core).

Figure 4.1 shows the two-dimensional model of the present benchmark system. This system consists of a two-region tungsten target injected by proton beam, MA fuelled core and reflectors, each of which is cooled by sodium flow. The optimised target is a stack of tungsten discs with two different thicknesses as shown in Figure 4.2(a). The MA nitride fuel pins are arranged in the core region as shown in Figure 4.2(b). Here the atom number densities are smeared in every region to simplify the benchmark problem; these homogenised number densities are presented in Table 4.3.

#### **4.2 Required cross-section library and code description**

Participants should use their own cross-section library and energy group structure and provide their description.

Code descriptions of the cascade code calculating the nuclear processes above 15 MeV energy and of the neutron transport code and the burn-up code for the energy range below 15 to 20 MeV should be provided. Specifically, the calculation method, energy group structure and the actinide chain considered in the burn-up calculations should be included in the code description.

### 4.3 Spallation neutron source spectrum

In the analysis of the spallation neutron, special codes such as HETC or NMTC/JAERI are required. For the participants who were not familiar with these codes, the spallation neutron source spectrum was provided. The spectrum was determined by calculational results determined by the NMTC/JAERI code and supplied by JAERI. Table 4.4 displays the 73 group-wised spectra at the interface between target and core.

### 4.4 Requested results

This hybrid system is expected to be driven by a proton beam of 1 GeV energy and a current of 10 mA in a sub-critical state of  $k_{\text{eff}} = 0.9$ . The neutron transport process in target/core may be calculated as the fixed source problem based on spallation neutron distributions using transport code or diffusion code. Burn-up calculations should be made for actinides in the energy range below 15 MeV with the fixed neutron spectrum to make one group cross-sections. Participants are requested to provide the benchmark results specified in points (a) through (c).

*(a) Spallation neutrons (energy range from 1 GeV to 15-20 MeV, initial core):*

- Number of spallation neutrons per incident proton.
- Region averaged spallation neutron spectra in target and core.
- Axial distribution of neutrons leaking from target at  $r = 150$  mm.
- Maximum and average heat power densities in target region.

*(b) Nuclear characteristics of transmutation target/core (energy range 15-20 MeV, initial core):*

- Effective neutron multiplication factor.
- Sodium void reactivity effect (include sodium in target region).
- Region averaged neutron spectra in target and core.
- Average neutron energy in core region.
- Axial neutron flux distributions at  $r = 75$  mm and  $r = 275$  mm.
- Average neutron flux in core region.
- Fission and capture reaction rates in whole core region.
- Maximum and average heat power density in core region.
- Amount of transmuted MA per year (only by fission).
- MA transmutation rate (only by fission).



(c) *Burn-up characteristics:*

- Atom number densities for actinides (at the constant flux of  $1.0 \times 10^{16}$  n/cm<sup>2</sup>/s) at burn-up steps of 10, 50, 100, 150, 200 GWd/tHM.
- Time evolution of  $k_{\text{eff}}$  with burn-up.

#### 4.5 Participants

For the ADS benchmark, there were only three participants. The list of participants, basic data and codes used for each stage of the calculations are presented in the following table.

Institution (country)	Participants	Basic data	Codes
JAERI (Japan)	T. Nishida T. Takizuka T. Sasa	JENDL-3.2	> 20 MeV • NMTC/JAERI < 20 MeV • TWODANT (neutron transport: 73 groups) • BURNER (burn-up) • NJOY-91.38/MILER/BONAMI-S (cross-sections)
PSI (Switzerland)	G. Youinou S. Pelloni P. Wydler	JEF-2.2	> 15 MeV • HETC-PSI < 15 MeV • TWODANT (neutron transport: 33 groups) • 2DTB (burn-up) • NJOY-89.62/MICROR/MICROX-2 (cross-sections)
IPPE (Russian Federation)	T.T. Ivanova V.F. Batyaev A.A Tsiboulia	ABBN-93 from FOND-2	> 20 MeV • HETC < 20 MeV • TWODANT (neutron transport: 28 groups) • CARE (burn-up) • CONSYST2 (cross-sections)

#### 4.6 Results and discussions

The number of neutrons produced by spallation is given in Table 4.5. Three results from JAERI, PSI and IPPE show a good agreement. Maximum and average heat densities in the target are summarised in Table 4.6. The variation in average heat densities is relatively small, however the variation in maximum heat densities is very large (a factor of 3) in both the thick and thin disk parts. A possible source of the discrepancies of heat power density results is the difference in the calculation models of the codes used.

The main neutronic characteristics of the core are given in Table 4.7. The initial  $k_{\text{eff}}$  of IPPE is quite different from that of JAERI and PSI. Sodium void reactivity is very similar for the PSI and JAERI solutions whereas the IPPE results are significantly different.

JAERI and PSI results give very similar values of average neutron energy for both MOX11 and MOX12 fuel, but about a 30% difference between JAERI and PSI results is observed for average neutron flux, maximum and average heat power density in the fuel.

Fission and capture rates for initial core and 200 GWd/tHM burn-up core are shown in Tables 4.8 and 4.9 respectively. These results show a good agreement for all solutions.

Burn-up characteristics of MOX11 and MOX 12 from PSI, JAERI and IPPE are shown in Tables 4.10-4.15. These tables show the change in  $k_{\text{eff}}$  and atomic number densities of isotopes as a function of burn-up; 0, 10, 50, 100, 150, 200 GWd/tHM.

Axial neutron distribution at  $r = 150$  mm shows a good agreement for all solutions as shown in Figure 4.3.

The average neutron energy spectrum in-core is given in Figure 4.4. An excellent agreement between the JAERI and PSI results for MOX11 can be observed.

The time evolution of  $k_{\text{eff}}$  is shown in Figures 4.5 and 4.6 for MOX11 and MOX 12, respectively. Significant discrepancies are observed. The shape of the curve is identical for IPPE and JAERI, but different for PSI with about a 3% difference in  $k_{\text{eff}}$  at zero burn-up. The difference between JAERI and PSI at the beginning of burn-up is relatively small, but it becomes larger after 100 GWd/tHM. JAERI made additional calculations to examine the influence of fission energy values and fission neutron energy spectrum on reactivity [3]. As for the fission energy value,  $Q$ , three different values were taken (190, 200 and 210 MeV). The difference caused by the fission energy value is less than 0.5% and the trend of the reactivity change with burn-up has not been affected. To determine the impact of the difference of the fission energy spectrum (the so-called chi-vector), the calculations were performed by substituting the chi-vector of  $^{237}\text{Np}$  in ENDF/B-VI, JENDL-3.2 and JEF-2.2. Other reaction cross-sections were based on the JENDL-3.2 library. ENDF/B-VI shows the highest  $k_{\text{eff}}$  at the start-up core. It is about 2% higher than that of JENDL-3.2 and 3% higher than that of JEF-2.2. The chi-vector in ENDF/B-VI is the highest among the libraries. This causes more threshold fission reactions than the other two libraries and then the highest initial  $k_{\text{eff}}$  value is given. With regard to discrepancies in the burn-up reactivity change, besides different treatment of fission products used by the participants in their burn-up calculations, the difference in the fission spectrum of  $^{237}\text{Np}$  between JENDL-3.2 and JEF-2.2 may be one of the origins of discrepancies [4].

Figures 4.7-4.10 show time evolution of number densities of  $^{237}\text{Np}$  and  $^{241}\text{Am}$ . An excellent agreement is observed for both of the isotopes for PSI and IPPE solutions. Overall the discrepancy in the results increases as the total MA content increases.

## 4.7 Conclusions

Neutronics of accelerator-driven transmutation system (ADS) has been studied for validation of codes and data on the international level. The study is composed of benchmark calculations of spallation neutrons, nuclear characteristics of transmutation target/core, and burn-up characteristics for the target and core of sodium-cooled nitride fuel ADS.

Three solutions were submitted for the benchmark. The following conclusions can be derived from the benchmark results:

- 1) Satisfactory agreements are observed in the number of spallation neutrons per incident proton and the axial distribution of leakage neutrons from the spallation target ( $> 15$  MeV). Large discrepancies are found in the maximum and average heat power densities in the thin and thick disk parts of the target.
- 2) The results of the average neutron spectrum show good agreement. Essential discrepancies are found in the  $k_{\text{eff}}$  and burn-up characteristics.
- 3) The discrepancies in  $k_{\text{eff}}$  and burn-up characteristics may be attributable to the treatment of the fission neutron energy spectrum, treatment of fission products including the preparation of fission product chains, lumped fission products and fission yields, differences in the microscopic cross-sections, etc.

The current ADS benchmark results are too discrepant and inconclusive. Therefore, the need for a further ADS benchmark is clearly evident. Its design should provide the necessary features for resolving the discrepancies found in the present study and should be the starting point for more complex investigations involving transient behaviour of ADS systems. This is very important to further improve the reliability for validation of codes and data.



## Chapter 5

### CONCLUSIONS AND RECOMMENDATIONS

In the framework of the OECD/NEA project on “Physics Aspects of Different Transmutation Concepts,” the physics of recovered plutonium and MA transmutation in the form of MOX fuel in PWR, FR and ADS has been studied.

The Secretariat received a total of 15 solutions: six for the PWR, six for the FR and three for the ADS.

For the PWR benchmark, in general, good agreement was observed among the submitted results. Overall, the results show consistency with limits of multiple plutonium recycling established by the NEA Working Party on Plutonium Fuels and Innovative Fuel Cycles (WPPR). In the PWR benchmark calculations, the discrepancies in  $k_{\text{eff}}$  values were about 2-3% between the ITEP and IPPE results, despite a good agreement being observed between the Japanese and German results. The fission products build-up of  $^{99}\text{Tc}$ ,  $^{129}\text{I}$  and  $^{135}\text{Cs}$  were in good agreement with each other. It was found the production of  $^{135}\text{Cs}$  depends considerably on the MA contents and MOX12 and MOX22 fuelled cases, that is on neutron spectra between  $\text{UO}_2$  and MOX fuels, standard and wide lattice cell and MA contents. For MA transmutation,  $^{237}\text{Np}$  and  $^{241}\text{Am}$  are transmuted and initial loading quantities are reduced, but  $^{243}\text{Am}$  and  $^{244}\text{Cm}$  increase by larger build-up rates than transmutation rates.

For the FR benchmark, very good general agreement was also observed among submitted results. Therefore, calculational code systems of participants have a fairly good agreement in the predictions of the nuclear characteristics of the MA loaded FR core. In the FR benchmark calculations, considerably good agreements were shown in the  $k_{\text{eff}}$  values, burn-up reactivity swings, spectral indices, sodium void reactivity, Doppler reactivity and transmutation rate. However, there were significant discrepancies for burn-up build-up of  $^{238}\text{Pu}$ ,  $^{242}\text{Pu}$ ,  $^{237}\text{Np}$ ,  $^{241}\text{Am}$ ,  $^{243}\text{Am}$  and  $^{244}\text{Cm}$ . Furthermore, FR benchmark calculations will be required for different (plutonium, MA) compositions such as the MOX22 case.

For the ADS benchmark, we observed good agreement for spallation neutron number/proton, axial neutron distribution from the target and so on. Large discrepancies were, however, observed in  $k_{\text{eff}}$  and burn-up characteristics. The major causes are due to fission neutron spectrum, treatment of fission products and capture and fission cross-sections used for MA nuclides in different nuclear data libraries.

In the ADS benchmark, considerable differences in calculated initial  $k_{\text{eff}}$  values and burn-up reactivity swings indicated the need for a further ADS benchmark. Its specification should provide the necessary features for resolving discrepancies identified in the present benchmark and can later be extended for more complex investigations such as beam trip transient behaviour of ADS systems. The detailed benchmark specification for the proposed ADS design can be found in Reference [5].



## REFERENCES

- [1] “OECD/NEA NSC Task Force on Physics Aspects of Different Transmutation Concepts – Benchmark Specifications”, NSC/DOC(96)10, 15 April 1996.
- [2] H. Takano *et al.*, “Benchmark Problems on Transmutation Calculation by the OECD/NEA Task Force on Physics Aspects of Different Transmutation Concepts”, Int. Conf. on the Physics of Nuclear Science and Technology, Long Island, NY, USA, 5-8 October 1998, p. 1 462.
- [3] T. Sasa, JAERI, private communications, December 1999.
- [4] “Present Status of Minor Actinide Data”, International Evaluation Co-operation, Volume 8, NEA/WPEC-8, 1999.
- [5] P. Wydler and H. Takano, “Comparison Calculations for an Accelerator-Driven Minor Actinide Burner”, NSC/DOC(99)13.





# TABLES



**Table 2.1. Benchmark cell specifications for PWR**

Parameter	Value
Moderator to fuel ratio	
<i>Standard</i>	1.929
<i>Wide</i>	3.0
Fuel radius (cm)	0.4095
Can radius (cm)	0.475
Lattice pitch (cm)	
<i>Standard</i>	1.333
<i>Wide</i>	1.513
Moderator radius (cm)	
<i>Standard</i>	0.741
<i>Wide</i>	0.8536
Specific power (MW/tHM)	38.30
Power rating (W/cm)	183.02
Theoretical UO <sub>2</sub> density (g/cm <sup>3</sup> )	10.96
Theoretical PuO <sub>2</sub> density (g/cm <sup>3</sup> )	11.46
Oxide fuel density (g/cm <sup>3</sup> )	10.29
Zirconium density (g/cm <sup>3</sup> )	6.55
Water density (g/cm <sup>3</sup> )	0.7136
Fuel temperature (°C)	660.0
Moderator temperature (°C)	363.3

**Table 2.2. Number densities of PWR UO<sub>2</sub> cell at BOL**

Zone	Isotope	Concentration (nuclei/cm <sup>3</sup> )	
		3.25% <sup>235</sup> U	4.65% <sup>235</sup> U
Fuel	O	4.5934E+22	4.5941E+22
	<sup>235</sup> U	7.5564E+20	1.0811E+21
	<sup>238</sup> U	2.2211E+22	2.1889E+22
Cladding	Zr	4.3365E+22	4.3365E+22
Moderator	H	4.7769E+2	4.7769E+22
	O	2.3885E+22	2.3885E+22

**Table 2.3. Actinide atom per cent fraction**

Fuel burn-up	MOX11	MOX21	MOX12	MOX22
	33 GWd/tHM	50 GWd/tHM	33 GWd/tHM	50 GWd/tHM
	Nuclide atom %			
<sup>238</sup> Pu	1.5	2.7	2.6	4.1
<sup>239</sup> Pu	59.3	55.3	44.5	41.9
<sup>240</sup> Pu	23.7	23.9	31.0	30.5
<sup>241</sup> Pu	8.7	9.5	10.7	10.6
<sup>242</sup> Pu	5.5	7.1	9.5	11.3
<sup>241</sup> Am	1.3	1.5	1.7	1.7
<b>Total</b>	<b>100</b>	<b>100</b>	<b>100</b>	<b>100</b>
<sup>237</sup> Np	44.6	46.4	4.5	4.4
<sup>241</sup> Am	43.6	37.1	62.5	58.3
<sup>243</sup> Am	9.7	12.7	24.3	26.1
<sup>243</sup> Cm	0.0	0.0	0.0	0.0
<sup>244</sup> Cm	2.1	3.8	8.7	11.3
<sup>245</sup> Cm	0.0	0.0	0.0	0.0
<b>Total</b>	<b>100</b>	<b>100</b>	<b>100</b>	<b>100</b>

**Table 2.4. Number densities of the normal PWR lattice**

MA(%)	MOX12 (33 GWd/tHM)			MOX22 (50 GWd/tHM)		
	0.0	1.0	2.5	0.0	1.0	2.5
<sup>235</sup> U	4.6618E-05	4.4263E-05	4.1190E-05	1.4144E-04	1.3547E-04	1.2639E-04
<sup>238</sup> U	2.0673E-02	1.9628E-02	1.8265E-02	1.9752E-02	1.8918E-02	1.7651E-02
<sup>237</sup> Np	0.0000E+00	1.0332E-05	2.5881E-05	0.0000E+00	1.0105E-05	2.5357E-05
<sup>238</sup> Pu	5.6777E-05	7.8873E-05	1.0646E-04	1.2477E-04	1.5081E-04	1.9044E-04
<sup>239</sup> Pu	9.7176E-04	1.3499E-03	1.8222E-03	1.2751E-03	1.5412E-03	1.9462E-03
<sup>240</sup> Pu	6.7695E-04	9.4041E-04	1.2694E-03	9.2817E-04	1.1219E-03	1.4167E-03
<sup>241</sup> Pu	2.3366E-04	3.2459E-04	4.3814E-04	3.1953E-04	3.8622E-04	4.8771E-04
<sup>242</sup> Pu	2.0745E-04	2.8819E-04	3.8900E-04	3.4388E-04	4.1564E-04	5.2487E-04
<sup>241</sup> Am	3.7123E-05	1.4349E-04	3.5946E-04	5.1734E-05	1.3366E-04	3.3540E-04
<sup>243</sup> Am	0.0000E+00	5.5790E-05	1.3976E-04	0.0000E+00	5.9941E-05	1.5041E-04
<sup>244</sup> Cm	0.0000E+00	1.9974E-05	5.0037E-05	0.0000E+00	2.5952E-05	6.5121E-05
O	4.5807E-02	4.5768E-02	4.5813E-02	4.5873E-02	4.5798E-02	4.5839E-02

**Table 2.5. Number densities of the wider PWR lattice**

MA(%)	MOX22 (50 GWd/tHM)		
	0.0	1.0	2.5
<sup>235</sup> U	1.4994E-04	1.4400E-04	1.3317E-04
<sup>238</sup> U	2.0939E-02	2.0109E-02	1.8596E-02
<sup>237</sup> Np	0.0000E+00	1.0084E-05	2.5286E-05
<sup>238</sup> Pu	7.3785E-05	9.9693E-05	1.4991E-04
<sup>239</sup> Pu	7.5405E-04	1.0188E-03	1.5320E-03
<sup>240</sup> Pu	5.4889E-04	7.4162E-04	1.1152E-03
<sup>241</sup> Pu	1.8896E-04	2.5531E-04	3.8392E-04
<sup>242</sup> Pu	2.0336E-04	2.7476E-04	4.1317E-04
<sup>241</sup> Am	3.0594E-05	1.3339E-04	3.3446E-04
<sup>243</sup> Am	0.0000E+00	5.9819E-05	1.4999E-04
<sup>244</sup> Cm	0.0000E+00	2.5899E-05	6.4939E-05
O	4.5873E-02	4.5798E-02	4.5839E-02

The plutonium enrichments are respectively: 0.0% MA: 4.15% Pu-f  
 1.0% MA: 5.6% Pu-f  
 2.5% MA: 8.4% Pu-f

**Table 2.6. Proposed macro steps for depletion calculations**

Step	Burn-up (MWd/tHM)	$\Delta T^*$ (day)
1	0	0.000
2	150	3.916
3	500	9.138
4	1 000	13.055
5	2 000	26.110
6	4 000	52.219
7	6 000	52.219
8	10 000	104.439
9	15 000	130.548
10	20 000	130.548
11	22 000	52.219
12	26 000	104.439
13	30 000	104.439
14	33 000	78.329
15	33 300	7.833
16	35 000	44.386
17	40 000	130.548
18	45 000	130.548
19	50 000	130.548

\* Power rating 183.02 W/cm

**Table 2.7. Fission products weight (kg) of <sup>99</sup>Tc, <sup>129</sup>I and <sup>135</sup>Cs generated at the burn-up 33 GWd/tHM and normalised to 1 t fuel**

Fuel	Nuclide	MA contents (%)		
		0.0	1.0	2.5
MOX12	<sup>99</sup> Tc	0.80	0.80	0.80
	<sup>129</sup> I	0.21	0.21	0.21
	<sup>135</sup> Cs	0.91	1.04	1.14
MOX22 (standard)	<sup>99</sup> Tc	0.81	0.81	0.80
	<sup>129</sup> I	0.21	0.21	0.20
	<sup>135</sup> Cs	1.04	1.10	1.17
MOX22 (wide)	<sup>99</sup> Tc	0.82	0.82	0.81
	<sup>129</sup> I	0.20	0.20	0.20
	<sup>135</sup> Cs	0.71	0.84	1.00

**Table 2.8. Index of MA transmutation which means negative or positive sign corresponding to decrease or increase from initial loading MA**

Nuclide	MOX12		MOX22-standard		MOX22-wide	
	1.0% MA	2.5% MA	1.0% MA	2.5% MA	1.0% MA	2.5% MA
<sup>237</sup> Np	0.0	-	0.0	-	- (+FZK)	-
<sup>241</sup> Am	-	-	-	-	-	-
<sup>243</sup> Am	+	0.0	+	+	+	0.0
<sup>244</sup> Am	+	+	+	+	+	+

**Table 2.9. Comparison of Doppler and void reactivities**

**Part I – MOX12**

**1. MOX12, 33 GWd, 5.3% Pu-f 0% MA**

a) Burn-up = 0 GWd/tHM (BOL)

	Tohoku Univ.	Itep	JAERI	IKE	FZK
<b>Void fraction</b>	<b>k0</b>				
0	1.10399	1.1296	1.10854	1.1081	1.10694
	<b><math>\Delta k = k' - k_0</math></b>				
0.4	-0.081	-0.0835	-0.0806	-0.0815	-0.0812
0.7	-0.1349	-0.1465	-0.1327	-0.1346	-0.1332
0.95	-0.1502	-0.1602	-0.1286	-0.1419	-0.1458
<b>Doppler (+300°C)</b>	-0.0099	-0.0106	-0.0098		-0.0102

b) Burn-up = 33 GWd/tHM (EOL)

	Tohoku Univ.	Itep	JAERI	IKE	FZK
<b>Void fraction</b>	<b>k0</b>				
0	0.99942	1.006	0.99728		0.98641
	<b><math>\Delta k = k' - k_0</math></b>				
0.4	-0.0803	-0.0797	-0.0808		-0.0791
0.7	-0.1358	-0.1334	-0.1362		-0.1322
0.95	-0.1462	-0.1403	-0.1304		-0.1399
<b>Doppler (+300°C)</b>	-0.0084	-0.008	-0.0086		-0.0088

**2. MOX12, 33 GWd, 7.5% Pu-f 1.0% MA**

a) Burn-up = 0 GWd/tHM (BOL)

	Tohoku Univ.	Itep	JAERI	IKE	FZK
<b>Void fraction</b>	<b>k0</b>				
0	1.07879	1.100	1.08437	1.0808	1.08431
	<b><math>\Delta k = k' - k_0</math></b>				
0.4	-0.0513	-0.0563	-0.0513	-0.0513	-0.0493
0.7	-0.0574	-0.0688	-0.0557	-0.0556	-0.0508
0.95	0.0033	-0.0075	0.0261	0.0138	0.018
<b>Doppler (+300°C)</b>	-0.0086	-0.0085	-0.0086		-0.0092

b) Burn-up = 33 GWd/tHM (EOL)

	Tohoku Univ.	Itep	JAERI	IKE	FZK
<b>Void fraction</b>	<b>k0</b>				
0	1.00916	1.0167	1.00721		0.99682
	<b><math>\Delta k = k' - k_0</math></b>				
0.4	-0.0524	-0.0543	-0.0532		-0.0501
0.7	-0.0631	-0.0684	-0.0637		-0.0568
0.95	-0.0047	-0.0052	0.0132		-0.0086
<b>Doppler (+300°C)</b>	-0.0079	-0.0075	-0.0080		-0.0083

### 3. MOX12, 33 GWd, 10.15% Pu-f 2.5% MA

a) Burn-up = 0 GWd/tHM (BOL)

	Tohoku Univ.	ITEP	JAERI	IKE	FZK
<b>Void fraction</b>	<b>k<sub>0</sub></b>				
0	1.06292	1.0766	1.06956	1.0641	1.07079
	<b><math>\Delta k = k' - k_0</math></b>				
0.4	-0.0179	-0.0222	-0.0184	-0.0172	-0.0151
0.7	0.0197	0.0059	0.0209	0.0229	0.0284
0.95	0.1495	0.1368	0.1733	0.1602	0.1691
<b>Doppler (+300°C)</b>	-0.0076	-0.0072	-0.0075		-0.0083

b) Burn-up = 33 GWd/tHM (EOL)

<b>Void Fraction</b>	<b>k<sub>0</sub></b>				
0	1.0148	1.0196	1.01334		1.00346
	<b><math>\Delta k = k' - k_0</math></b>				
0.4	-0.0205	-0.0222	-0.0217		-0.0182
0.7	0.0117	0.006	0.0108		0.0193
0.95	0.1381	0.1343	0.1576		0.1548
<b>Doppler (+300°C)</b>	-0.0071	-0.0069	-0.0072		-0.0077



**Table 2.9. Comparison of Doppler and void reactivities (continued)**

**Part II – MOX22**

**1. MOX22, 50 GWd, 7% Pu-f 0.0% MA**

a) Burn-up = 0 GWd/tHM (BOL)

	Tohoku Univ.	ITEP	JAERI	IKE	FZK
<b>Void fraction</b>	<b>k0</b>				
0	1.1247	1.1494	1.12957	1.1286	1.12585
	<b><math>\Delta k = k' - k0</math></b>				
0.4	-0.0543	-0.06	-0.0542	-0.0547	-0.0569
0.7	-0.0673	-0.0809	-0.0655	-0.0664	-0.0653
0.95	-0.0215	-0.0328	0.0010	-0.0119	-0.0148
<b>Doppler (+300°C)</b>	-0.0094	-0.0089	-0.0093		-0.0100

b) Burn-up = 50 GWd/tHM (EOL)

	Tohoku Univ.	ITEP	JAERI	IKE	FZK
<b>Void fraction</b>	<b>k0</b>				
0	0.99221	0.9991	0.98943		0.9741
	<b><math>\Delta k = k' - k0</math></b>				
0.4	-0.0597	-0.0595	-0.0610		-0.0587
0.7	-0.0809	-0.0827	-0.0829		-0.0783
0.95	-0.0350	-0.0305	-0.0210		-0.0288
<b>Doppler (+300°C)</b>	-0.0078	-0.0078	-0.0081		-0.0082

**2. MOX22, 50 GWd, 8.45% Pu-f 1.0% MA**

a) Burn-up = 0 GWd/tHM (BOL)

	Tohoku Univ.	ITEP	JAERI	IKE	FZK
<b>Void fraction</b>	<b>k0</b>				
0	1.10426	1.1257	1.10968	1.1069	1.10371
	<b><math>\Delta k = k' - k0</math></b>				
0.4	-0.0346	-0.0404	-0.0348	-0.0347	-0.0338
0.7	-0.0186	-0.0328	-0.0170	-0.0167	-0.0148
0.95	0.0752	0.0626	0.0988	0.0858	0.0855
<b>Doppler (+300°C)</b>	-0.0085	-0.0089	-0.0084		-0.0091

b) Burn-up = 50 GWd/tHM (EOL)

	Tohoku Univ.	ITEP	JAERI	IKE	FZK
<b>Void fraction</b>	<b>k0</b>				
0	1.00207	1.0089	0.99864		0.97986
	<b><math>\Delta k = k' - k0</math></b>				
0.4	-0.0405	-0.0430	-0.0420		-0.0400
0.7	-0.0342	-0.0400	-0.0360		-0.0319
0.95	0.0547	0.0544	0.0707		0.0617
<b>Doppler (+300°C)</b>	-0.0075	-0.0076	-0.0077		-0.0079

### 3. MOX22, 50 GWd, 10.65% Pu-f 2.5% MA

a) Burn-up = 0 GWd/tHM (BOL)

	Tohoku Univ.	ITEP	JAERI	IKE	FZK
<b>Void fraction</b>	<b>k<sub>0</sub></b>				
0	1.08556	1.0989	1.09186	1.0874	1.08391
	<b><math>\Delta k = k' - k_0</math></b>				
0.4	-0.0070	-0.0132	-0.0075	-0.0064	-0.0056
0.7	0.0437	0.0293	0.0450	0.0468	0.0492
0.95	0.1948	0.1811	0.2193	0.2051	0.2083
<b>Doppler (+300°C)</b>	-0.0075	-0.007	-0.0075		-0.0082

b) Burn-up = 50 GWd/tHM (EOL)

<b>Void fraction</b>	<b>k<sub>0</sub></b>				
0	1.01163	1.014	1.00707		0.98577
	<b><math>\Delta k = k' - k_0</math></b>				
0.4	-0.0137	-0.0166	-0.0154		-0.0108
0.7	0.0274	0.0215	0.0255		0.0300
0.95	0.1722	0.1685	0.1900		0.1812
<b>Doppler (+300°C)</b>	-0.0069	-0.0069	-0.0071		-0.0074

**Table 2.9. Comparison of Doppler and void reactivities (continued)**

**Part III – MOX22 (wide)**

**1. Wide lattice MOX22, 50 GWd, 4.15% Pu-f 0.0% MA**

a) Burn-up = 0 GWd/tHM (BOL)

	Tohoku Univ.	ITEP	JAERI	IKE	FZK
<b>Void fraction</b>	<b>k<sub>0</sub></b>				
0	1.18209	1.2014	1.18597	1.1868	1.18373
	<b>Δk = k' - k<sub>0</sub></b>				
0.4	-0.1024	-0.1024	-0.1018	-0.1027	-0.1034
0.7	-0.2126	-0.2126	-0.2106	-0.2126	-0.2130
0.95	-0.2795	-0.2795	-0.2561	-0.2736	-0.2754
<b>Doppler (+300°C)</b>	-0.0090	-0.0080	-0.0089		-0.0090

b) Burn-up = 50 GWd/tHM (EOL)

	Tohoku Univ.	ITEP	JAERI	IKE	FZK
<b>Void fraction</b>	<b>k<sub>0</sub></b>				
0	0.97236	0.9676	0.96829		0.94994
	<b>Δk = k' - k<sub>0</sub></b>				
0.4	-0.1005	-0.0954	-0.1008		-0.0987
0.7	-0.2228	-0.2151	-0.2233		-0.2179
0.95	-0.3171	-0.3003	-0.3008		-0.3051
<b>Doppler (+300°C)</b>	-0.0066	-0.0062	-0.0067		-0.0072

**2. Wide lattice, MOX22, 50 GWd, 5.6% Pu-f 1.0% MA**

a) Burn-up = 0 GWd/tHM (BOL)

	Tohoku Univ.	ITEP	JAERI	IKE	FZK
<b>Void fraction</b>	<b>k<sub>0</sub></b>				
0	1.12559	1.1427	1.13115	1.1286	1.12469
	<b>Δk = k' - k<sub>0</sub></b>				
0.4	-0.0904	-0.0864	-0.0902	-0.0911	-0.0908
0.7	-0.1622	-0.1648	-0.1611	-0.1621	-0.1608
0.95	-0.1404	-0.1479	-0.1161	-0.1316	-0.1318
<b>Doppler (+300°C)</b>	-0.0081	-0.0069	-0.0080		-0.0083

b) Burn-up = 50 GWd/tHM (EOL)

	Tohoku Univ.	ITEP	JAERI	IKE	FZK
<b>Void fraction</b>	<b>k<sub>0</sub></b>				
0	0.99288	0.993	0.98909		0.96772
	<b>Δk = k' - k<sub>0</sub></b>				
0.4	-0.0936	-0.0898	-0.0944		-0.0923
0.7	-0.1826	-0.1794	-0.1840		-0.179
0.95	-0.1935	-0.1818	-0.1764		-0.1845
<b>Doppler (+300°C)</b>	-0.0069	-0.0095	-0.0070		-0.0072

### 3. Wide lattice, MOX22, 50 GWd, 8.45% Pu-f 2.5% MA

a) Burn-up = 0 GWd/tHM (BOL)

	Tohoku Univ.	ITEP	JAERI	IKE	FZK
<b>Void fraction</b>	<b>k0</b>				
0	1.0905	1.1039	1.09784	1.0929	1.08806
	<b><math>\Delta k = k' - k0</math></b>				
0.4	-0.0628	-0.0639	-0.0633	-0.0634	-0.0626
0.7	-0.0791	-0.0882	-0.0790	-0.0783	-0.0756
0.95	0.0408	0.0289	0.0667	0.0505	0.0534
<b>Doppler (+300°C)</b>	-0.0072	-0.0082	-0.0071		-0.0077

b) Burn-up = 50 GWd/tHM (EOL)

<b>Void fraction</b>	<b>k0</b>				
0	1.0076	1.0077	1.00385		0.98165
	<b><math>\Delta k = k' - k0</math></b>				
0.4	-0.0695	-0.0670	-0.0708		-0.0690
0.7	-0.1025	-0.1009	-0.1048		-0.1005
0.95	-0.0077	-0.0040	0.0114		0.0005
<b>Doppler (+300°C)</b>	-0.0065	-0.0070	-0.0067		-0.0069

**Table 3.1. Plutonium isotopic composition (PWR UO<sub>2</sub> fuel 50 GWd/tHM, seven years cooling)**

	<sup>238</sup> Pu	<sup>239</sup> Pu	<sup>240</sup> Pu	<sup>241</sup> Pu	<sup>242</sup> Pu	<sup>241</sup> Am
<b>at%</b>	2.76	53.74	24.24	10.63	6.98	1.65

Table 3.2. Homogenised atomic density

Nuclide	Reference core		MA 2.5% core		MA 5.0% core		Axial blanket	Radial blanket	Upper shield	Radial shield	Sodium follower
	Inner core (Pu 15.4%)	Outer core (Pu 19.1%)	Inner core (Pu 15.22%)	Outer core (Pu 18.96%)	Inner core (Pu 15.13%)	Outer core (Pu 18.84%)					
<sup>238</sup> Pu	3.9035E-05	4.8493E-05	3.8605E-05	4.8156E-05	3.8376E-05	4.7861E-05					
<sup>239</sup> Pu	7.5686E-04	9.4025E-04	7.4853E-04	9.3371E-04	7.4409E-04	9.2799E-04					
<sup>240</sup> Pu	3.3997E-04	4.2234E-04	3.3622E-04	4.1940E-04	3.3423E-04	4.1683E-04					
<sup>241</sup> Pu	1.4847E-04	1.8444E-04	1.4683E-04	1.8316E-04	1.4596E-04	1.8203E-04					
<sup>242</sup> Pu	9.7084E-05	1.2061E-04	9.6015E-05	1.1977E-04	9.5446E-05	1.1903E-04					
<sup>241</sup> Am	2.3043E-05	2.8627E-05	2.2770E-05	2.8410E-05	2.2690E-05	2.8230E-05					
<sup>235</sup> U	2.3607E-05	2.2611E-05	2.2954E-05	2.1948E-05	2.2281E-05	2.1281E-05	2.8822E-05	3.8136E-05			
<sup>238</sup> U	7.7462E-03	7.4196E-03	7.5321E-03	7.2020E-03	7.3112E-03	6.9830E-03	9.4576E-03	1.2514E-02			
O	1.8165E-02	1.8190E-02	1.8162E-02	1.8187E-02	1.8159E-02	1.8184E-02	1.8973E-02	2.5104E-02			
Na	8.3436E-03	8.3436E-03	8.3436E-03	8.3436E-03	8.3436E-03	8.3436E-03	8.3436E-03	6.0635E-03	8.3453E-03	4.4484E-03	2.0547E-02
Fe	1.0343E-02	1.0343E-02	1.0343E-02	1.0343E-02	1.0343E-02	1.0343E-02	1.0343E-02	8.4772E-03	1.0344E-02	4.1922E-02	3.9941E-03
Cr	2.7421E-03	2.7421E-03	2.7421E-03	2.7421E-03	2.7421E-03	2.7421E-03	2.7421E-03	2.2475E-03	2.7425E-03	1.1115E-02	1.0589E-03
Ni	3.1476E-03	3.1476E-03	3.1476E-03	3.1476E-03	3.1476E-03	3.1476E-03	3.1476E-03	2.5799E-03	3.1482E-03	1.2759E-02	1.2156E-03
Mo	2.4785E-04	2.4785E-04	2.4785E-04	2.4785E-04	2.4785E-04	2.4785E-04	2.4785E-04	2.0315E-04	2.4791E-04	1.0047E-03	9.5721E-05
Mn	3.3971E-04	3.3971E-04	3.3971E-04	3.3971E-04	3.3971E-04	3.3971E-04	3.3971E-04	2.7844E-04	3.3977E-04	1.3770E-03	1.3119E-04
<sup>237</sup> Np			1.1586E-04	1.1605E-04	2.3172E-04	2.3210E-04					
<sup>241</sup> Am*			7.8930E-05	7.9060E-05	1.5780E-04	1.5810E-04					
<sup>242m</sup> Am			1.8071E-07	1.8101E-07	3.6141E-07	3.6200E-07					
<sup>243</sup> Am			2.5443E-05	2.5485E-05	5.0884E-05	5.0967E-05					
<sup>243</sup> Cm			1.1248E-07	1.1267E-07	2.2495E-07	2.2532E-07					
<sup>244</sup> Cm			7.4829E-06	7.4951E-06	1.4965E-05	1.4989E-05					
<sup>245</sup> Cm			4.4624E-07	4.4697E-07	8.9245E-07	8.9390E-07					

\* <sup>241</sup>Am in MA MA (Mass); MA/(MA + Pu + U)

**Table 3.3.1.  $k_{\text{eff}}$  at 0, 365, 1 460, 1 825 EFPD (reference core)**

Burn-up (EFPD)	JAERI	CEA	JNC	MITSUBISHI	TOSHIBA	IPPE
0	1.03086	1.02948	1.03075	1.02802	1.02792	1.03352
365	1.01904	1.01855	1.01986	1.0167	1.01683	1.02064
1 460	1.0155	1.01534	1.01646	1.01268	1.01314	1.01654
1 825	1.00214	1.00243	1.00356	0.99845	0.99827	1.00053

**Table 3.3.2.  $k_{\text{eff}}$  at 0, 365, 1 460, 1 825 EFPD (2.5% MA core)**

Burn-up (EFPD)	JAERI	CEA	JNC	MITSUBISHI	TOSHIBA	IPPE
0	1.01374	1.01248	1.01298	1.011	1.01033	1.0198
365	1.00889	1.00865	1.00896	1.0061	1.00610	1.01346
1 460	1.00815	1.00831	1.00828	1.0048	1.00511	1.01062
1 825	1.00276	1.00366	1.00332	0.9982	0.99826	1.00198

**Table 3.3.3.  $k_{\text{eff}}$  at 0, 365, 1 460, 1 825 EFPD (5% MA core)**

Burn-up (EFPD)	JAERI	CEA	JNC	MITSUBISHI	TOSHIBA	IPPE
0	1.00272	1.0012	1.00064	1.00004	0.99896	1.01163
365	1.00301	1.00269	1.00182	0.99984	0.99970	1.01012
1 460	1.00433	1.00455	1.00325	1.00054	1.00075	1.00822
1 825	1.00497	1.0063	1.0045	0.99977	0.99999	1.00517

**Table 3.4.1. Spectral indices at 0 EFPD (reference core)**

Spectrum indices	JAERI	CEA	JNC	MITSUBISHI	TOSHIBA	IPPE
$C (^{238}\text{U})/F (^{239}\text{Pu})$	0.1597	0.1632	0.1692		0.1601	0.1591
$F (^{238}\text{U})/F (^{239}\text{Pu})$	0.0247	0.0222	0.026		0.0239	0.0243
$F (^{240}\text{Pu})/F (^{239}\text{Pu})$	0.2066	0.1859	0.216		0.1995	0.2003
$F (^{241}\text{Pu})/F (^{239}\text{Pu})$	1.4214	1.3968	1.50		1.4299	1.385

**Table 3.4.2. Spectral indices at 0 EFPD (2.5% MA core)**

Spectrum indices	JAERI	CEA	JNC	MITSUBISHI	TOSHIBA	IPPE
$C (^{238}\text{U})/F (^{239}\text{Pu})$	0.157	0.1614	0.165		0.1585	0.157
$F (^{238}\text{U})/F (^{239}\text{Pu})$	0.0258	0.0232	0.0269		0.0249	0.0253
$F (^{240}\text{Pu})/F (^{239}\text{Pu})$	0.2131	0.1919	0.2203		0.2060	0.2063
$F (^{241}\text{Pu})/F (^{239}\text{Pu})$	1.4072	1.3877	1.477		1.4166	1.3692

**Table 3.4.3. Spectral indices at 0 EFPD (5% MA core)**

Spectrum indices	JAERI	CEA	JNC	mitsubishi	TOSHIBA	IPPE
C ( <sup>238</sup> U)/F ( <sup>239</sup> Pu)	0.1542	0.1594	0.1611		0.1560	0.1552
F ( <sup>238</sup> U)/F ( <sup>239</sup> Pu)	0.0269	0.0242	0.0279		0.0260	0.0262
F ( <sup>240</sup> Pu)/F ( <sup>239</sup> Pu)	0.2196	0.1978	0.2247		0.2124	0.2114
F ( <sup>241</sup> Pu)/F ( <sup>239</sup> Pu)	1.3933	1.3785	1.456		1.4025	1.3593

**Table 3.5.1. Reactivity losses over five cycles (reference core)**

(%Δk/k')

Burn-up (EFPD)	JAERI	CEA	JNC	mitsubishi	TOSHIBA	IPPE
<b>0-365</b>	1.679	1.574	1.547	1.619	1.691	1.764
<b>365-730</b>	1.336	1.288	1.279	1.424	1.494	1.534
<b>730-1 095</b>	1.297	1.257	1.253	1.396	1.458	1.521
<b>1 095-1 460</b>	1.31	1.269	1.264	1.407	1.47	1.567
<b>1 460-1 825</b>	1.311	1.27	1.265	1.407	1.47	1.574

**Table 3.5.2. Reactivity losses over five cycles (2.5% MA core)**

(%Δk/k')

Burn-up (EFPD)	JAERI	CEA	JNC	mitsubishi	TOSHIBA	IPPE
<b>0-365</b>	0.686	0.558	0.573	0.707	0.706	0.858
<b>365-730</b>	0.483	0.399	0.436	0.61	0.635	0.767
<b>730-1 095</b>	0.511	0.437	0.473	0.635	0.665	0.818
<b>1 095-1 460</b>	0.532	0.458	0.491	0.653	0.683	0.851
<b>1 460-1 825</b>	0.533	0.458	0.491	0.653	0.684	0.853

**Table 3.5.3. Reactivity losses over five cycles (5% MA core)**

(%Δk/k')

Burn-up (EFPD)	JAERI	CEA	JNC	mitsubishi	TOSHIBA	IPPE
<b>0-365</b>	-0.071	-0.234	0.2	0.009	-0.044	0.175
<b>365-730</b>	-0.161	-0.291	-0.227	-0.005	-0.021	0.188
<b>730-1 095</b>	-0.092	-0.202	-0.145	0.055	0.054	0.28
<b>1 095-1 460</b>	-0.067	-0.178	-0.125	0.076	0.076	0.304
<b>1 460-1 825</b>	-0.065	-0.177	-0.124	0.077	0.076	0.301

**Table 3.6.1. Isotopic composition variation (EOC-BOC) (reference core, inner core)**

(Δ kg)

Isotope	JAERI	CEA	JNC	MITSUBISHI	TOSHIBA	IPPE
<sup>238</sup> Pu	-17.97	-13.7	-16.1	-16	-16.44	-15.33
<sup>239</sup> Pu	129.14	124	127	128	126.23	109.04
<sup>240</sup> Pu	42.80	60.53	40.1	39.4	39.38	47.56
<sup>241</sup> Pu	-88.35	-91.27	-87.1	-86.1	-86.54	-82.64
<sup>242</sup> Pu	-3.72	-9.678	-5.8	-3.1	-3.14	-4.53
<sup>235</sup> U	-18.67	-18.49	-18.3	-18	-18.06	-17.32
<sup>236</sup> U	–	4.101	–	–	–	–
<sup>238</sup> U	-1 102.81	-1 072	-1 068.5	-1 030	-1 035.67	-1 045.39
<sup>237</sup> Np	2.98	4.559	2.9	2.7	2.77	2.91
<sup>239</sup> Np	–	4.22	–	–	–	–
<sup>241</sup> Am	0.30	-0.3019	0.9	1.6	1.48	0.93
<sup>242m</sup> Am	2.45	2.512	2.4	1.9	2.43	1.64
<sup>243</sup> Am	17.37	20.43	17	16.7	16.81	15.76
<sup>242</sup> Cm	–	4.309	–	–	–	–
<sup>243</sup> Cm	0.23	0.2823	0.3	0.2	0.22	0.22
<sup>244</sup> Cm	3.62	4.372	3.4	3.3	3.33	2.49
<sup>245</sup> Cm	0.23	0.2167	0.2	0.2	0.20	0.14

**Table 3.6.2. Isotopic composition variation (EOC-BOC) (2.5% MA core, inner core)**

(Δ kg)

Isotope	JAERI	CEA	JNC	MITSUBISHI	TOSHIBA	IPPE
<sup>238</sup> Pu	50.58	56.5	55.2	51.9	50.98	43.61
<sup>239</sup> Pu	115.76	111.3	112.1	115	113.53	98.53
<sup>240</sup> Pu	36.29	53.18	34.7	33	32.13	41.35
<sup>241</sup> Pu	-86.96	-89.34	-85.5	-84.5	-85.1	-81.18
<sup>242</sup> Pu	2.05	-9.61	-5.8	2.7	2.41	0.99
<sup>235</sup> U	-17.52	-17.34	-17.2	-16.8	-16.99	-16.26
<sup>236</sup> U	–	3.841	–	–	–	–
<sup>238</sup> U	-1 030.55	-999.3	-995.5	-960	-972.42	-979.39
<sup>237</sup> Np	-74.43	-67.21	-72.6	-71	-71.64	-64.94
<sup>239</sup> Np	–	3.917	–	–	–	–
<sup>241</sup> Am	-53.80	-55.79	-51.9	-49.4	-50.11	-49.20
<sup>242m</sup> Am	8.14	8.412	8.1	6.4	8.05	5.35
<sup>243</sup> Am	0.68	3.601	0.8	1.2	1.26	3.79
<sup>242</sup> Cm	–	13.96	–	–	–	–
<sup>243</sup> Cm	0.62	0.8097	0.8	0.6	0.60	0.62
<sup>244</sup> Cm	11.05	12.29	10.8	10.4	10.61	6.91
<sup>245</sup> Cm	2.02	1.587	2	1.9	1.91	1.12



**Table 3.6.3. Isotopic composition variation (EOC-BOC) (5% MA core, inner core)**

(Δ kg)

Isotope	JAERI	CEA	JNC	MITSUBISHI	TOSHIBA	IPPE
<sup>238</sup> Pu	113.92	121.5	121.2	114	113.26	98.15
<sup>239</sup> Pu	98.49	94.96	94.2	98	96.86	84.38
<sup>240</sup> Pu	30.51	46.77	30	27.3	25.67	35.88
<sup>241</sup> Pu	-86.01	-87.96	-84.3	-83.4	-84.22	-80.16
<sup>242</sup> Pu	7.33	-9.612	-5.8	8	7.48	6.08
<sup>235</sup> U	-16.45	-16.28	-16.1	-15.7	-15.99	-15.27
<sup>236</sup> U	–	3.599	–	–	–	–
<sup>238</sup> U	-963.68	-933.2	-928.5	-890	-917.08	-918.38
<sup>237</sup> Np	-146.16	-133.7	-142.6	-138.7	-140.84	-127.80
<sup>239</sup> Np	–	3.64	–	–	–	–
<sup>241</sup> Am	-103.95	-107.7	-101	-96.1	-97.99	-96.05
<sup>242m</sup> Am	13.52	14.08	13.4	10.5	13.37	8.92
<sup>243</sup> Am	-14.67	11.88	-14	-13	-13.08	-7.10
<sup>242</sup> Cm	–	23.02	–	–	–	–
<sup>243</sup> Cm	0.93	1.231	1.2	0.9	0.89	0.93
<sup>244</sup> Cm	17.81	19.49	17.5	16.9	17.24	10.71
<sup>245</sup> Cm	3.58	2.784	3.5	3.3	3.41	1.98

**Table 3.7.1. Sodium reactivity worth at the beginning of the fourth cycle (BOC)**

(reference core, sodium void whole core)

(Δk/kk')

Component	JAERI	CEA	JNC	MITSUBISHI	TOSHIBA	IPPE
<b>Axial leak</b>	-0.689%	-0.696%	-0.68%	-0.671%	-0.659%	-0.669%
<b>Radial leak</b>	-0.335%	-0.328%	-0.34%	-0.318%	-0.319%	-0.340%
<b>Scattering</b>	3.068%	2.888%	3.05%	2.969%	3.012%	1.998%
<b>Absorption</b>	0.453%	0.424%	0.45%	0.438%	0.429%	1.231%
<b>Production</b>	-0.030%	-0.024%	3.47%	3.407%	-0.023%	-0.206%
<b>Total</b>	2.466%	2.264%	2.45%	2.418%	2.440%	2.014%

**Table 3.7.2. Sodium reactivity worth at the beginning of the fourth cycle (BOC)**

(2.5% MA core, sodium void whole core)

(Δk/kk')

Component	JAERI	CEA	JNC	MITSUBISHI	TOSHIBA	IPPE
<b>Axial leak</b>	-0.673%	-0.677%	-0.67%	-0.665%	-0.647%	-0.654%
<b>Radial leak</b>	-0.331%	-0.323%	-0.34%	-0.318%	-0.316%	-0.337%
<b>Scattering</b>	3.472%	3.335%	3.46%	3.348%	3.426%	3.065%
<b>Absorption</b>	0.381%	0.355%	0.38%	0.458%	0.363%	0.519%
<b>Production</b>	-0.026%	-0.021%	3.82%	3.906%	-0.019%	-0.228%
<b>Total</b>	2.824%	2.669%	2.82%	2.823%	2.806%	2.364%

**Table 3.7.3. Sodium reactivity worth at the beginning of the fourth cycle (BOC)**  
(5% MA core, sodium void whole core)

( $\Delta k/kk'$ )

Component	JAERI	CEA	JNC	mitsubishi	TOSHIBA	IPPE
<b>Axial leak</b>	-0.657%	-0.659%	-0.65%	-0.644%	-0.636%	-0.638%
<b>Radial leak</b>	-0.324%	-0.315%	-0.33%	-0.310%	-0.311%	-0.331%
<b>Scattering</b>	3.815%	3.728%	3.81%	3.669%	3.785%	3.452%
<b>Absorption</b>	0.322%	0.297%	0.32%	0.371%	0.310%	0.433%
<b>Production</b>	-0.022%	-0.018%	4.11%	4.040%	-0.017%	-0.250%
<b>Total</b>	3.135%	3.033%	3.13%	3.085%	3.131%	2.666%

**Table 3.8.1. Doppler reactivity worth at the fourth cycle (reference core)**

(% $\Delta k/kk'$ )

	JAERI	CEA	JNC	mitsubishi	TOSHIBA	IPPE
<b>BOC</b>	-2.40E-01	-2.57E-01	-2.53E-01	-2.58E-01	-2.61E-01	-2.50E-01
<b>EOC</b>	-2.26E-01	-2.46E-01	-2.36E-01	-2.39E-01	-2.44E-01	-2.31E-01

**Table 3.8.2. Doppler reactivity worth at the fourth cycle (2.5% MA core)**

(% $\Delta k/kk'$ )

	JAERI	CEA	JNC	mitsubishi	TOSHIBA	IPPE
<b>BOC</b>	-1.90E-01	-2.07E-01	-2.01E-01	-2.05E-01	-2.09E-01	-2.00E-01
<b>EOC</b>	-1.83E-01	-2.02E-01	-1.91E-01	-1.95E-01	-1.99E-01	-1.90E-01

**Table 3.8.3. Doppler reactivity worth at the fourth cycle (5% MA core)**

(% $\Delta k/kk'$ )

	JAERI	CEA	JNC	mitsubishi	TOSHIBA	IPPE
<b>BOC</b>	-1.52E-01	-1.67E-01	-1.59E-01	-1.63E-01	-1.67E-01	-1.61E-01
<b>EOC</b>	-1.49E-01	-1.66E-01	-1.56E-01	-1.59E-01	-1.63E-01	-1.56E-01

**Table 3.9.1. Decay heat at different cooling times (reference core, inner core)**

(Unit: watt)

Time	JAERI	CEA	JNC	mitsubishi	TOSHIBA	IPPE
<b>0 sec</b>	4.972E+05	4.596E+05	3.96E+05			
<b>1 day</b>	5.034E+04	4.515E+04	4.47E+04			
<b>1 month</b>	1.193E+04	1.202E+04	1.33E+04			
<b>3 months</b>	7.100E+03	7.381E+03	8.43E+03			
<b>1 year</b>	3.012E+03	2.811E+03				

**Table 3.9.2. Decay heat at different cooling times (2.5% MA core, inner core)**

(Unit: watt)

Time	JAERI	CEA	JNC	mitsubishi	TOSHIBA	IPPE
<b>0 sec</b>	4.972E+05		3.94E+05			
<b>1 day</b>	5.144E+04		4.85E+04			
<b>1 month</b>	1.279E+04		1.70E+04			
<b>3 months</b>	7.928E+03		1.15E+04			
<b>1 year</b>	3.774E+03					

**Table 3.9.3. Decay heat at different cooling times (5% MA core, inner core)**

(Unit: watt)

Time	JAERI	CEA	JNC	mitsubishi	TOSHIBA	IPPE
0 sec	4.983E+05		3.93E+05			
1 day	5.262E+04		5.25E+04			
1 month	1.365E+04		2.06E+04			
3 months	8.750E+03		1.45E+04			
1 year	4.518E+03					

**Table 3.10.1. Neutron source at different cooling times (reference core, inner core)**

(Unit: n/sec)

Time	JAERI	CEA	JNC	mitsubishi	TOSHIBA	IPPE
0 sec	8.855E+08	8.321E+08	1.03E+09			
1 day	8.849E+08	8.317E+08	1.03E+09			
1 month	8.325E+08	7.703E+08	9.66E+08			
3 months	7.409E+08	6.628E+08	8.60E+08			
1 year	5.179E+08	4.040E+08				

**Table 3.10.2. Neutron source at different cooling times (2.5% MA core, inner core)**

(Unit: n/sec)

Time	JAERI	CEA	JNC	mitsubishi	TOSHIBA	IPPE
0 sec	3.277E+09		3.03E+09			
1 day	3.274E+09		3.02E+09			
1 month	3.123E+09		2.87E+09			
3 months	2.859E+09		2.60E+09			
1 year	2.203E+09					

**Table 3.10.3. Neutron source at different cooling times (5% MA core, inner core)**

(Unit: n/sec)

Time	JAERI	CEA	JNC	mitsubishi	TOSHIBA	IPPE
0 sec	5.579E+09		5.02E+09			
1 day	5.576E+09		5.01E+09			
1 month	5.330E+09		4.77E+09			
3 months	4.901E+09		4.34E+09			
1 year	3.834E+09					

**Table 3.11. Transmutation rate of MA\***

(%)

MA content	JAERI	CEA	JNC	mitsubishi	TOSHIBA	IPPE
2.5%	30.1	27.5	29.3	28.9	28.0	27.6
5.0%	33.8	30.1	33.0	32.5	31.8	30.9

Definition of transmutation rate:  $\text{Transmutation rate} = \frac{(\text{Loaded mass of MA at BOC}) - (\text{Discharged mass of MA at EOC})}{(\text{Loaded mass of MA at BOC})}$

**Table 4.1. Specification of target/core transmutation system**

<b>Proton beam</b>	1.0 GeV, 10 mA
Beam radius	15 cm
Beam profile	Uniform
<b>Beam duct radius</b>	15 cm
<b>Target/core</b>	Concentric cylinders with height of 1 m
Radii	15 cm/40 cm
<b>Target</b>	Tungsten (disk layer type)
Upper region	Height 80 cm, radius 15 cm
Lower region	Height 26 cm, disk thickness 1.5 cm
<b>Fuel</b>	(90 MA-10 Pu)N (nitride pin-bundle type)
Pin outside diameter	7.3 cm
Pin pitch	9.9 cm
Pin height	80 cm
Fuel pellet diameter	6 cm
Sodium bond thickness	0.35 mm
Cladding thickness	0.3 mm (HT9 SS)
<b>Reflector</b>	Stainless steel
Inner/outer radii	40 cm/90 cm
Top thickness	30 cm
Bottom thickness	40 cm
<b>Sodium volume fraction</b>	
Target upper region	86%
Target lower region	37.2%
Core	61.7%
Reflector	41.3%

**Table 4.2. Actinide atom per cent fraction**

<b>Fuel burn-up</b>	<b>MOX11 33 GWd/tHM</b>	<b>MOX21 50 GWd/tHM</b>	<b>MOX12 33 GWd/tHM</b>	<b>MOX22 50 GWd/tHM</b>
<b>Nuclide atom %</b>				
<sup>238</sup> Pu	1.5	2.7	2.6	4.1
<sup>239</sup> Pu	59.3	55.3	44.5	41.9
<sup>240</sup> Pu	23.7	23.9	31.0	30.5
<sup>241</sup> Pu	8.7	9.5	10.7	10.6
<sup>242</sup> Pu	5.5	7.1	9.5	11.3
<sup>241</sup> Am	1.3	1.5	1.7	1.7
<b>Total</b>	<b>100</b>	<b>100</b>	<b>100</b>	<b>100</b>
<sup>237</sup> Np	44.6	46.4	4.5	4.4
<sup>241</sup> Am	43.6	37.1	62.5	58.3
<sup>243</sup> Am	9.7	12.7	24.3	26.1
<sup>243</sup> Cm	–	–	–	–
<sup>244</sup> Cm	2.1	3.8	8.7	11.3
<sup>245</sup> Cm	–	–	–	–
<b>Total</b>	<b>100</b>	<b>100</b>	<b>100</b>	<b>100</b>

**Table 4.3. Homogenised atomic number densities ( $\times 10^{24}/\text{cm}^3$ )**

Nuclide	TARGET	
	Upper region	Lower region
$^{182}\text{W}$	2.688E-03	1.075E-02
$^{183}\text{W}$	1.453E-03	5.814E-03
$^{184}\text{W}$	3.103E-03	1.241E-02
$^{186}\text{W}$	2.859E-03	1.144E-02
$^{23}\text{Na}$	1.821E-02	7.806E-03

Nuclide	FUEL			
	MOX11 33 GWd/tHM	MOX21 50 GWd/tHM	MOX12 33 GWd/tHM	MOX22 50 GWd/tHM
$^{238}\text{Pu}$	1.251E-05	2.252E-05	2.169E-05	3.420E-05
$^{239}\text{Pu}$	4.947E-04	4.613E-04	3.712E-04	3.495E-04
$^{240}\text{Pu}$	1.977E-04	1.994E-04	2.586E-04	2.544E-04
$^{241}\text{Pu}$	7.257E-05	7.924E-05	8.925E-05	8.842E-05
$^{242}\text{Pu}$	4.588E-05	5.922E-05	7.924E-05	9.426E-05
$^{241}\text{Am}$	1.084E-05	1.251E-05	1.418E-05	1.418E-05
$^{237}\text{Np}$	3.353E-03	3.488E-03	3.383E-04	3.308E-04
$^{241}\text{Am}$	3.278E-03	2.789E-03	4.699E-03	4.375E-03
$^{243}\text{Am}$	7.293E-04	9.548E-04	1.827E-03	1.962E-03
$^{244}\text{Cm}$	1.579E-04	2.857E-04	6.541E-04	8.495E-04
$^{15}\text{N}$	8.352E-03			
$^{23}\text{Na}$	1.296E-02			
$^{182}\text{W}$	2.735E-06			
$^{183}\text{W}$	1.555E-06			
$^{184}\text{W}$	3.092E-06			
$^{186}\text{W}$	2.868E-06			
$^{12}\text{C}$	5.626E-05			
$^{\text{nat}}\text{Si}$	3.671E-05			
$^{51}\text{V}$	2.094E-05			
$^{\text{nat}}\text{Cr}$	8.206E-04			
$^{55}\text{Mn}$	3.107E-05			
$^{\text{nat}}\text{Fe}$	5.391E-03			
$^{\text{nat}}\text{Ni}$	3.029E-05			
$^{\text{nat}}\text{Mo}$	3.781E-05			

Nuclide	REFLECTOR
$^{23}\text{Na}$	8.673E-03
$^{\text{nat}}\text{Cr}$	8.599E-03
$^{55}\text{Mn}$	5.061E-04
$^{\text{nat}}\text{Fe}$	3.424E-02
$^{\text{nat}}\text{Ni}$	6.000E-03
$^{\text{nat}}\text{Mo}$	1.265E-03

**Table 4.4. Normalised spallation neutron spectrum from the target**

Energy boundary (eV)	Source	Lethargy width
2.0000E+07 to 1.6487E+07	1.56%	0.19
1.6487E+07 to 1.2840E+07	2.47%	0.25
1.2840E+07 to 1.0000E+07	3.23%	0.25
1.0000E+07 to 7.7880E+06	4.27%	0.25
7.7880E+06 to 6.0653E+06	5.62%	0.25
6.0653E+06 to 4.7237E+06	7.01%	0.25
4.7237E+06 to 3.6788E+06	8.26%	0.25
3.6788E+06 to 2.8650E+06	9.06%	0.25
2.8650E+06 to 2.2313E+06	9.36%	0.25
2.2313E+06 to 1.7377E+06	9.15%	0.25
1.7377E+06 to 1.3534E+06	8.48%	0.25
1.3534E+06 to 1.0540E+06	7.50%	0.25
1.0540E+06 to 8.2085E+05	5.99%	0.25
8.2085E+05 to 6.3928E+05	4.79%	0.25
6.3928E+05 to 4.9787E+05	3.81%	0.25
4.9787E+05 to 3.8774E+05	2.93%	0.25
3.8774E+05 to 3.0197E+05	2.20%	0.25
3.0197E+05 to 2.3518E+05	1.63%	0.25
2.3518E+05 to 1.8316E+05	1.18%	0.25
1.8316E+05 to 1.4264E+05	0.88%	0.25
1.4264E+05 to 1.1109E+05	0.61%	0.25

**Table 4.5. Number of spallation neutrons per incident proton (n/p)**

JAERI	PSI	IPPE
25.54	23.18	24.596

**Table 4.6. Maximum and average heat power densities in target region**

Parameters	Thin disk part			Thick disk part		
	JAERI	PSI	IPPE	JAERI	PSI	IPPE
Max. (W/cc/10 mA)	99.0	309	131	255.1	692	378
Av. (W/cc/10 mA)	86.2	130	89.9	98.1	92	83.4

**Table 4.7. Nuclear characteristics results**

Parameters	MOX11			MOX12		
	JAERI	PSI	IPPE	JAERI	PSI	IPPE
$k_{eff}$	0.8993	0.8966	0.9308	0.9180	0.9205	0.9533
Sodium void reactivity (% $\Delta k/kk'$ )	7.16	7.31	4.65	7.30	7.44	4.99
Average neutron energy (MeV)	0.827	0.828	–	0.809	0.838	–
Average neutron flux ( $10^{15}$ n/cm <sup>2</sup> /s/10 mA)	2.39	1.58	–	2.92	1.99	–
Maximum heat power density ( $10^{-4}$ W/cc/10 mA)	6.03	4.72	–	6.66	5.42	–
Average heat power density ( $10^{-4}$ W/cc/10 mA)	3.73	2.75	–	4.22	3.31	–

**Table 4.8. Fission and capture rate (initial core)**

MOX11	Fission			Capture		
	JAERI	PSI	IPPE	JAERI	PSI	IPPE
<sup>237</sup> Np	0.3699	0.3707	0.3671	0.4151	0.3616	0.3966
<sup>238</sup> Pu	0.0037	0.0032	0.003	0.0006	0.0005	0.0006
<sup>239</sup> Pu	0.1599	0.1639	0.1519	0.017	0.0153	0.0176
<sup>240</sup> Pu	0.0223	0.0238	0.0217	0.009	0.0076	0.0089
<sup>241</sup> Pu	0.0279	0.0278	0.0262	0.003	0.0037	0.0025
<sup>242</sup> Pu	0.0037	0.0043	0.0039	0.0018	0.0015	0.0017
<sup>241</sup> Am	0.3346	0.3256	0.3441	0.4484	0.5029	0.499
<sup>243</sup> Am	0.0576	0.0583	0.0615	0.0889	0.0902	0.0541
<sup>244</sup> Cm	0.0223	0.0221	0.0206	0.0088	0.0071	0.008
Structural material	0	0	0	0.0076	0.0097	0.011
MOX12	Fission			Capture		
	JAERI	PSI	IPPE	JAERI	PSI	IPPE
<sup>237</sup> Np	0.0395	0.0398	0.0385	0.0429	0.0348	0.0421
<sup>238</sup> Pu	0.0066	0.0059	0.0055	0.0011	0.0008	0.001
<sup>239</sup> Pu	0.1301	0.1286	0.1206	0.0131	0.011	0.0138
<sup>240</sup> Pu	0.0313	0.0331	0.0296	0.012	0.0094	0.012
<sup>241</sup> Pu	0.0379	0.0355	0.0342	0.0038	0.0044	0.0032
<sup>242</sup> Pu	0.0082	0.0079	0.0071	0.003	0.0024	0.0031
<sup>241</sup> Am	0.5041	0.4962	0.5148	0.6541	0.6858	0.7387
<sup>243</sup> Am	0.1499	0.1554	0.1609	0.226	0.2145	0.1408
<sup>244</sup> Cm	0.0939	0.0976	0.0889	0.0363	0.0277	0.0338
Structural material	0	0	0	0.0077	0.0092	0.0115

**Table 4.9. Fission and capture rate (200 GWd/tHM burn-up)**

MOX11	Fission		Capture	
	JAERI	PSI	JAERI	PSI
<sup>237</sup> Np	0.2202	0.2354	0.3284	0.3104
<sup>238</sup> Np	0.0020	0.0063	0.0003	0.0002
<sup>238</sup> Pu	0.2352	0.2096	0.0605	0.0392
<sup>239</sup> Pu	0.1038	0.1015	0.0140	0.0121
<sup>240</sup> Pu	0.0213	0.0219	0.0111	0.0093
<sup>241</sup> Pu	0.0189	0.0180	0.0025	0.0029
<sup>242</sup> Pu	0.0140	0.0161	0.0077	0.0075
<sup>241</sup> Am	0.1898	0.1859	0.3483	0.3847
<sup>242</sup> Am	0.0007	0.0021	0.0001	0.0003
<sup>242m</sup> Am	0.0581	0.0551	0.0073	0.0061
<sup>243</sup> Am	0.0360	0.0380	0.0783	0.0798
<sup>242</sup> Cm	0.0474	0.0577	0.0125	0.0167
<sup>243</sup> Cm	0.0067	0.0063	0.0006	0.0003
<sup>244</sup> Cm	0.0355	0.0368	0.0195	0.0156
<sup>245</sup> Cm	0.0104	0.0084	0.0010	0.0007
Fission products	0	0	0.0976	0.1051
Structural material	0	0	0.0088	0.0090

**Table 4.10. PSI results (MOX11)**

Nuclide	Burn-up (GWd/tHM)					
	0	10	50	100	150	200
k <sub>eff</sub>	8.966E-01	9.025E-01	9.112E-01	9.171E-01	9.183E-01	9.149E-01
<sup>234</sup> U	0.000E00	1.193E-08	2.329E-07	8.545E-07	1.754E-06	2.820E-06
<sup>235</sup> U	0.000E00	7.536E-10	6.296E-09	2.684E-08	6.944E-08	1.360E-07
<sup>236</sup> U	0.000E00	4.187E-08	1.972E-07	3.682E-07	5.188E-07	6.529E-07
<sup>237</sup> Np	3.353E-03	3.280E-03	3.001E-03	2.683E-03	2.392E-03	2.124E-03
<sup>238</sup> Np	0.000E00	1.049E-05	1.245E-05	1.222E-05	1.180E-05	1.139E-05
<sup>236</sup> Pu	0.000E00	2.676E-08	1.185E-07	2.062E-07	2.719E-07	3.211E-07
<sup>238</sup> Pu	1.251E-05	4.583E-05	2.220E-04	4.330E-04	6.190E-04	7.764E-04
<sup>239</sup> Pu	4.947E-04	4.796E-04	4.257E-04	3.699E-04	3.239E-04	2.854E-04
<sup>240</sup> Pu	1.977E-04	1.970E-04	1.940E-04	1.897E-04	1.851E-04	1.802E-04
<sup>241</sup> Pu	7.257E-05	7.058E-05	6.333E-05	5.554E-05	4.884E-05	4.297E-05
<sup>242</sup> Pu	4.588E-05	5.399E-05	8.637E-05	1.206E-04	1.491E-04	1.728E-04
<sup>241</sup> Am	3.289E-03	3.202E-03	2.877E-03	2.512E-03	2.184E-03	1.887E-03
<sup>242</sup> Am	0.000E00	4.633E-06	4.745E-06	4.518E-06	4.297E-06	4.097E-06
<sup>242m</sup> Am	0.000E00	9.412E-06	4.109E-05	7.038E-05	9.144E-05	1.064E-04
<sup>243</sup> Am	7.293E-04	7.139E-04	6.563E-04	5.914E-04	5.328E-04	4.791E-04
<sup>242</sup> Cm	0.000E00	3.578E-05	1.541E-04	2.447E-04	2.991E-04	3.322E-04
<sup>243</sup> Cm	0.000E00	7.891E-08	1.459E-06	4.139E-06	6.912E-06	9.447E-06
<sup>244</sup> Cm	1.579E-04	1.656E-04	1.930E-04	2.208E-04	2.429E-04	2.603E-04
<sup>245</sup> Cm	0.000E00	8.639E-07	4.325E-06	8.542E-06	1.253E-05	1.623E-05
<sup>246</sup> Cm	0.000E00	1.547E-09	3.785E-08	1.464E-07	3.176E-07	5.444E-07



**Table 4.11. PSI results (MOX12)**

Nuclide	Burn-up (GWd/tHM)					
	0	10	50	100	150	200
$k_{eff}$	0.92054	0.92494	0.9312	0.93538	0.93518	0.93069
$^{234}\text{U}$	0.00E+00	1.04E-08	1.09E-07	4.14E-07	9.03E-07	1.52E-06
$^{235}\text{U}$	0.00E+00	5.97E-10	4.01E-09	1.50E-08	3.87E-08	7.73E-08
$^{236}\text{U}$	0.00E+00	5.48E-09	2.60E-08	4.92E-08	7.04E-08	9.06E-08
$^{237}\text{Np}$	3.38E-04	3.31E-04	3.03E-04	2.71E-04	2.41E-04	2.14E-04
$^{238}\text{Np}$	0.00E+00	1.06E-06	1.25E-06	1.22E-06	1.18E-06	1.14E-06
$^{236}\text{Pu}$	0.00E+00	2.61E-09	1.15E-08	2.00E-08	2.62E-08	3.09E-08
$^{238}\text{Pu}$	2.17E-05	2.68E-05	8.30E-05	1.84E-04	2.89E-04	3.85E-04
$^{239}\text{Pu}$	3.71E-04	3.59E-04	3.16E-04	2.71E-04	2.33E-04	2.01E-04
$^{240}\text{Pu}$	2.59E-04	2.57E-04	2.53E-04	2.47E-04	2.42E-04	2.36E-04
$^{241}\text{Pu}$	8.93E-05	8.67E-05	7.77E-05	6.80E-05	5.97E-05	5.25E-05
$^{242}\text{Pu}$	7.92E-05	9.11E-05	1.38E-04	1.87E-04	2.27E-04	2.60E-04
$^{241}\text{Am}$	4.71E-03	4.58E-03	4.10E-03	3.55E-03	3.07E-03	2.63E-03
$^{242}\text{Am}$	0.00E+00	6.58E-06	6.69E-06	6.35E-06	6.02E-06	5.73E-06
$^{242m}\text{Am}$	0.00E+00	1.40E-05	6.06E-05	1.03E-04	1.33E-04	1.54E-04
$^{243}\text{Am}$	1.83E-03	1.79E-03	1.63E-03	1.46E-03	1.31E-03	1.17E-03
$^{242}\text{Cm}$	0.00E+00	5.32E-05	2.26E-04	3.55E-04	4.31E-04	4.76E-04
$^{243}\text{Cm}$	0.00E+00	1.35E-07	2.27E-06	6.27E-06	1.03E-05	1.39E-05
$^{244}\text{Cm}$	6.54E-04	6.69E-04	7.19E-04	7.66E-04	7.99E-04	8.22E-04
$^{245}\text{Cm}$	0.00E+00	3.61E-06	1.72E-05	3.25E-05	4.59E-05	5.76E-05
$^{246}\text{Cm}$	0.00E+00	6.76E-09	1.57E-07	5.79E-07	1.21E-06	2.00E-06

**Table 4.12. JAERI results (MOX11)**

MOX11 (Unit: atoms/barn-cm)

Nuclide	Burn-up (GWd/tHM)					
	0	10	50	100	150	200
$k_{eff}$	0.8993	0.9027	0.9392	0.9099	0.9126	0.8974
$^{237}\text{Np}$	3.353E-03	3.265E-03	2.936E-03	2.568E-03	2.240E-03	1.943E-03
$^{238}\text{Np}$	0.000E+00	7.923E-06	7.105E-06	6.311E-06	5.687E-06	5.173E-06
$^{238}\text{Pu}$	1.251E-05	5.768E-05	2.648E-04	5.001E-04	6.963E-04	8.492E-04
$^{239}\text{Pu}$	4.947E-04	4.777E-04	4.190E-04	3.627E-04	3.218E-04	2.926E-04
$^{240}\text{Pu}$	1.977E-04	1.968E-04	1.930E-04	1.876E-04	1.819E-04	1.760E-04
$^{241}\text{Pu}$	7.257E-05	7.053E-05	6.320E-05	5.557E-05	4.929E-05	4.406E-05
$^{242}\text{Pu}$	4.588E-05	5.298E-05	7.971E-05	1.074E-04	1.298E-04	1.477E-04
$^{241}\text{Am}$	3.289E-03	3.200E-03	2.870E-03	2.502E-03	2.174E-03	1.880E-03
$^{242}\text{Am}$	0.000E+00	2.155E-06	1.930E-06	1.707E-06	1.531E-06	1.386E-06
$^{243}\text{Am}$	7.293E-04	7.129E-04	6.522E-04	5.847E-04	5.248E-04	4.708E-04
$^{244}\text{Am}$	0.000E+00	1.692E-08	1.547E-08	1.408E-08	1.305E-08	1.226E-08
$^{242m}\text{Am}$	0.000E+00	1.114E-05	4.753E-05	7.876E-05	9.814E-05	1.087E-04
$^{244m}\text{Am}$	0.000E+00	1.382E-08	1.264E-08	1.150E-08	1.066E-08	1.001E-08
$^{242}\text{Cm}$	0.000E+00	3.425E-05	1.362E-04	2.006E-04	2.253E-04	2.290E-04
$^{243}\text{Cm}$	0.000E+00	8.193E-08	1.726E-06	5.262E-06	9.096E-06	1.255E-05
$^{244}\text{Cm}$	1.579E-04	1.657E-04	1.927E-04	2.192E-04	2.391E-04	2.539E-04
$^{245}\text{Cm}$	0.000E+00	1.139E-06	5.706E-06	1.138E-05	1.686E-05	2.209E-05
$^{246}\text{Cm}$	0.000E+00	2.356E-09	5.788E-08	2.290E-07	5.105E-07	9.024E-07
$^{247}\text{Cm}$	0.000E+00	2.520E-12	2.973E-10	2.276E-09	7.429E-09	1.721E-08
$^{248}\text{Cm}$	0.000E+00	3.604E-15	2.120E-12	3.266E-11	1.618E-10	5.090E-10
$^{249}\text{Cm}$	0.000E+00	3.066E-20	1.806E-17	2.837E-16	1.459E-15	4.827E-15
$^{249}\text{Bk}$	0.000E+00	1.900E-18	5.410E-15	1.626E-13	1.189E-12	4.943E-12
$^{250}\text{Bk}$	0.000E+00	2.215E-22	6.307E-19	1.929E-17	1.462E-16	6.387E-16
$^{249}\text{Cf}$	0.000E+00	1.370E-20	1.921E-16	1.129E-14	1.198E-13	6.383E-13
$^{250}\text{Cf}$	0.000E+00	3.844E-21	5.526E-17	3.404E-15	3.840E-14	2.198E-13
$^{251}\text{Cf}$	0.000E+00	3.609E-24	2.462E-19	2.993E-17	5.040E-16	3.849E-15
$^{252}\text{Cf}$	0.000E+00	1.282E-27	4.300E-22	1.044E-19	2.649E-18	2.729E-17
$^{238}\text{U}$ (FP)	0.000E+00	3.630E-05	1.853E-04	3.819E-04	5.893E-04	8.062E-04
$^{239}\text{Pu}$ (FP)	0.000E+00	1.731E-05	8.210E-05	1.564E-04	2.268E-04	2.964E-04
$^{241}\text{Pu}$ (FP)	0.000E+00	4.236E-05	2.114E-04	4.185E-04	6.168E-04	8.049E-04

FP – fission product

**Table 4.13. JAERI results (MOX12)**

MOX12 (Unit: atoms/barn-cm)

Nuclide	Burn-up (GWd/tHM)					
	0	10	50	100	150	200
$k_{eff}$	0.9180	0.9215	0.9293	0.9317	0.9260	0.9126
$^{237}\text{Np}$	3.383E-04	3.289E-04	2.941E-04	2.555E-04	2.213E-04	1.907E-04
$^{238}\text{Np}$	0.000E+00	8.181E-07	7.285E-07	6.404E-07	5.712E-07	5.149E-07
$^{238}\text{Pu}$	2.169E-05	2.841E-05	9.453E-05	2.148E-04	3.371E-04	4.414E-04
$^{239}\text{Pu}$	3.712E-04	3.573E-04	3.080E-04	2.592E-04	2.228E-04	1.962E-04
$^{240}\text{Pu}$	2.586E-04	2.572E-04	2.514E-04	2.442E-04	2.370E-04	2.295E-04
$^{241}\text{Pu}$	8.925E-05	8.662E-05	7.727E-05	6.773E-05	6.002E-05	5.373E-05
$^{242}\text{Pu}$	7.924E-05	9.024E-05	1.311E-04	1.724E-04	2.049E-04	2.300E-04
$^{241}\text{Am}$	4.713E-03	4.575E-03	4.065E-03	3.503E-03	3.010E-03	2.573E-03
$^{242}\text{Am}$	0.000E+00	3.134E-06	2.777E-06	2.419E-06	2.138E-06	1.910E-06
$^{253}\text{Am}$	1.827E-03	1.782E-03	1.616E-03	1.432E-03	1.269E-03	1.122E-03
$^{244}\text{Am}$	0.000E+00	4.291E-08	3.886E-08	3.482E-08	3.174E-08	2.934E-08
$^{242m}\text{Am}$	0.000E+00	1.755E-05	7.384E-05	1.201E-04	1.470E-04	1.600E-04
$^{244m}\text{Am}$	0.000E+00	3.504E-08	3.174E-08	2.844E-08	2.592E-08	2.397E-08
$^{242}\text{Cm}$	0.000E+00	5.404E-05	2.097E-04	3.004E-04	3.292E-04	3.274E-04
$^{243}\text{Cm}$	0.000E+00	1.436E-07	2.949E-06	8.728E-06	1.469E-05	1.977E-05
$^{244}\text{Cm}$	6.541E-04	6.697E-04	7.213E-04	7.664E-04	7.945E-04	8.090E-04
$^{245}\text{Cm}$	0.000E+00	5.029E-06	2.391E-05	4.497E-05	6.342E-05	7.942E-05
$^{246}\text{Cm}$	0.000E+00	1.150E-08	2.723E-07	1.028E-06	2.200E-06	3.746E-06
$^{247}\text{Cm}$	0.000E+00	1.364E-11	1.560E-09	1.141E-08	3.578E-08	7.978E-08
$^{248}\text{Cm}$	0.000E+00	2.149E-14	1.233E-11	1.821E-10	8.691E-10	2.640E-09
$^{249}\text{Cm}$	0.000E+00	1.860E-19	1.067E-16	1.602E-15	7.908E-15	2.521E-14
$^{249}\text{Bk}$	0.000E+00	1.251E-17	3.476E-14	9.999E-13	7.030E-12	2.817E-11
$^{250}\text{Bk}$	0.000E+00	1.487E-21	4.131E-18	1.206E-16	8.752E-16	3.678E-15
$^{249}\text{Cf}$	0.000E+00	9.782E-20	1.343E-15	7.575E-14	7.753E-13	3.986E-12
$^{250}\text{Cf}$	0.000E+00	2.802E-20	3.949E-16	2.333E-14	2.537E-13	1.402E-12
$^{251}\text{Cf}$	0.000E+00	2.883E-23	1.936E-18	2.255E-16	3.655E-15	2.693E-14
$^{252}\text{Cf}$	0.000E+00	1.133E-26	3.747E-21	8.703E-19	2.125E-17	2.111E-16
$^{238}\text{U}$ (FP)	0.000E+00	4.656E-06	2.984E-05	8.077E-05	1.561E-04	2.555E-04
$^{239}\text{Pu}$ (FP)	0.000E+00	1.529E-05	7.118E-05	1.317E-04	1.852E-04	2.349E-04
$^{241}\text{Pu}$ (FP)	0.000E+00	7.569E-05	3.774E-04	7.438E-04	1.092E-03	1.418E-03

FP – fission product

**Table 4.14. IPPE results (MOX11)**

Burn-up: GWd/tHM, Nuclide: atom/b/cm

Nuclide	Burn-up (GWd/tHM)					
	0	10	50	100	150	200
$k_{eff}$	0.9308	0.9317	0.9391	0.9418	0.9383	0.9299
<sup>238</sup> Pu	1.251E-05	5.225E-05	2.305E-04	4.378E-04	6.123E-04	7.512E-04
<sup>239</sup> Pu	4.947E-04	4.782E-04	4.209E-04	3.656E-04	3.247E-04	2.945E-04
<sup>240</sup> Pu	1.977E-04	1.969E-04	1.933E-04	1.884E-04	1.834E-04	1.784E-04
<sup>241</sup> Pu	7.257E-05	7.060E-05	6.358E-05	5.645E-05	5.073E-05	4.610E-05
<sup>242</sup> Pu	4.588E-05	5.349E-05	8.126E-05	1.093E-04	1.313E-04	1.485E-04
<sup>241</sup> Am	3.289E-03	3.198E-03	2.866E-03	2.509E-03	2.208E-03	1.951E-03
<sup>237</sup> Np	3.353E-03	3.272E-03	2.973E-03	2.648E-03	2.366E-03	2.123E-03
<sup>243</sup> Am	7.293E-04	7.173E-04	6.727E-04	6.235E-04	5.804E-04	5.423E-04
<sup>244</sup> Cm	1.579E-04	1.608E-04	1.706E-04	1.802E-04	1.873E-04	1.928E-04
<sup>242m</sup> Am	0.000E+00	8.953E-06	3.742E-05	6.082E-05	7.481E-05	8.239E-05
<sup>242</sup> Cm	0.000E+00	3.608E-05	1.398E-04	2.036E-04	2.275E-04	2.310E-04
<sup>243</sup> Cm	0.000E+00	7.434E-08	1.495E-06	4.488E-06	7.678E-06	1.053E-05
<sup>245</sup> Cm	0.000E+00	9.213E-07	4.256E-06	7.860E-06	1.093E-05	1.354E-05
Fission product	0.000E+00	0.000E+00	4.032E-04	8.690E-04	1.305E-03	1.712E-03

**Table 4.15. IPPE results (MOX12)**

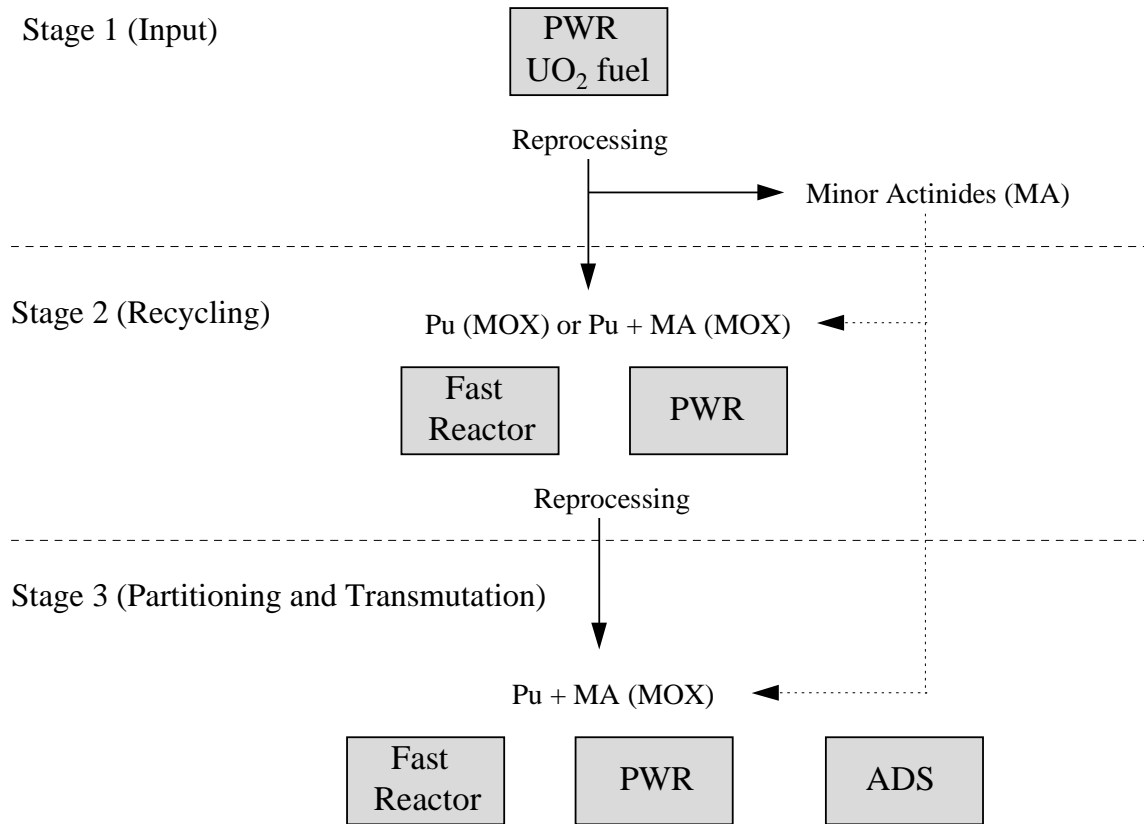
Burn-up: GWd/tHM, Nuclide: atom/b/cm

Nuclide	Burn-up (GWd/tHM)					
	0	10	50	100	150	200
$k_{eff}$	0.9533	0.9537	0.9568	0.9551	0.9481	0.9372
<sup>238</sup> Pu	2.169E-05	2.706E-05	8.117E-05	1.815E-04	2.863E-04	3.810E-04
<sup>239</sup> Pu	3.712E-04	3.592E-04	3.166E-04	2.742E-04	2.417E-04	2.170E-04
<sup>240</sup> Pu	2.586E-04	2.575E-04	2.529E-04	2.470E-04	2.415E-04	2.360E-04
<sup>241</sup> Pu	8.925E-05	8.698E-05	7.891E-05	7.074E-05	6.419E-05	5.889E-05
<sup>242</sup> Pu	7.924E-05	8.973E-05	1.280E-04	1.665E-04	1.966E-04	2.203E-04
<sup>241</sup> Am	4.713E-03	4.586E-03	4.125E-03	3.633E-03	3.216E-03	2.861E-03
<sup>237</sup> Np	3.383E-04	3.307E-04	3.026E-04	2.720E-04	2.456E-04	2.227E-04
<sup>243</sup> Am	1.827E-03	1.798E-03	1.689E-03	1.568E-03	1.462E-03	1.368E-03
<sup>244</sup> Cm	6.541E-04	6.565E-04	6.628E-04	6.668E-04	6.675E-04	6.660E-04
<sup>242m</sup> Am	0.000E+00	1.260E-05	5.271E-05	8.593E-05	1.061E-04	1.176E-04
<sup>242</sup> Cm	0.000E+00	5.076E-05	1.980E-04	2.912E-04	3.286E-04	3.371E-04
<sup>243</sup> Cm	0.000E+00	1.038E-07	2.089E-06	6.284E-06	1.080E-05	1.489E-05
Fission product	0.000E+00	0.000E+00	3.742E-04	8.076E-04	1.211E-03	1.585E-03

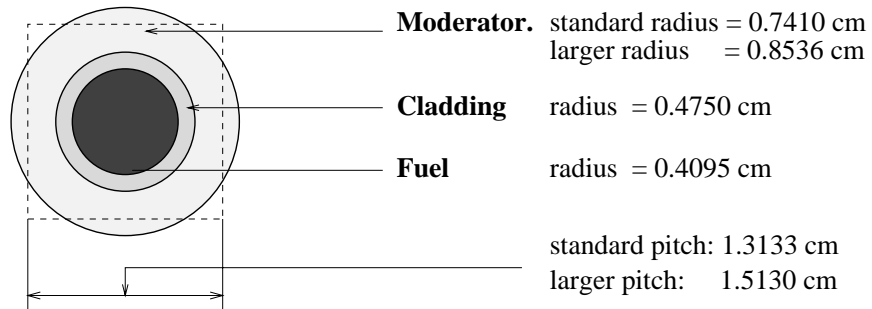
# FIGURES



**Figure 1.1. Schematic fuel cycle scenario for the benchmark proposal**



**Figure 2.1. Benchmark cell geometry**



**Figure 2.2.  $k_{\infty}$  as a function of burn-up for MOX12 (33 GWd/tHM) and MA 0.0%**

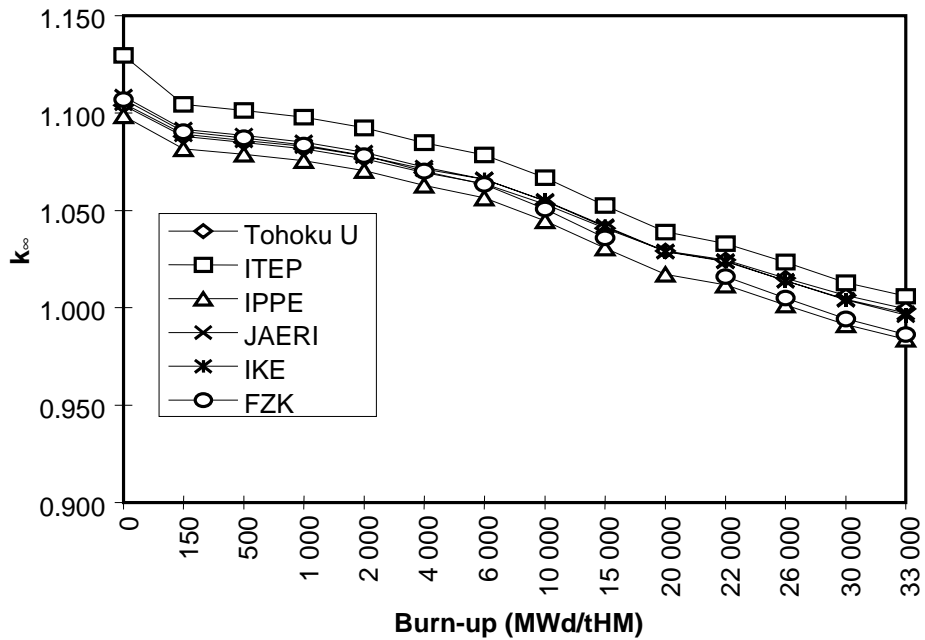




Figure 2.3.  $k_{\infty}$  as a function of burn-up for MOX12 (33 GWd/tHM) and MA 1.0%

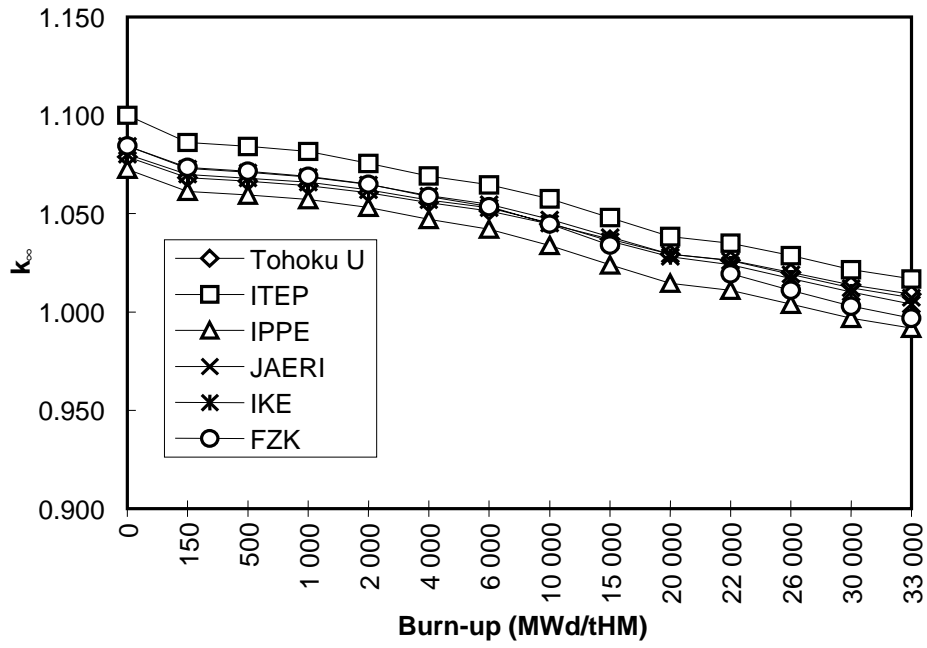


Figure 2.4.  $k_{\infty}$  as a function of burn-up for MOX12 (33 GWd/tHM) and MA 2.5%

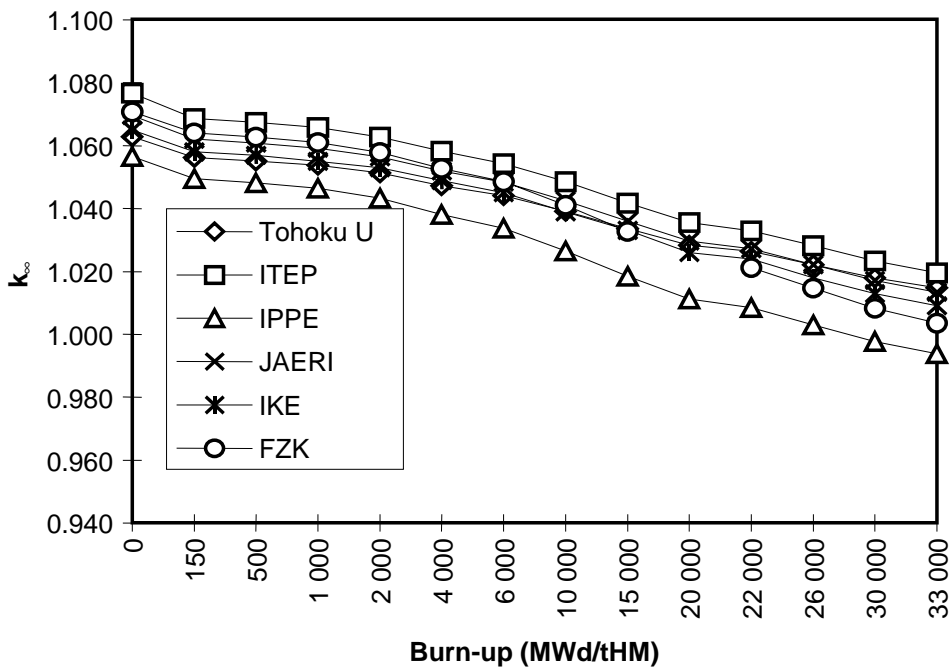


Figure 2.5.  $k_{\infty}$  as a function of burn-up for MOX22 (50 GWd/tHM) and MA 0.0%

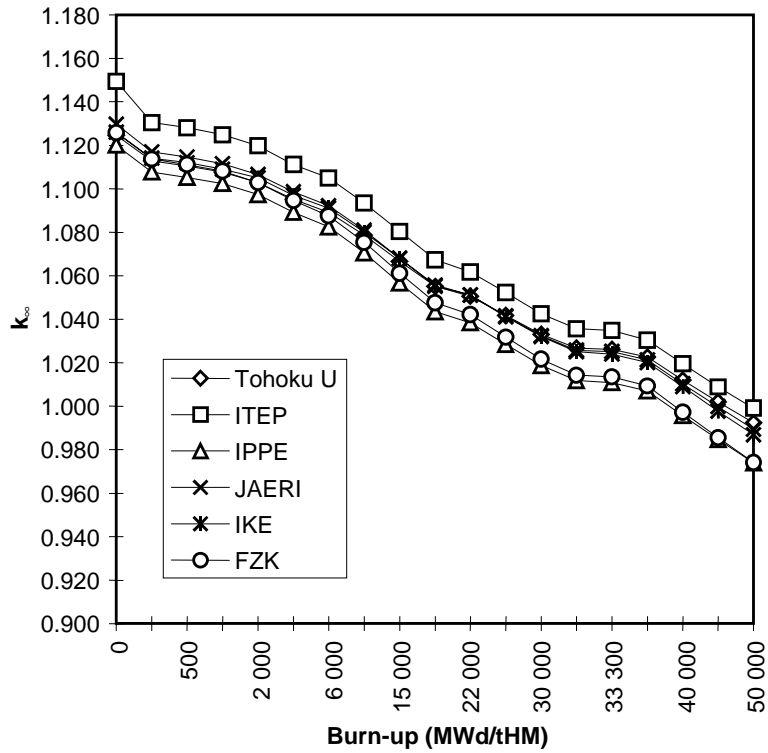


Figure 2.6.  $k_{\infty}$  as a function of burn-up for MOX22 (50 GWd/tHM) and MA 1.0%

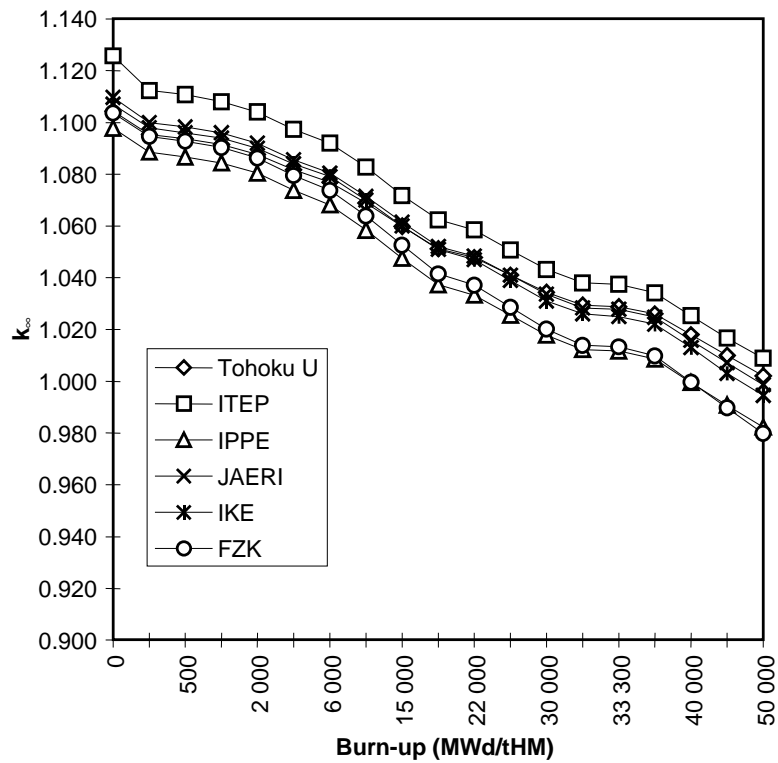


Figure 2.7.  $k_{\infty}$  as a function of burn-up for MOX22 (50 GWd/tHM) and MA 2.5%

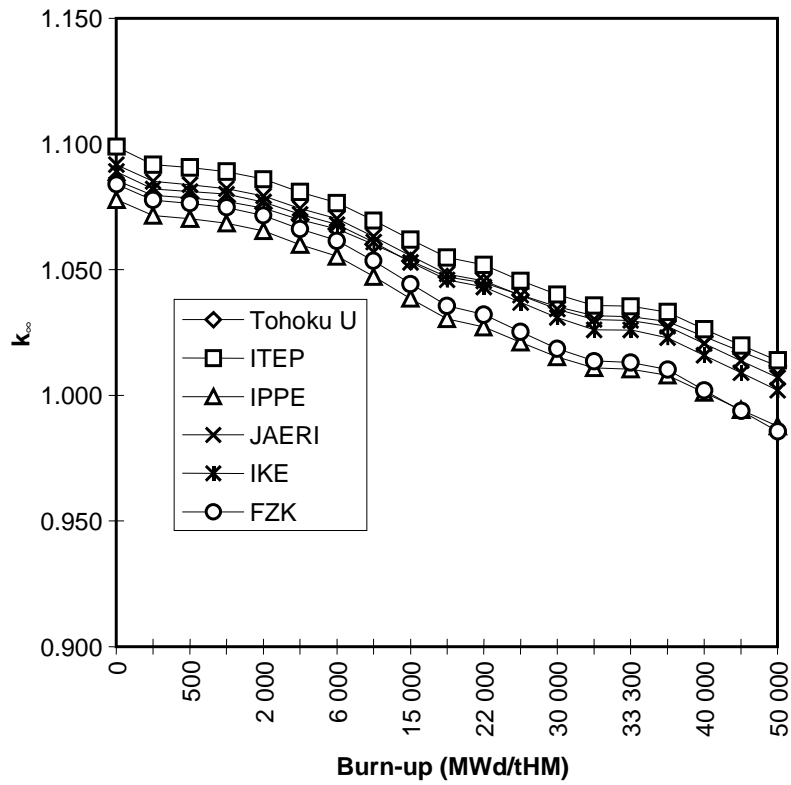


Figure 2.8.  $k_{\infty}$  as a function of burn-up for MOX22 (50 GWd/tHM) wide lattice and MA 0.0%

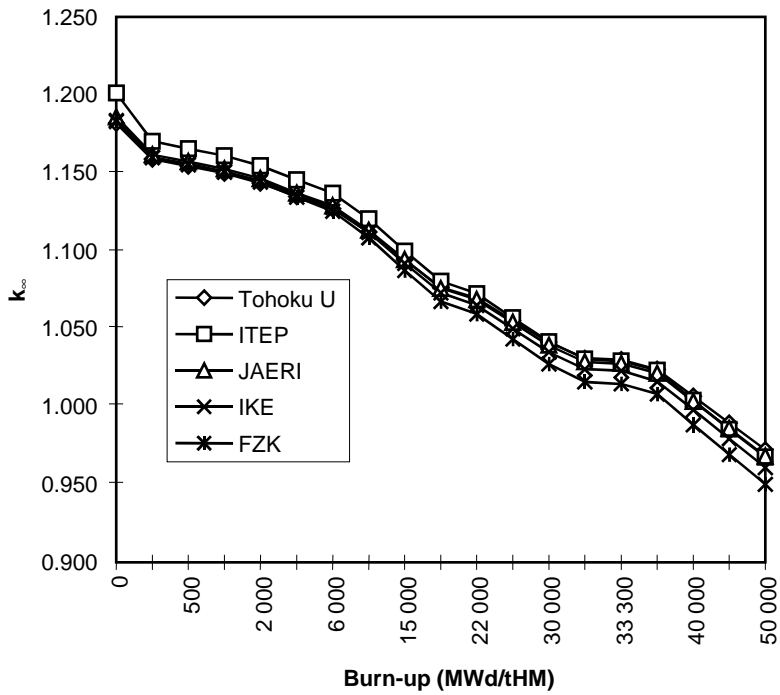


Figure 2.9.  $k_{\infty}$  as a function of burn-up for MOX22 (50 GWd/tHM) wide lattice and MA 1.0%

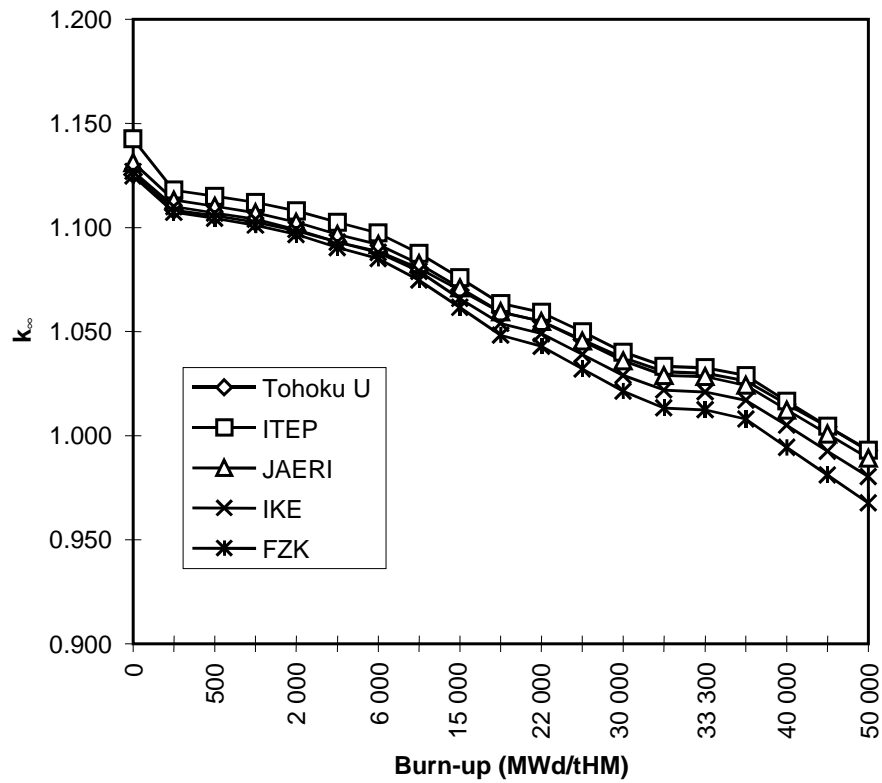
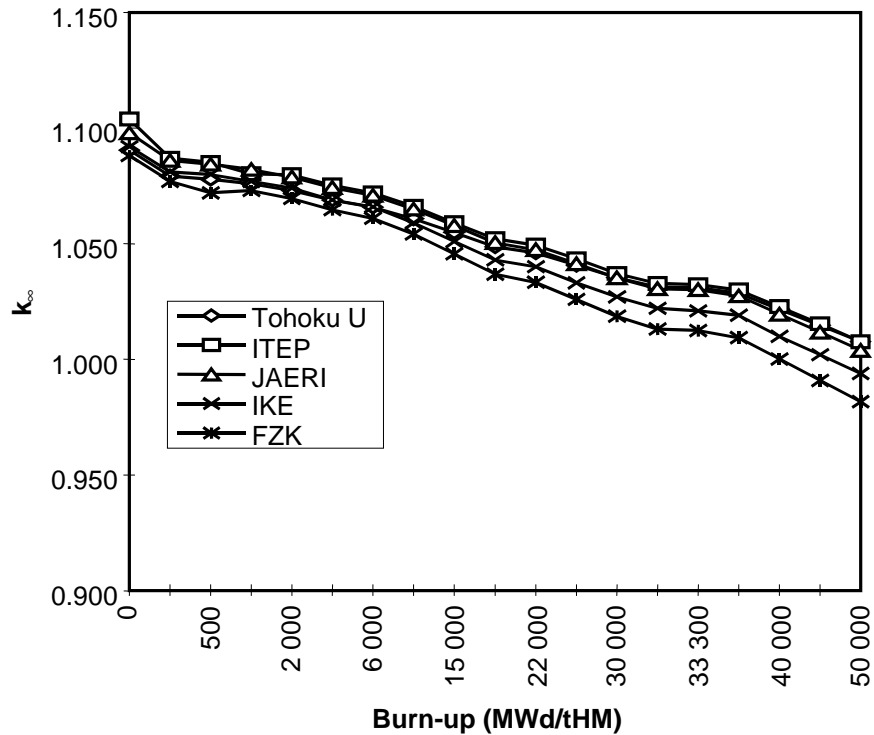
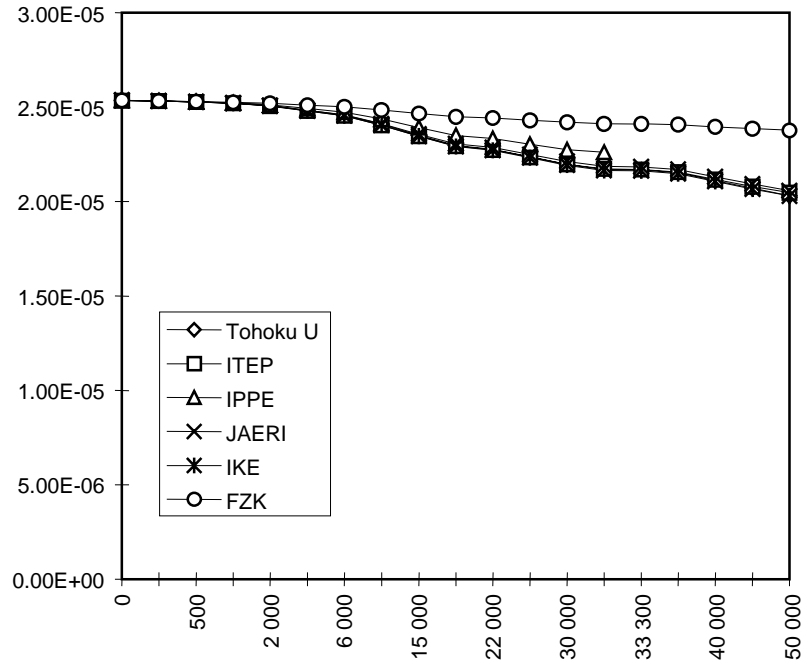


Figure 2.10.  $k_{\infty}$  as a function of burn-up for MOX22 (50 GWd/tHM) wide lattice and MA 2.5%



**Figure 2.11. Atomic number density of  $^{237}\text{Np}$  as a function of burn-up for MOX22 (50 GWd/tHM) and MA 2.5%**



**Figure 2.12. Atomic number density of  $^{241}\text{Pu}$  as a function of burn-up for MOX22 (50 GWd/tHM) and MA 2.5%**

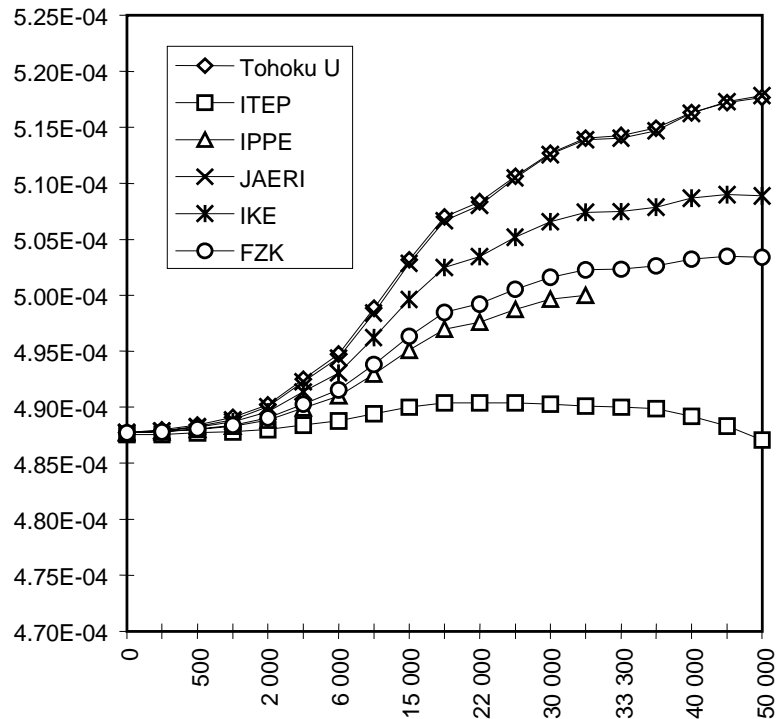


Figure 2.13. Atomic number density of  $^{242}\text{Pu}$  as a function of burn-up for MOX22 (50 GWd/tHM) and MA 2.5%

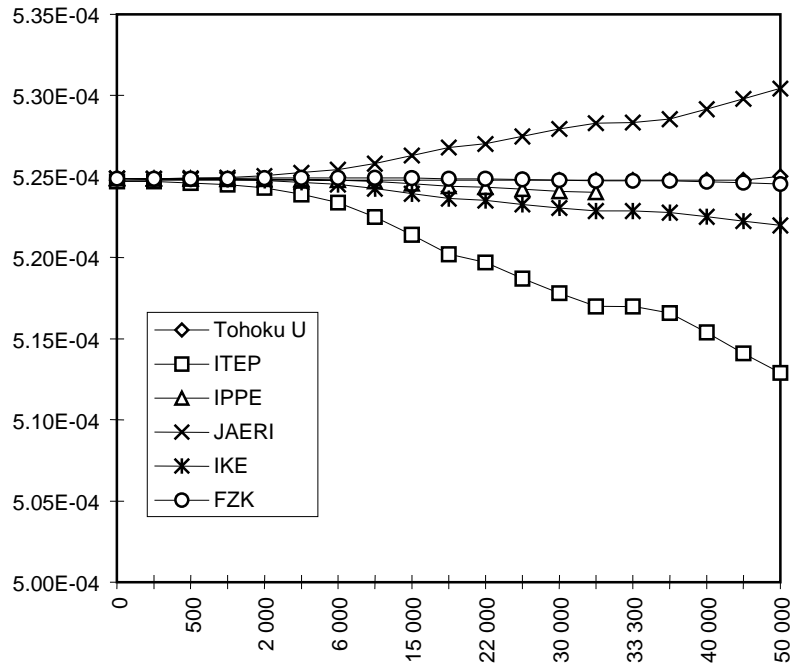
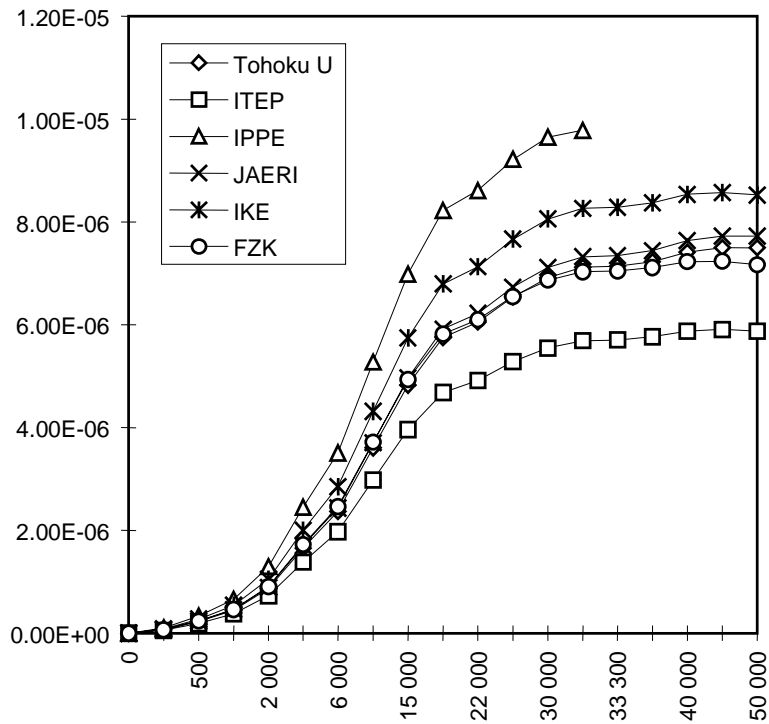
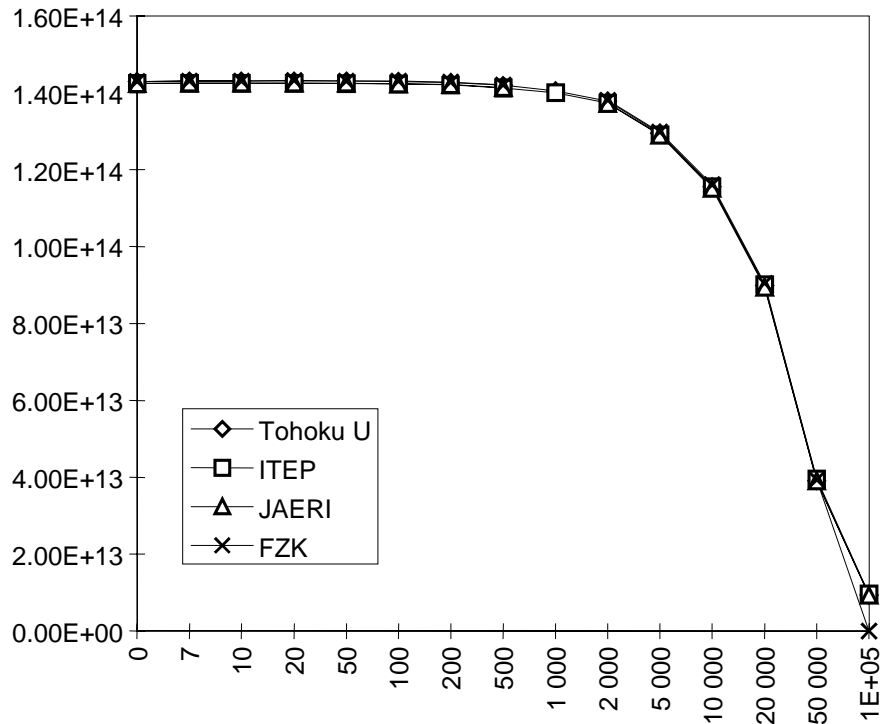


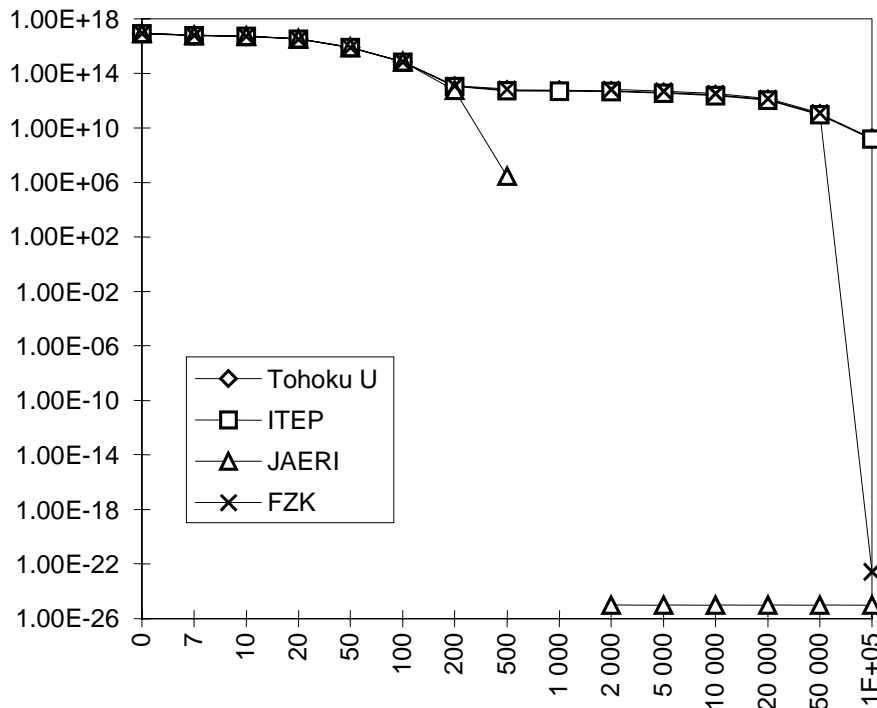
Figure 2.14. Atomic number density of  $^{242m}\text{Am}$  as a function of burn-up for MOX22 (50 GWd/tHM) and MA 2.5%



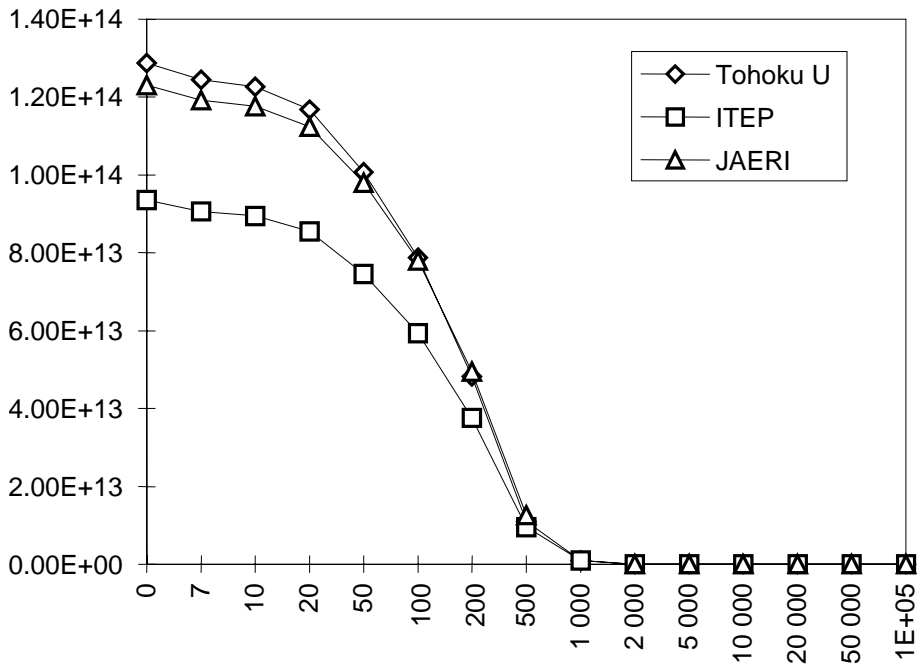
**Figure 2.15. Radioactivity of  $^{239}\text{Pu}$  (Bq) as a function of decay time (years) for MOX22 (50 GWd/tHM) and MA 2.5%**



**Figure 2.16. Radioactivity of  $^{241}\text{Pu}$  (Bq) as a function of decay time (years) for MOX22 (50 GWd/tHM) and MA 2.5%**



**Figure 2.17. Radioactivity of  $^{242m}\text{Am}$  (Bq) as a function of decay time (years) for MOX22 (50 GWd/tHM) and MA 2.5%**



**Figure 2.18. Radioactivity of  $^{243}\text{Cm}$  (Bq) as a function of decay time (years) for MOX22 (50 GWd/tHM) and MA 2.5%**

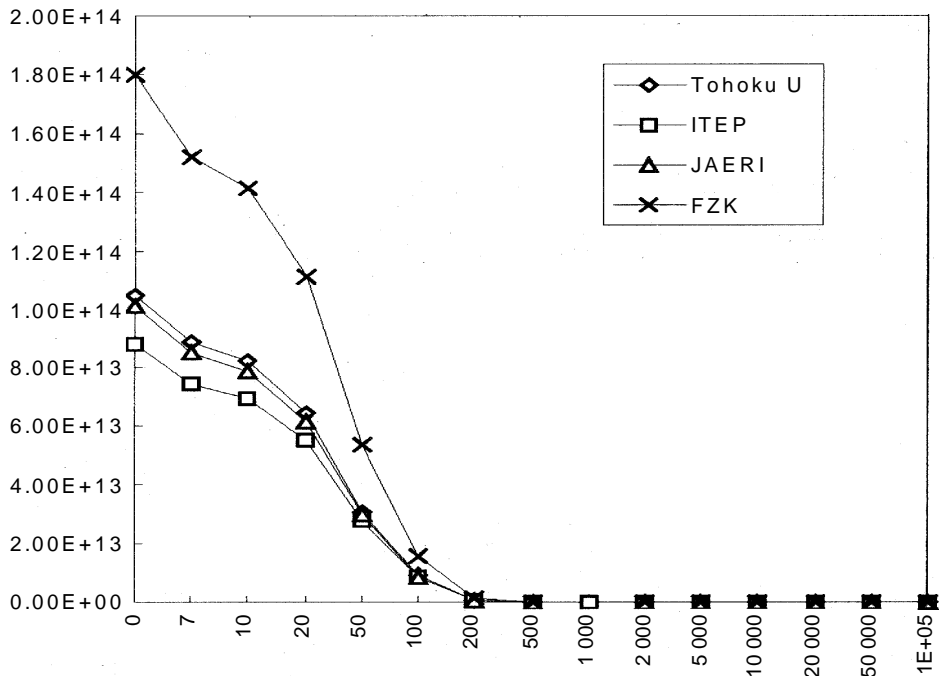




Figure 3.1. Reference core (1 000 MWe class FBR)

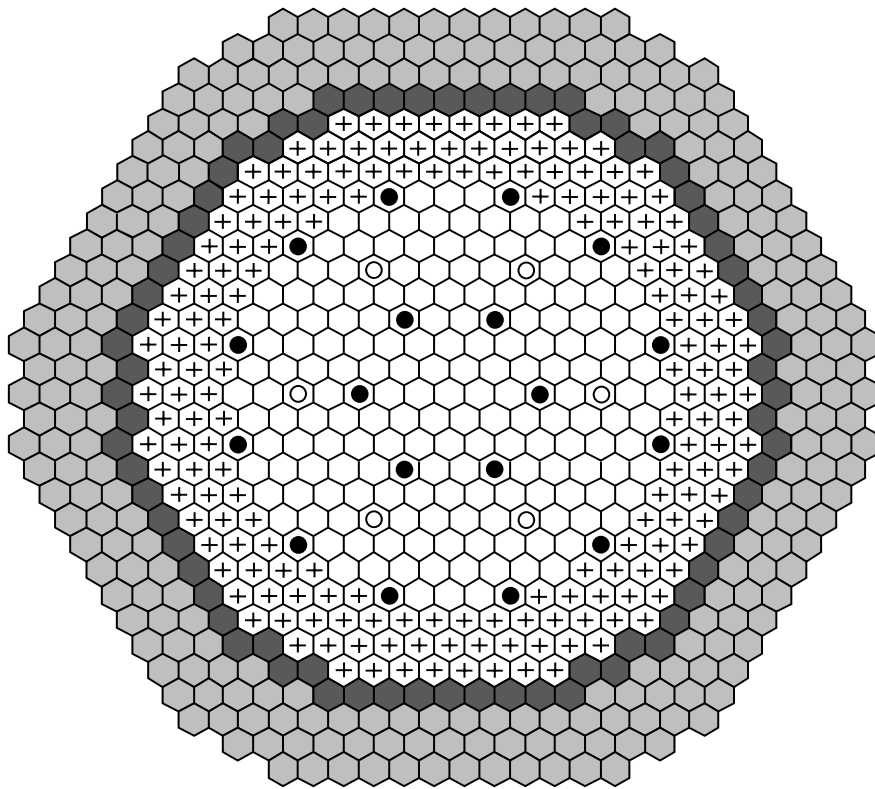
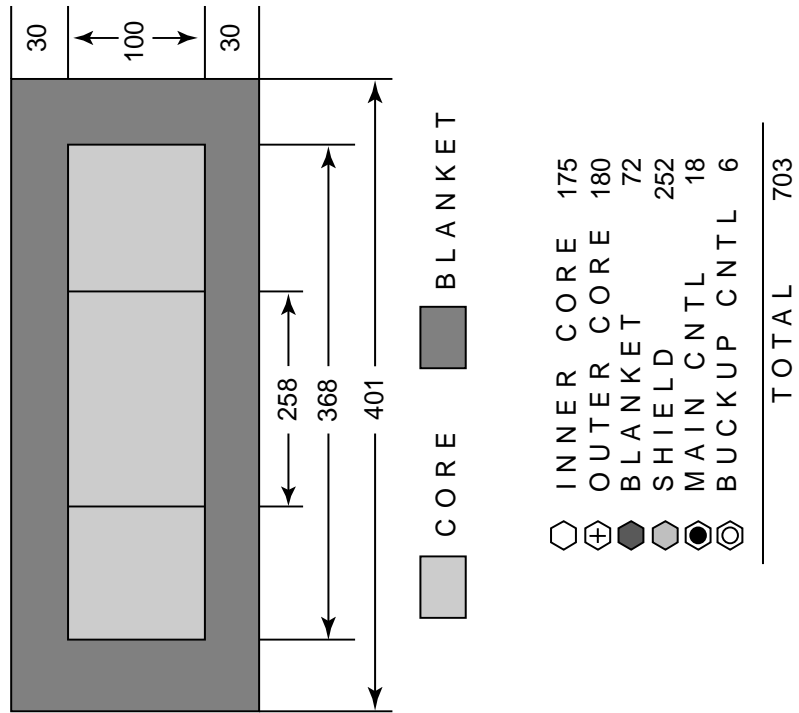


Figure 3.2. Dependence of  $k_{\text{eff}}$  on burn-up (reference core)

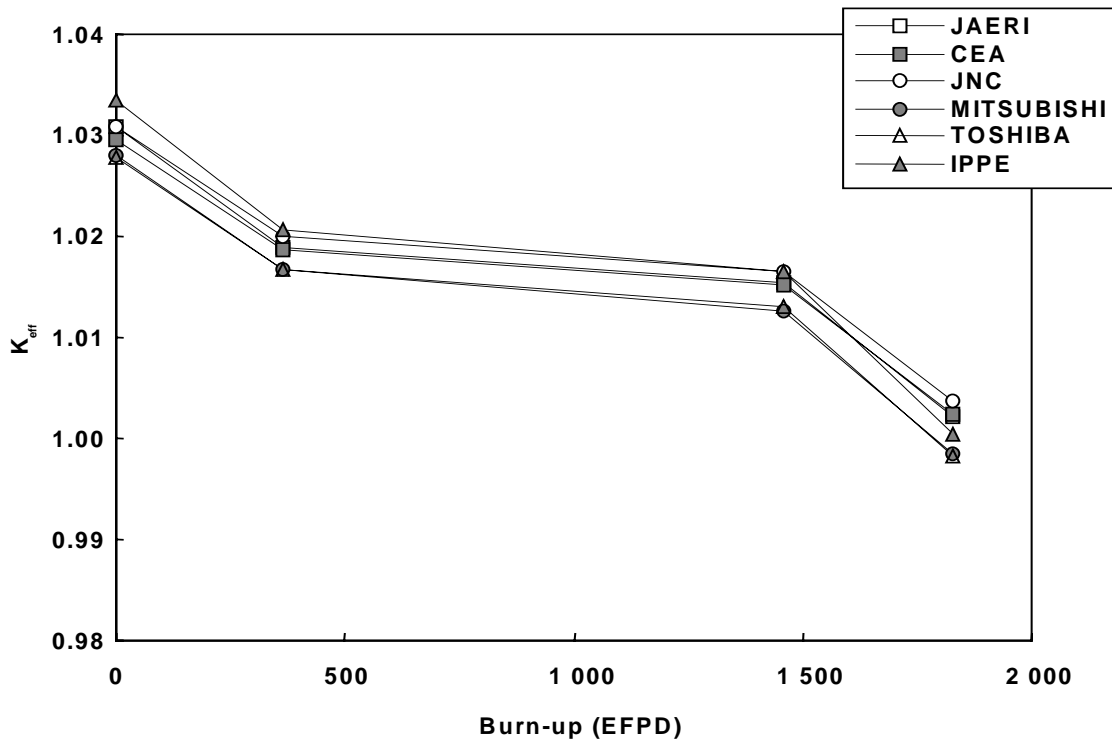


Figure 3.3. Dependence of  $k_{\text{eff}}$  on burn-up (2.5% MA core)

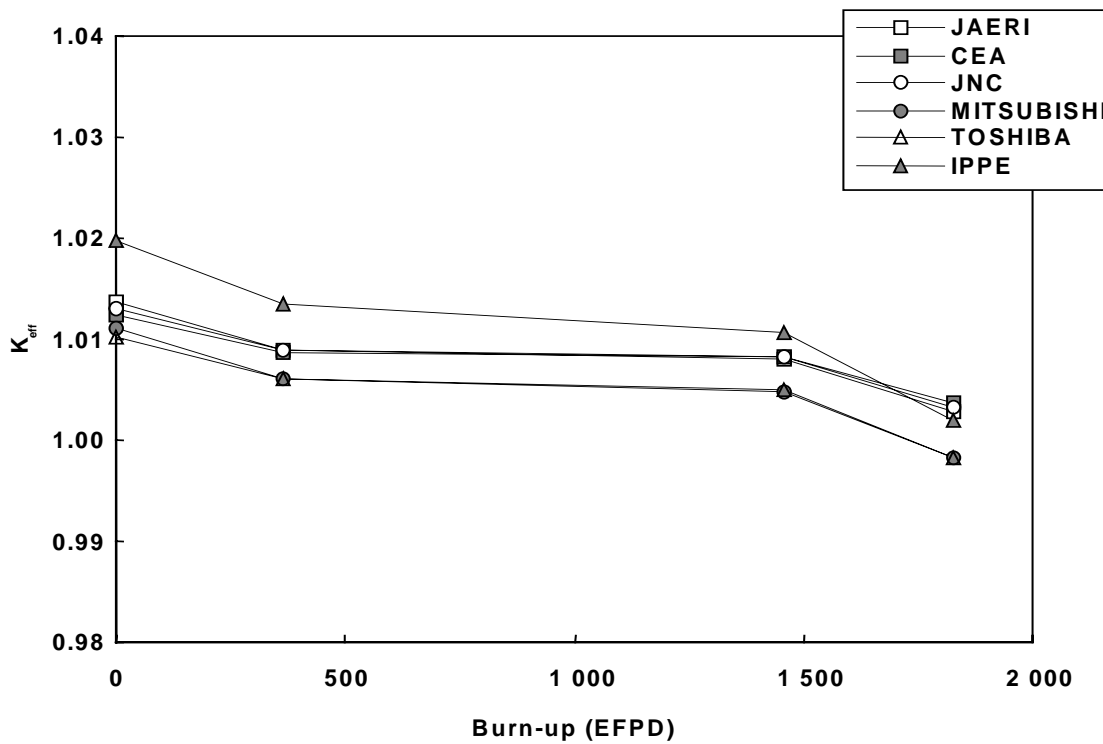


Figure 3.4. Dependence of  $k_{eff}$  on burn-up (5% MA core)

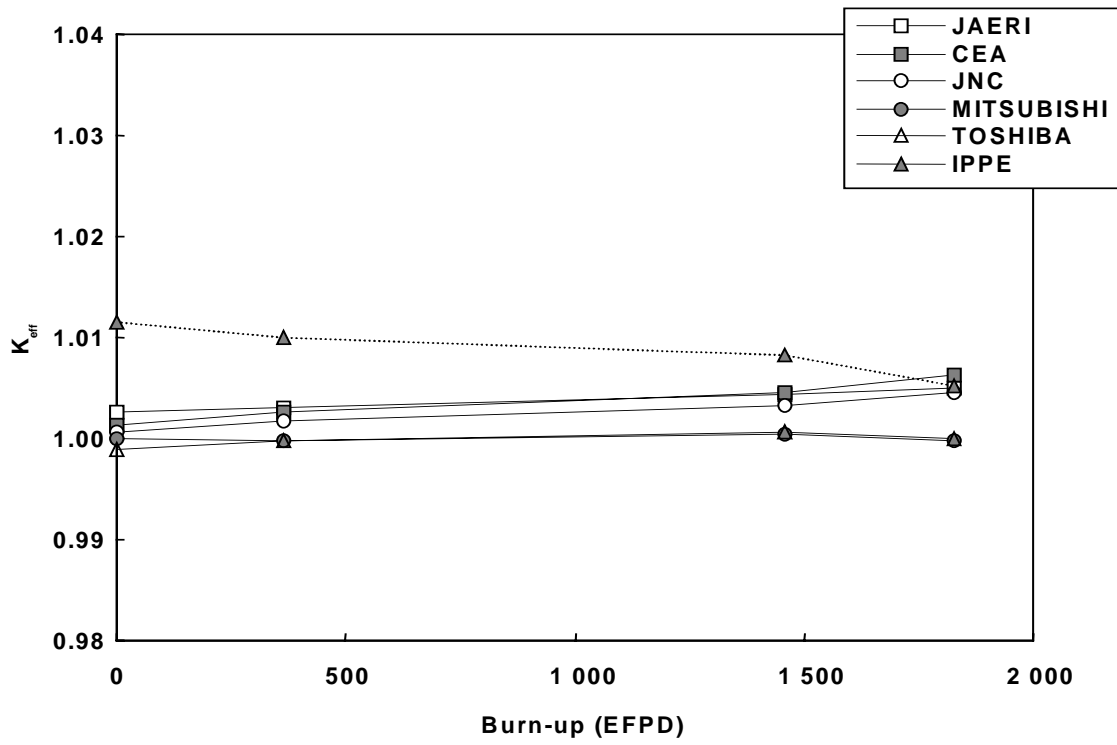
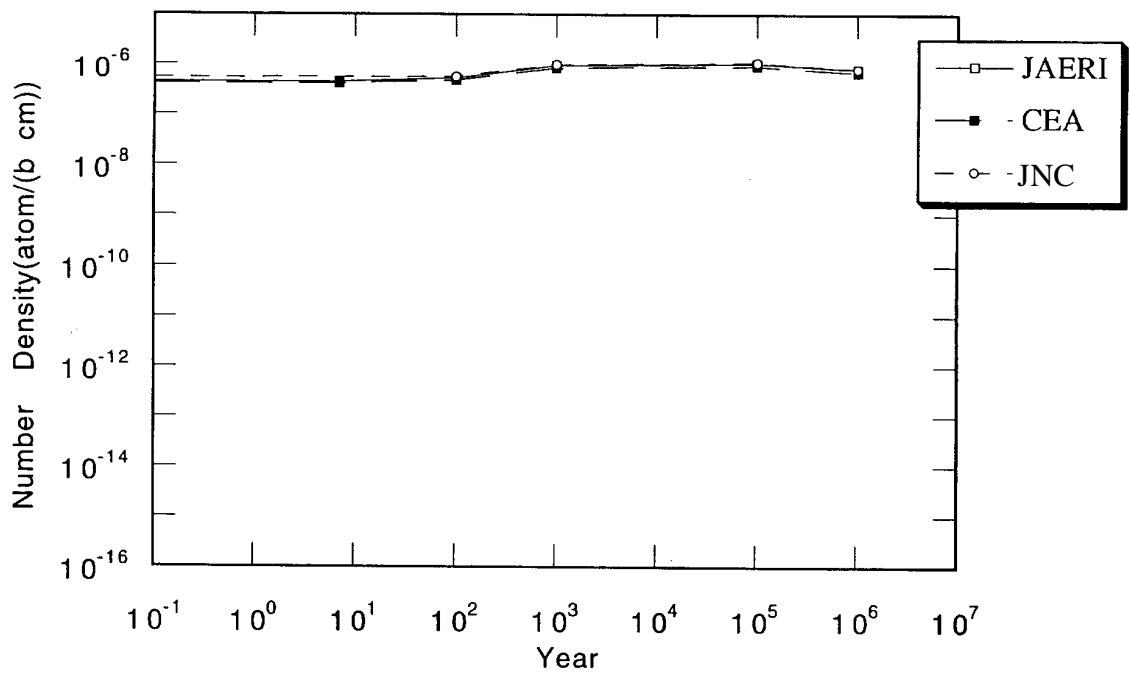
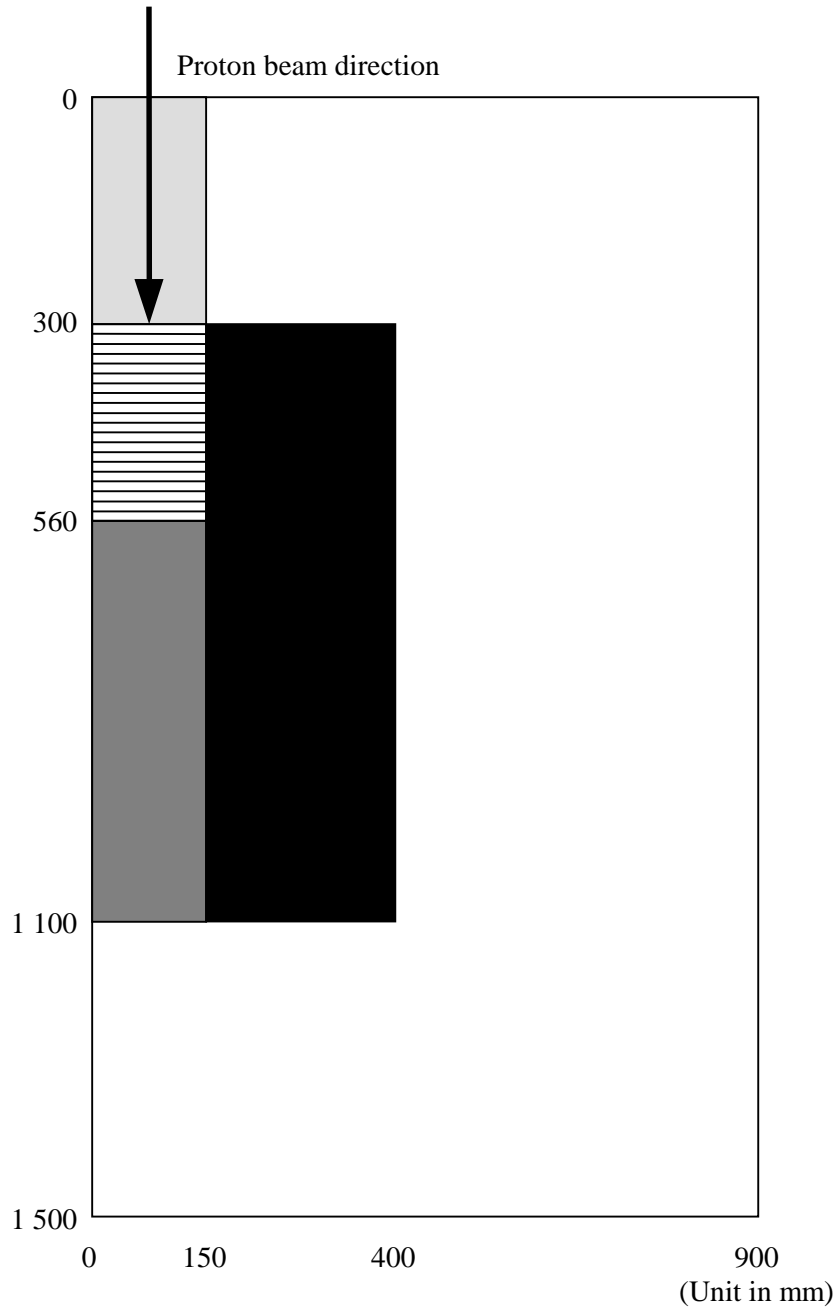
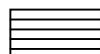
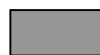

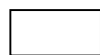



Figure 3.5. Number density of  $^{237}\text{Np}$  at various cooling times (2.5% MA core)



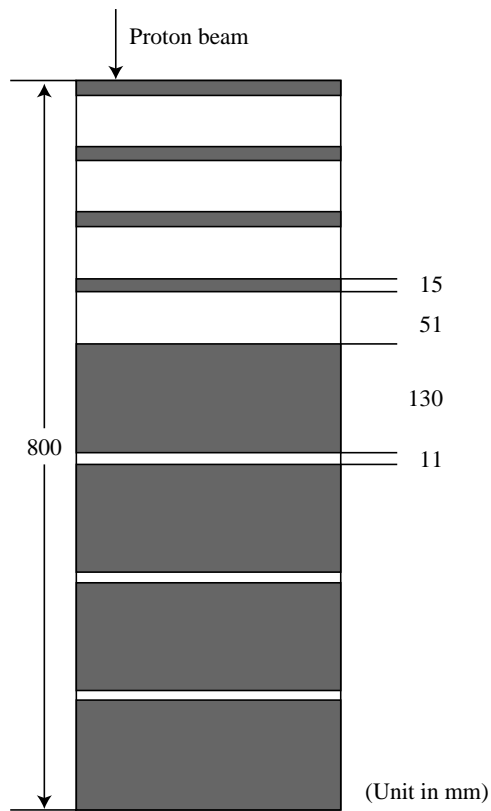
**Figure 4.1. Calculational model**



-  Tungsten target (thin disk part)
-  Tungsten target (thick disk part)
-  Pin-bundle type nitride fuel [(84MA-16Pu)<sub>1.0</sub>N<sub>1.0</sub>]
-  Stainless steel reflector
-  Beam duct (void)

**Figure 4.2. Target and fuel configurations**

*a) Disk-type tungsten target on which many flow holes are distributed for sodium coolant*



*b) Hexagonal arrangement of MA nitride fuel pins in the core region*

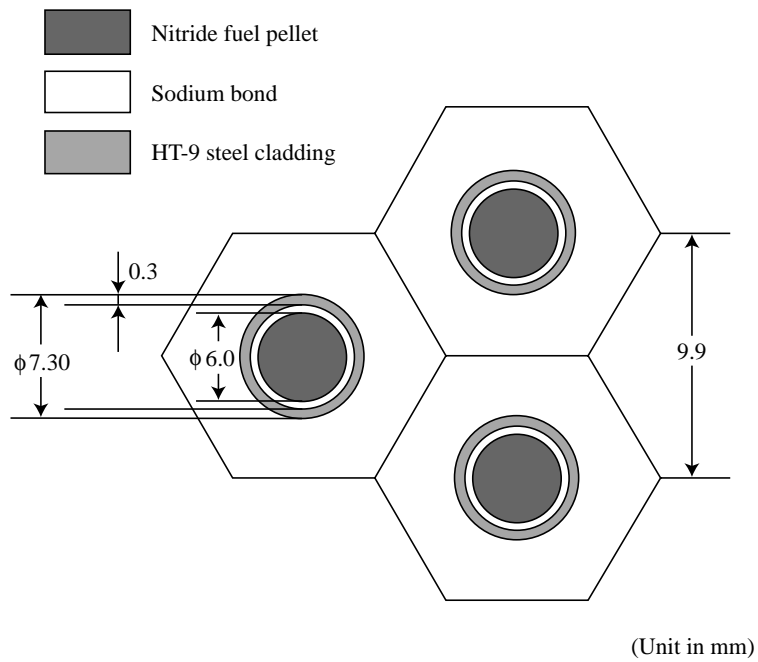


Figure 4.3. Axial distribution of neutrons (> 15 MeV) leaking from target at r = 150 mm

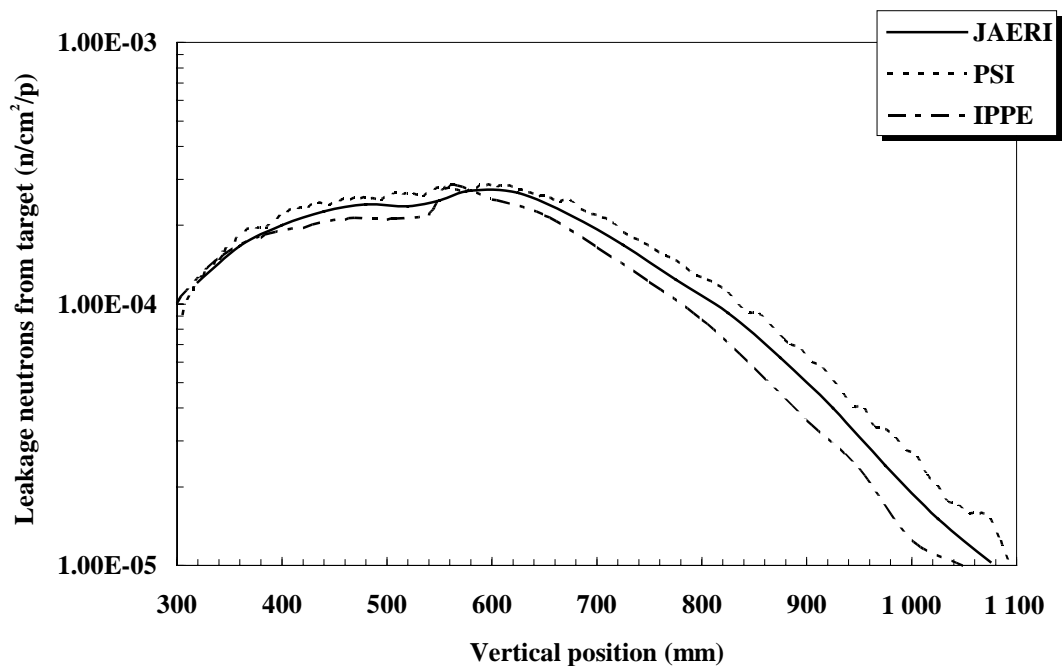


Figure 4.4. Average neutron spectrum in-core (MOX11)

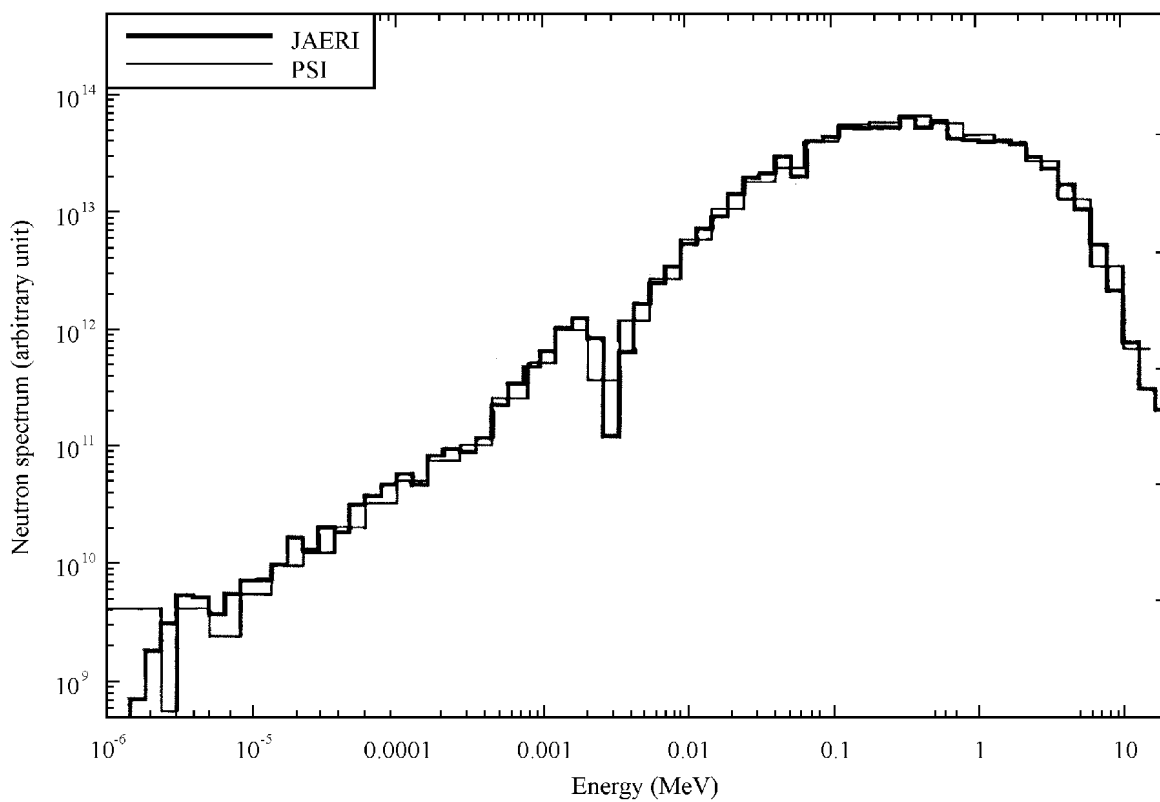


Figure 4.5. Time evolution of  $k_{eff}$  (MOX11)

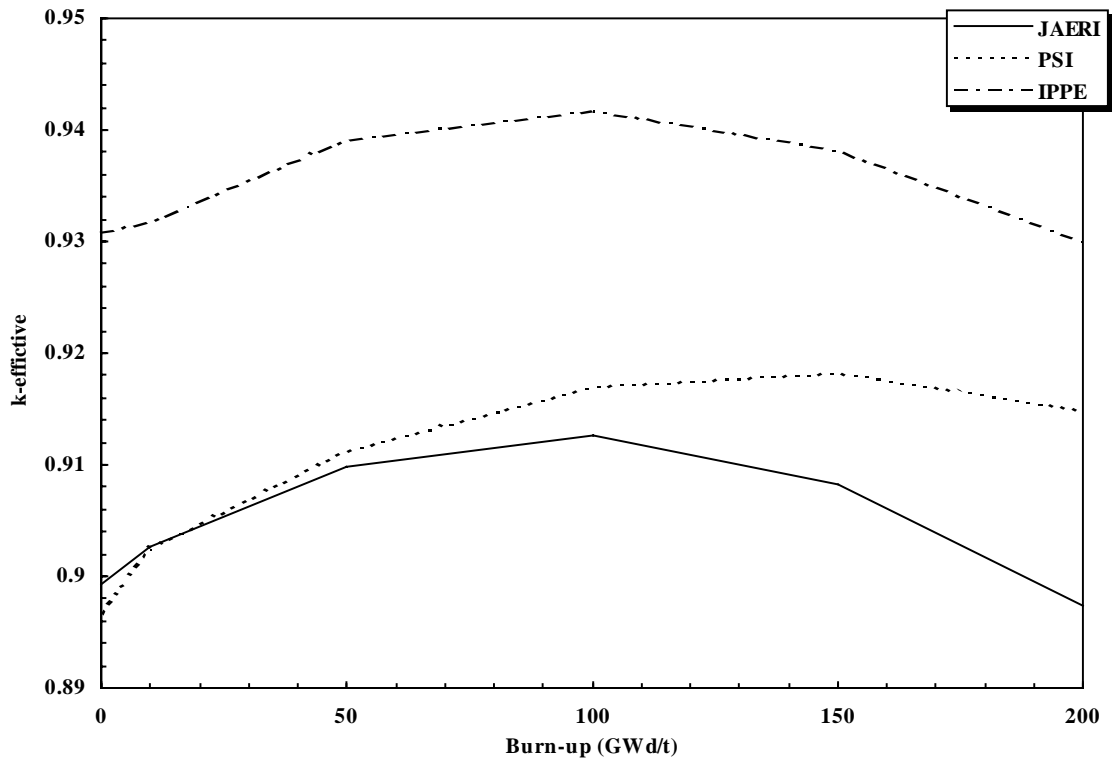


Figure 4.6. Time evolution of  $k_{eff}$  (MOX12)

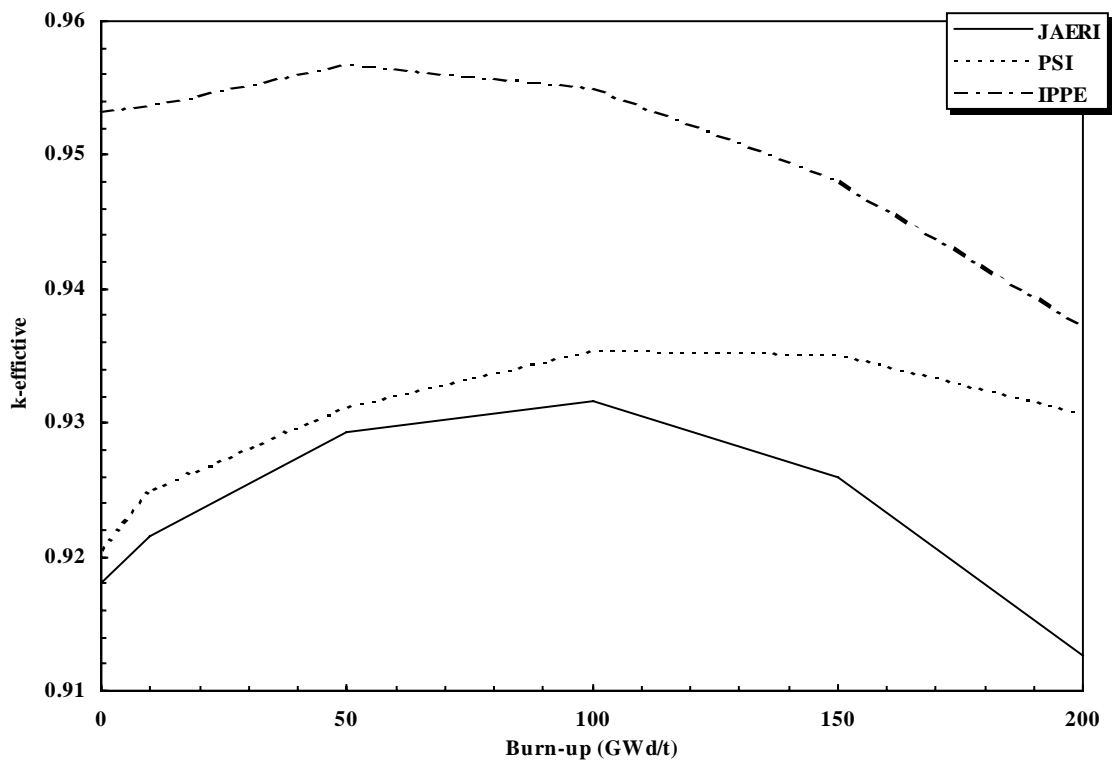


Figure 4.7. Time evolution of  $^{237}\text{Np}$  number density (MOX11)

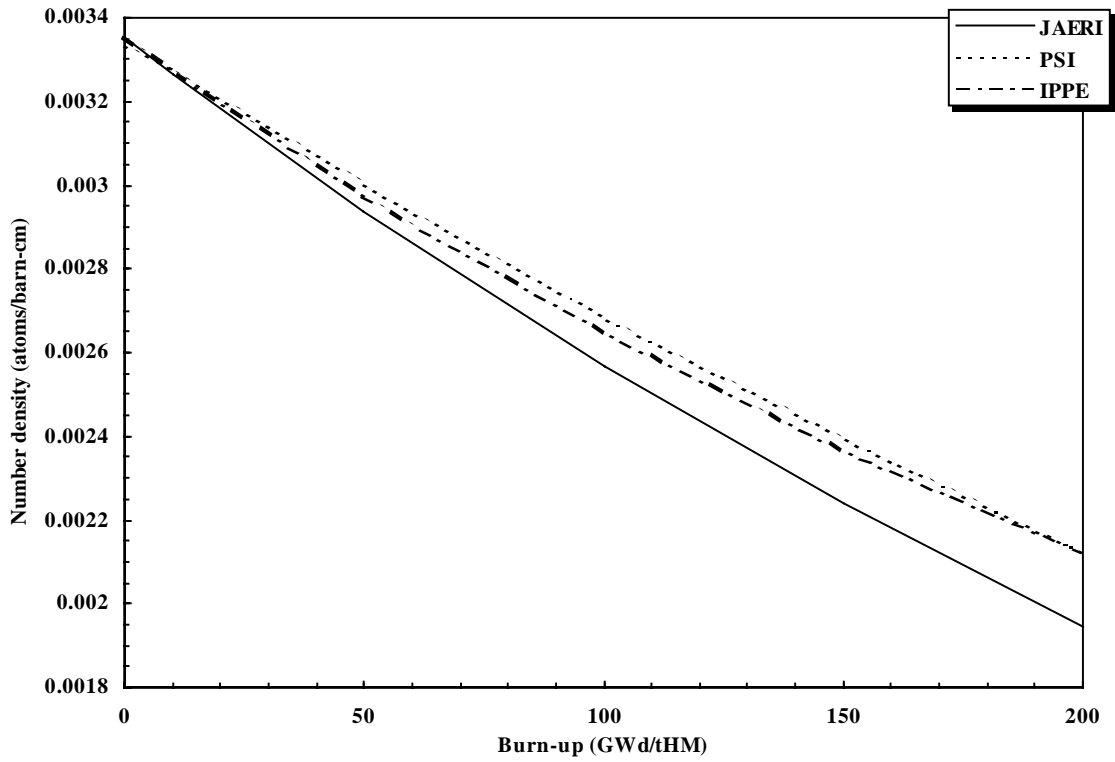


Figure 4.8. Time evolution of  $^{237}\text{Np}$  number density (MOX12)

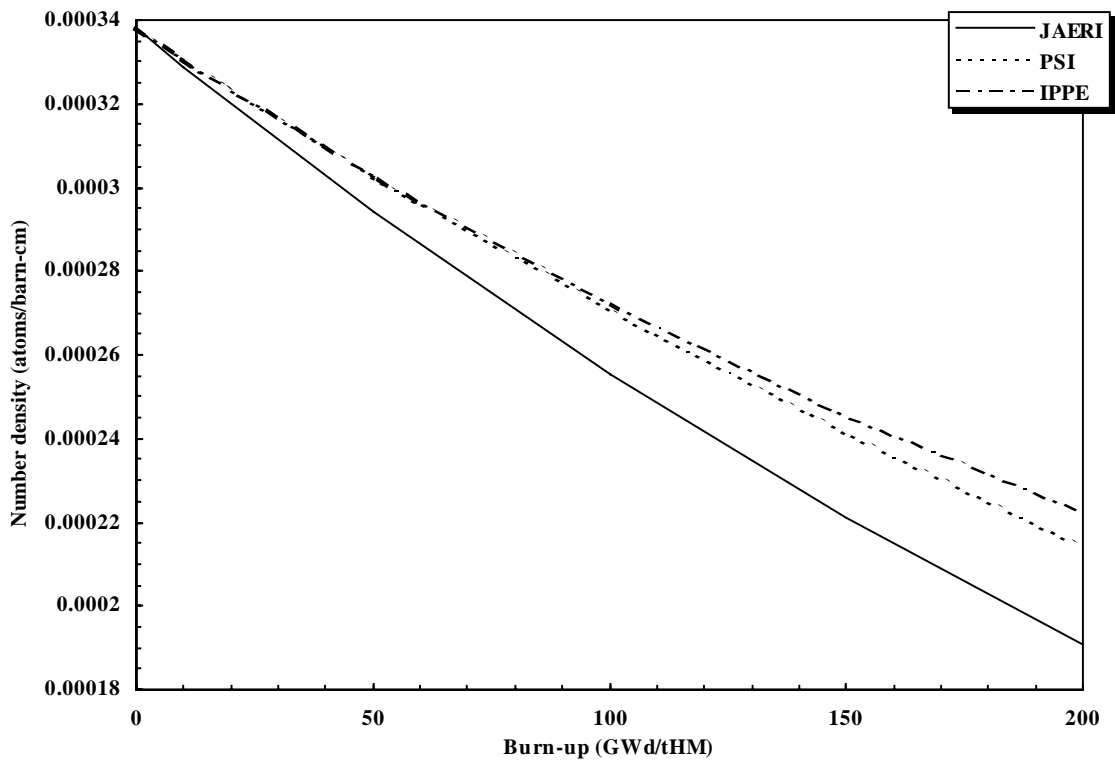




Figure 4.9. Time evolution of  $^{241}\text{Am}$  number density (MOX11)

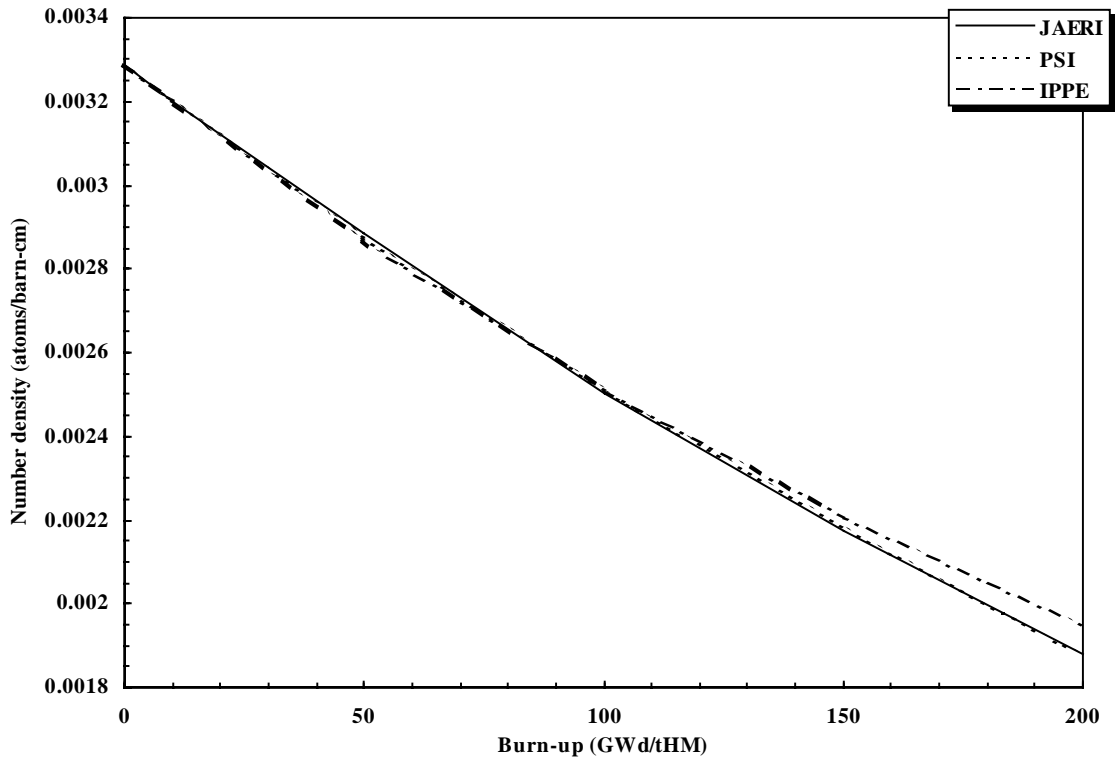
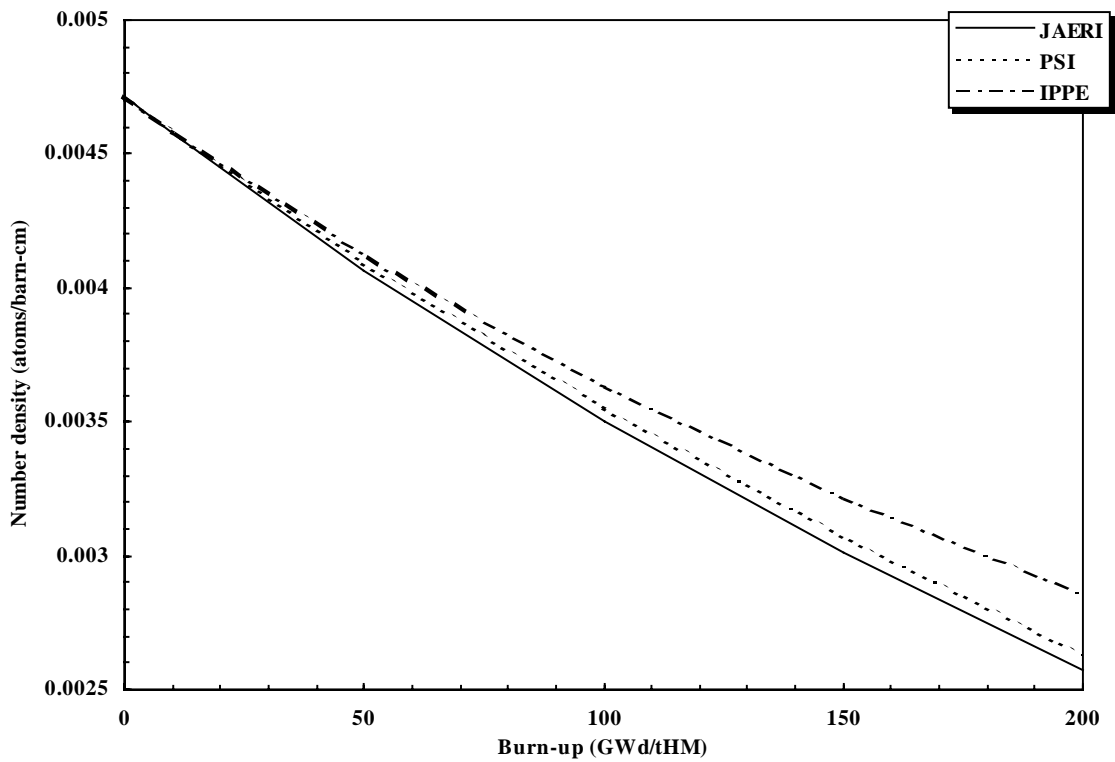


Figure 4.10. Time evolution of  $^{241}\text{Am}$  number density (MOX12)





# **APPENDIX A**

## **Benchmark Specifications**



## *Appendix A.1*

### **NEA/NSC benchmark on physics aspects of different transmutation concepts – specifications for PWRs**

**C. Broeders, H. Küsters, L. Payen**  
FZK, Institut für Neutronenphysik  
und Reaktortechnik  
Postfach 3640, 76021 Karlsruhe

**J. Vergnes**  
EDF/DER  
Département Physique des réacteurs  
1, avenue du Général de Gaulle

#### **Introduction**

The Nuclear Energy Agency's Nuclear Science Committee (NEA/NSC) is investigating the physical aspects of partitioning and transmutation (P-T) of actinides and fission products in several task forces [1,2]. One result of these efforts was a proposal to instigate benchmarks for a set of common transmutation system models [1]. At the task force meeting at Cadarache on 15 December 1994 it was agreed to propose a rather simple and realistic benchmark, close to actual scenarios. The objective is to compare the calculated activities for individual isotopes as a function of time (0 to 100 000 years) for different stages of proposed scenarios. The calculated activities must be normalised to the power produced.

The following stages are defined in Ref. [2]:

1. The initial stage (input data):
  - a) The activity, after seven years cooling, of UO<sub>2</sub> fuel (burn-up = 45 GWd/tHM) from a typical PWR reactor, where the minor actinides are taken out.
2. The second stage (recycling stage), that would input both plutonium and minor actinides to the third stage (seven years cooling), contains either:
  - a) A standard MOX fuelled fast reactor.
  - b) A standard MOX fuelled PWR.
3. The third and last stage (transmutation stage) contains either:
  - a) A standard fast reactor.
  - b) A special actinide burning fast reactor.
  - c) A PWR with moderator to fuel ratio of about 3.
  - d) An accelerator-driven transmutation system based on a fast neutron flux.
  - e) An accelerator-driven transmutation system based on a thermal neutron flux.
  - f) A special electron linear accelerator for the transmutation of fission products.

In Ref. [2] it was agreed, that FZK (formerly KZK) would specify the benchmark for the first stage (PWR UO<sub>2</sub> fuel), and would collaborate with BNFL the PWRs for Stages 2 and 3.

The characteristics should be representative for the type of system described. It was agreed to recommend that simple calculation methods, such as cell calculations, be used by the participants.

Because of the common experience of EDF and FZK with joined benchmarks on plutonium recycling in PWRs [3,4] the co-operation between EDF and FZK was extended for the new NEA/NSC benchmarks.

The proposal was discussed with representatives of BNFL at FZK on 20 April 1995 [5].

### **General discussion of the fuel cycle stages**

In this section we discuss the background and arguments for the specific data of the benchmark proposal. The detailed benchmark specifications are given in the section entitled *Detailed benchmark specification*.

All calculations will be based on simplified cell models. The basic cell is the same as in the earlier NEA/NSC benchmark for plutonium recycling in PWRs [6]. This square lattice cell was also considered in the EDF/KFK plutonium recycling benchmarks [3] and is representative of modern French PWRs. The outer fuel pin diameter of 9.5 mm is also used in modern German PWRs.

#### ***Stage 1: Initial stage with UO<sub>2</sub> PWRs***

Instead of the value of 45 GWd/tHM target burn-up in Ref. [2], we propose to investigate two different burn-up values:

- 1) 33 GWd/tHM, having been representative of most spent PWR fuel up to now.
- 2) 50 GWd/tHM, being an often mentioned target burn-up for the near future. The EDF/KFK benchmark of Ref. [4] specifies this burn-up value.

The results for these two burn-up values will give us quantitative information about the impact of target burn-up increase on long-term radiological consequences. Very probably these data will justify the increased benchmark efforts.

#### ***Stage 2: Plutonium recycling in PWRs***

In this stage only the plutonium from Stage 1 is put into a follow-up PWR core. Other transurania and fission products eventually have to be treated in a Stage 3 scenario. The (PuU)O<sub>2</sub> mixed oxide (MOX) may be manufactured with natural or depleted uranium. At present, there is a tendency to utilise depleted uranium for the MOX in order to consume a maximum amount of plutonium in the expensive MOX fuel assemblies (plutonium burning).

The results of Ref. [4] indicate that plutonium may be recycled more than once in PWRs. However, the planned benchmark will only consider one recycling step before the final transmutation stage. For the plutonium recycling in PWRs we have to select the applied full core model:

- A full MOX core.
- A mixed core with MOX and UO<sub>2</sub> fuel assemblies.

Although full MOX PWR cores are feasible and even have some advantages, e.g. related to power distributions, no real application seems to be planned for the near future. Therefore a mixed MOX/UO<sub>2</sub> core is proposed for this benchmark. The characteristics of the MOX and of the UO<sub>2</sub> fuel assemblies have to be determined by independent cell calculations for the corresponding lattices. This choice leads to two open questions:

1) *Which partition of the mixed core will be MOX?*

Some investigations consider the use of self-generated MOX in a mixed MOX/UO<sub>2</sub> core. In practical cases, however, the MOX comes from different reactors and its partition is fixed in some way. Usually the licensing procedures allow up to about 50% MOX content in the core. For the benchmark we propose to use a fixed partition of e.g. 30% MOX.

2) *What are the criteria for MOX and UO<sub>2</sub> fuel assemblies being utilised together in a full reactor core model?*

The criteria for equivalency of UO<sub>2</sub> and MOX fuel assemblies are not well defined. In practice it must be possible to run the full core in a satisfactory manner over the whole reactor cycle. The first experiences in French and German PWRs for target burn-ups of ≈35 GWd/tHM indicate that for burn-up calculations without boron in the coolant, the following relation for the end of cycle  $k_{\infty}$  values is reasonable:

$$k_{\infty,MOX}^{EOC} = k_{\infty,UOX}^{EOC} - 0.03 \quad (1)$$

For the benchmark we propose to apply this formula. This means that a  $Pu_{fis}$  value must be determined to match Eq. (1) for a given UO<sub>2</sub> lattice.

### ***Stage 3: Partition and transmutation in PWRs***

In Ref. [2] it is proposed to investigate a PWR with a moderator to fuel ratio of about 3 (highly moderated PWR). In order to obtain systematic information about the potential of modern PWRs for partition and transmutation (P&T) purposes, we propose to also consider the PWR specification of Stages 1/2. The following problem areas may be identified for the benchmark specification:

1. The maximum Pu content of the MOX fuel, eventually admixed with other transurania and/or fission products. It is well known that too high Pu contents may lead to problems with safety parameters, e.g. the moderator density reactivity coefficient (void effect).
2. Choice of the uranium composition for the MOX fuel. Here a balance must be found between colliding requirements such as maximum transurania consumption and upper transurania limits due to safety considerations. In addition to natural and depleted uranium, <sup>235</sup>U enriched uranium may also become of interest.

3. Technical feasibility of separation of individual transurania isotopes and fission products. At present, only the extraction of plutonium, neptunium and selected fission products seems to be feasible [5]. For the benchmark we propose to study the following alternatives:
  - a) Transmutation of plutonium and neptunium. This would be possible with current techniques. With this option it should be emphasised that  $^{237}\text{Np}$  will be produced by the americium on store. The transmuted  $^{237}\text{Np}$  is converted to  $^{238}\text{Pu}$ .
  - b) Transmutation of plutonium and all other transurania (neptunium, americium and curium). Technical developments are required to realise this option. The disadvantage of this procedure is the high radioactivity of curium.
  - c) Transmutation of plutonium, neptunium and americium. Technical developments are required to realise this most desirable option.
  - d) Burning of selected fission products. It is of interest to clarify the capabilities of fission product incineration in PWRs in a benchmark investigation.
4. For the highly moderated PWRs no actual design for  $\text{UO}_2$  fuel is available with the proposed moderator to fuel ratio of 3. Thus there is no basis for a mixed PWR core with  $\text{UO}_2$  and MOX fuel assemblies. To avoid further complications we propose to consider a full MOX highly moderated PWR. The  $\text{Pu}_{\text{fis}}$  fraction should be determined on the basis of fundamental mode diffusion calculations with the requirement  $k_{\text{eff}}^{\text{EOC}} = 1$ . For a reasonable geometrical buckling, e.g. for a realistic 3 000 MWth reactor.

### Detailed benchmark specification

All calculations should be performed on the basis of the cylindrical Wigner-Seitz cell as specified in Figure 1 and Table 1. The pitch and the equivalent outer cell radius are given twice: the smaller one for the standard PWR of the Stages 1-3 and a larger one for the highly moderated PWR of Stage 3. For simplicity the influences of the water boration and of the fuel assembly structures are neglected in this benchmark. The effects of these simplifications have been studied in some detail. They are not significant for fuel inventory calculations [7]. The determination of the one-group cross-sections for the depletion calculations should be based on cell flux calculations with critical buckling.

### *Specifications for the fuel*

For this benchmark we have three different sources for the manufacturing of the fuel:

- 1) Uranium oxide ( $\text{UO}_2$ ) with a theoretical density of  $10.96 \text{ g/cm}^3$  (see Table 1). Natural uranium with 0.711%  $^{235}\text{U}$  or depleted uranium with 0.225%  $^{235}\text{U}$  will be used in the MOX in most cases. Only the isotopes  $^{235}\text{U}$  and  $^{238}\text{U}$  will be considered in the fresh uranium fuel.
- 2) Plutonium oxide ( $\text{PuO}_2$ ) with a theoretical density of  $11.46 \text{ g/cm}^3$  (see Table 1). The origin and history of the plutonium strongly affect its composition. At reactor beginning of cycle (BOC) we assume reprocessed plutonium after three years fabrication time. This fuel contains the plutonium isotopes  $^{238}\text{Pu}$ ,  $^{239}\text{Pu}$ ,  $^{240}\text{Pu}$ ,  $^{241}\text{Pu}$ ,  $^{242}\text{Pu}$  and  $^{241}\text{Am}$  from the  $\beta^-$ -decay of  $^{241}\text{Pu}$  ( $T_{1/2} = 14.4$  years).



- 3) Additives like neptunium, americium, curium and fission products. These materials can be specified in several ways. For the benchmark it is recommended to replace uranium by these additives.

The density of the oxide fuel has to be kept constant for all cases:  $\rho_{ox} = 10.29 \text{ g/cm}^3$ . This means that for different fractions of plutonium to the MOX, the ratio of the actual oxide density to the theoretical value varies.

### *Isotopic composition of plutonium mixtures*

The isotopic composition of the plutonium very strongly depends on its irradiation history. The higher isotopes increase with increasing irradiation, e.g. by higher target burn-ups or by recyclings. An increase of higher plutonium isotopes determines a decrease in the fissile fraction  $f_{Pu_{fis}} = f_{^{239}\text{Pu}} + f_{^{241}\text{Pu}}$ . Low  $f_{Pu_{fis}}$  values are disadvantageous for use in PWRs. The usability of highly irradiated plutonium can be improved by mixing it with better quality plutonium. The isotopic composition of plutonium from a mixture of different charges can be determined by mass weighting of the fractions of the single charges. For  $N$  charges with weight  $W_i$ , ( $i = 1, N$ ), we obtain the isotopic fraction  $f_j$  of isotope  $j$ , ( $j = ^{238}\text{Pu}, ^{239}\text{Pu}, ^{240}\text{Pu}, ^{241}\text{Pu}, ^{242}\text{Pu}, ^{241}\text{Am}$ ) with the following formula:

$$f_j = \sum_{i=1, N} \frac{W_i \cdot f_j^i}{W_{tot}} \quad (2)$$

with  $f_j^i$  the isotopic fraction of isotope  $j$  in charge  $i$  and:

$$W_{tot} = \sum_{i=1, N} W_i \quad (3)$$

### ***Stage 1: Initial stage with UO<sub>2</sub> PWRs***

For the initial stage number densities are specified for two target burn-ups. Recommendations are given for the detailed burn-up scheme, including the burn-ups steps and the list of isotopes for explicit treatment. Finally the required results to be reported are specified.

#### *Specification of the number densities*

For the initial Stage 1, two  $^{235}\text{U}$  enrichments are specified:

- 1) 3.25% for the target burn-up of 33 GWd/tHM. This value is in accordance with experience gained while running PWRs with three batches. The mean end of cycle (EOC) burn-up amounts 22 GWd/tHM.
- 2) 4.65% for the target burn-up of 50 GWd/tHM. This is the same value as for the EDF/KFK benchmark investigations of Refs. [3,4]. In a three batch reactor system the mean EOC burn-up amounts 33.3 GWd/tHM.

Table 2 contains the isotopic concentrations in the fuel, cladding and moderator zones for these enrichments. These number densities have been obtained by the Karlsruhe KARBUS code [8]. *They are defined to be the starting conditions for the benchmark calculations.*

### *Specification of the burn-up steps*

For both enrichments depletion calculations must be performed up to the specified target burn-up. Although inventory calculations are not very sensitive to the interval scheme for the recalculation of one-group cross-sections (macro steps for the depletion calculations), it is recommended to apply rather small steps as specified in Table 3. The accumulated burn-up and the corresponding incremental time steps are tabulated at a power rating of 183.02 W/cm (see also Table 1).

### *Specification of the explicitly treated isotopes*

For the cell flux and the one-group cross-section calculations the following isotopes should be treated explicitly if possible:

- Uranium:  $^{234}\text{U}$ ,  $^{235}\text{U}$ ,  $^{236}\text{U}$  and  $^{238}\text{U}$ .
- Neptunium:  $^{237}\text{Np}$  and  $^{239}\text{Np}$ .
- Plutonium:  $^{238}\text{Pu}$ ,  $^{239}\text{Pu}$ ,  $^{240}\text{Pu}$ ,  $^{241}\text{Pu}$  and  $^{242}\text{Pu}$ .
- Americium:  $^{241}\text{Am}$ ,  $^{242}\text{Am}$ ,  $^{242\text{m}}\text{Am}$  and  $^{243}\text{Am}$ .
- Curium:  $^{242}\text{Cm}$ ,  $^{243}\text{Cm}$ ,  $^{244}\text{Cm}$  and  $^{245}\text{Cm}$ .
- Fission products: the long-lived fission products  $^{99}\text{Tc}$ ,  $^{129}\text{I}$  and  $^{135}\text{Cs}$  will be considered in Stage 3. Thus, they must be treated explicitly. For other fission products it is recommended to consider as much as available.

### *Evaluation of the results*

Tabulated results should be prepared for the *in situ* burn-up and for the long-term depletion. For the burn-up calculations the following results have to be tabulated for all isotopes listed in the above section *Specification of the explicitly treated isotopes* and the burn-up steps of Table 3 with an additional seven years cooling time:

- $k_{\infty}$ .
- Number densities (atoms/cm<sup>3</sup>).
- Weights (kg), normalised to 1 t of initial heavy metal (TIHM).

For the long-term, the depletion of the radioactivity of the same isotopes, with the exception of the short-lived  $^{239}\text{Np}$  and  $^{242}\text{Cm}$  has to be determined for the following time scale:

- Reactor shutdown, seven years cooling time, 10, 20, 50, 100, 200, 500, 1 000, 2 000, 5 000, 10 000, 20 000, 50 000 and 100 000 years decay.

Ref. [2] proposes to normalise to the power produced (Bq/GWh). Here one has to decide between thermal or electric power produced. For a benchmark on P&T systems with different efficiencies, electric (net) power seems to be preferable. In the case electric power normalisation is required, the efficiency factor  $\eta_p$  of the PWR (in the range 0.32-0.35) must be defined, e.g.  $\eta_p = 1/3$ .

Further, the calculation of the activity of individual isotopes has to be clarified. Two alternative methods are discussed:

- 1) The time dependence of the radioactivity of the single isotopes within the unloaded fuel. In fact this means a continuation of the reactor burn-up calculations with zero neutron flux (decay processes).
- 2) Determination of the long-term behaviour of the individual isotopes after unloading from the core. The proper activity of each isotope as well as the activity of its successors is considered. Separate decay calculations, starting with only the single unloaded individual isotopes, have to be performed.

The second method seems to be more suitable for the judgement of hazard potential after fuel unloading from reactors. In spite of possible complications with calculational procedures, the second option is recommended.

### ***Stage 2: Plutonium recycling in PWRs***

In this stage, the plutonium gained in Stage 1 is reused in a PWR. Other transurania and fission products stay on store. After seven years cooling and reprocessing time and three years fabrication time, the MOX fuel assemblies (FA) are loaded in a PWR core together with UO<sub>2</sub> FA. The partition of MOX and UO<sub>2</sub> FA is fixed: 30% MOX and 70% UO<sub>2</sub>.

For the benchmark it is assumed that enough material with the mean characteristics of the obtained "Stage 1" plutonium is available for the production of 30% MOX FA. In this first plutonium recycling depleted uranium is preferred for the MOX. The plutonium content in the MOX FA is determined by the required fissile plutonium ( $Pu_{fis}$ ) to match the equivalency criteria of Eq. (1) (under the section entitled *General discussion of the fuel cycle stages*, see the sub-section *Stage 2: Plutonium recycling in PWRs*).

Two cases should be calculated:

- 1) For the plutonium coming from the target burn-up of 33 GWd/tHM the  $Pu_{fis}$  value has to be determined for the same target burn-up in a core along with 3.25% enriched UO<sub>2</sub>.
- 2) For the plutonium coming from the target burn-up of 50 GWd/tHM the  $Pu_{fis}$  value has to be determined for the same target burn-up in a core along with 4.65% enriched UO<sub>2</sub>.

For both cases the required  $Pu_{fis}$  value and the same results as specified for Stage 1 must be reported.

### ***Stage 3: Partition and transmutation in PWRs***

The definition of the Stage 3 benchmark specifications is not as straightforward as the first two stages. Too many material compositions are possible. Table 4 summarises possible materials for incineration studies for PWRs. The identifications of the second column will be used below. U325FA and U465FA are UO<sub>2</sub> fuel assemblies, whereas U020, U070 and Uxyz define admixed uranium to the MOX fuel assemblies.

For Stage 3 the specification of the materials of Table 4 may be provided for use in all transmutation concepts, e.g. on the basis of KARBUS/APOLLO [4] calculations.

The plutonium from Stage 1, MOX33<sub>1</sub> and MOX50<sub>1</sub>, is the same as the input for Stage 2. The Stage 2 output plutonium, MOX33<sub>2</sub> and MOX50<sub>2</sub>, is the mixture of 70% UO<sub>2</sub> and 30% MOX FA. The plutonium composition of MOX<sub>xx2</sub> can be determined by Eq. (2).

In Ref. [2] no information is given about the amount of admixed transurania or fission products to the plutonium or about the uranium in the MOX.

For PWRs it seems worthwhile to study the feasibility to incinerate the self-generated long-lived isotopes, both with the standard and with the highly moderated lattice. Thus for selected cases it is proposed to make the same calculations as those described in the sub-section of *Detailed benchmark specification*, entitled *Stage 1: Initial stage with UO<sub>2</sub> PWRs*. It may be assumed that the additional materials may be admixed homogeneously to the MOX fuel. The preference for the uranium in this MOX is:

- a) Depleted uranium if possible. This leads to a maximum amount of transurania in the expensive MOX FA.
- b) Natural or even enriched uranium in cases, where the need for high Pu<sub>fiss</sub> contents with depleted uranium would lead to safety concerns.

In Ref. [2] it is proposed to use the second generation MOX<sub>xx2</sub> plutonium in the “transmutation PWR”. However, it might also be of general interest to investigate the P&T potential of PWRs with first generation plutonium MOX<sub>xx1</sub>. Thus we propose to consider all available plutonium compositions from Stages 1 and 2 for the incineration studies of Stage 3. The transurania fraction of the fuel should not exceed 10%. Some possibilities for the additives are:

- NP33<sub>1</sub>, NP33<sub>2</sub> and NP33<sub>1</sub> + NP33<sub>2</sub> in a 33 GWd/tHM PWR with U325FA.
- NP50<sub>1</sub>, NP50<sub>2</sub> and NP50<sub>1</sub> + NP50<sub>2</sub> in a 50 GWd/tHM PWR with U465FA.
- NPAM33<sub>1</sub>, NPAM33<sub>2</sub> and NPAM33<sub>1</sub> + NPAM33<sub>2</sub> 33 GWd/tHM PWR with U325FA.
- NPAM50<sub>1</sub>, NPAM50<sub>2</sub> and NPAM50<sub>1</sub> + NPAM50<sub>2</sub> 50 GWd/tHM PWR with U465FA.
- TRU33<sub>1</sub>, TRU33<sub>2</sub> and TRU33<sub>1</sub> + TRU33<sub>2</sub> in a 33 GWd/tHM PWR with U325FA.
- TRU50<sub>1</sub>, TRU50<sub>2</sub> and TRU50<sub>1</sub> + TRU50<sub>2</sub> in a 50 GWd/tHM PWR with U465FA.
- TC33<sub>1</sub>, TC33<sub>2</sub> and TC33<sub>1</sub> + TC33<sub>2</sub> in a 33 GWd/tHM PWR with U325FA.
- TC50<sub>1</sub>, TC50<sub>2</sub> and TC50<sub>1</sub> + TC50<sub>2</sub> in a 50 GWd/tHM PWR with U465FA.
- I33<sub>1</sub>, I33<sub>2</sub> and I33<sub>1</sub> + I33<sub>2</sub> in a 33 GWd/tHM PWR with U325FA.
- I50<sub>1</sub>, I50<sub>2</sub> and I50<sub>1</sub> + I50<sub>2</sub> in a 50 GWd/tHM PWR with U465FA.
- CS33<sub>1</sub>, CS33<sub>2</sub> and CS33<sub>1</sub> + CS33<sub>2</sub> in a 33 GWd/tHM PWR with U325FA.
- CS50<sub>1</sub>, CS50<sub>2</sub> and CS50<sub>1</sub> + CS50<sub>2</sub> in a 50 GWd/tHM PWR with U465FA.

The most interesting case from the physics point of view is the transmutation of neptunium and americium together (NPAM<sub>xx</sub>).

For caesium technical problems may occur with <sup>137</sup>Cs. This isotope with  $T_{1/2} = 30$  years is also a fission product and must be taken into account in some way (e.g. 100 years cooling time).

In the case some of these investigations are successful for PWRs, larger amounts of the materials may be admixed to the fuel, e.g. the inventories of 2,3,...,  $N_{max}$  reactor systems. These specifications could be fixed in a later stage of the benchmark investigations.

### *Specifications for the highly moderated PWR*

The cell specifications for the highly moderated PWR with moderator to fuel ratio 3 are given in Table 1. The determination of the required  $Pu_{fis}$  in the MOX should be performed on the basis of a 3 000 MW<sub>th</sub> full MOX PWR. With fundamental mode diffusion calculations the end of cycle reactivity condition  $k_{eff}^{EOC} = 1$  must be satisfied. It is proposed to use the geometrical buckling of a cylindrical core with height to diameter ratio one ( $H/D=1$ ). For this conditions we obtain:

- For the geometry  $H = D = 362.8$  cm.
- For the geometrical buckling:  $B_g^2 = 2.50 \cdot 10^{-4} \text{ cm}^{-2}$ .

### **Summary**

Within the framework of an international NEA/NSC benchmark on P&T of transurania and fission products with available concepts, this paper proposes the specifications for PWRs.

Figure 2 gives an overview for the three stages:

- 1) The initial stage with PWRs, producing the first generation plutonium, other transurania and fission products.
- 2) The recycling stage with reload of the first generation plutonium to PWRs, producing second generation plutonium and further transurania and fission products.
- 3) The transmutation stage. Among various transmutation concepts, the use of PWRs is also considered.

Two target burn-up values (33 and 50 GWd/tHM) are proposed for Stage 1 to obtain quantitative information about the impact of target burn-up increase on long-term radiological consequences.

In accordance with actual developments for MOX loading in PWRs, for Stage 2 a mixed core with UO<sub>2</sub> and MOX fuel assemblies is proposed. The partition of MOX FA to the core amounts 30%. The proposed equivalency criteria for UO<sub>2</sub> and MOX FA in the same PWR core is based on initial experiences in French and German PWRs with UO<sub>2</sub>/MOX loadings.

For the transmutation stage with PWRs, it is proposed to investigate both standard and highly moderated PWRs. Depleted uranium should preferably be used in the MOX FA because this leads to maximum plutonium consumption. For cases where criticality requirements lead to too high plutonium fractions with depleted uranium, natural or even enriched uranium may be taken into account.

## REFERENCES TO APPENDIX A.1

- [1] S. Matsuura, *et al.*, “Overview of Physics Aspects of Different Transmutation Concepts”, NEA/NSC/DOC(94)11 (1994).
- [2] S. Matsuura, *et al.*, “Summary Record of the NSC Task Force Meeting on Physics Aspects of Different Transmutation Concepts”, NEA/NSC/DOC(94)34 (1994).
- [3] J. Vergnes, “First Proposition of Scenario for the Second Part of the CEA-EDF-KfK-Siemens Benchmark on Plutonium Multi-Recycling in PWR”, private communication (1993).
- [4] J. Vergnes, C. Broeders, L. Payen, “Plutonium Multi-Recycling in PWRs: Benchmark EDF-KfK”, EDF Note HT-11/95/003/A (1995).
- [5] Discussion on NEA/NSC/DOC(94)34 at FZK, 20/04/1995. Participants: P. Little (BNFL), C. Zimmermann (BNFL), C. Broeders (FZK), H. Küsters (FZK).
- [6] D. Lutz, W. Bernnat, E. Sartori, “Physics of Plutonium Recycling, Vol. 2, Benchmark on Plutonium Recycling in PWRs”, OECD/NEA (1995).
- [7] C. Broeders, L. Payen, private communication (1995).
- [8] C.H.M. Broeders, “Entwicklungsarbeiten für die neutronenphysikalische Auslegung von Fortschrittlichen Druckwasserreaktoren (FDWR) mit kompakten Dreiecksgittern in hexagonalen Brennelemente”, KfK5072 (1992).

**Table 1. Benchmark cell specifications for PWR**

Parameter	Name	Unity	Value
Moderator to fuel ratio $\left( \frac{V_m}{V_f} = \frac{r_m^2 - r_c^2}{r_f^2} \right)$	$R_{m,std}$ $R_{m,high}$		1.929 3.
Fuel radius	$r_f$	cm	0.4095
Can radius	$r_c$	cm	0.4750
Lattice pitch	$p_{std}$ $p_{high}$	cm	1.3133 1.5130
Moderator radius	$r_{m,std}$ $r_{m,high}$	cm	0.7410 0.8536
Specific power	$P_s$	MW/tHM	38.30
Power rating	$P_l$	W/cm	183.02
Theoretical UO <sub>2</sub> density	$\rho_{UO_2}$	g/cm <sup>3</sup>	10.96
Theoretical PuO <sub>2</sub> density	$\rho_{PuO_2}$	g/cm <sup>3</sup>	11.46
Oxide fuel density	$\rho_{ox}$	g/cm <sup>3</sup>	10.29
Zirconium density	$\rho_{zy}$	g/cm <sup>3</sup>	6.55
Water density	$\rho_{H_2O}$	g/cm <sup>3</sup>	0.7136
Fuel temperature	$T_f$	°C	660.0
Moderator temperature	$T_m$	°C	306.3

**Table 2. Benchmark BOL number density specifications for PWR UO<sub>2</sub> cell**

Zone	Isotope	Concentration (Nuclei/ cm <sup>3</sup> )	
		3.25% <sup>235</sup> U	4.65% <sup>235</sup> U
<b>Fuel</b>	O	4.59339 10 <sup>22</sup>	4.59410 10 <sup>22</sup>
	<sup>235</sup> U	7.55641 10 <sup>22</sup>	1.08113 10 <sup>22</sup>
	<sup>238</sup> U	2.22113 10 <sup>22</sup>	2.18894 10 <sup>22</sup>
<b>Cladding</b>	Zr	4.33646 10 <sup>22</sup>	4.33646 10 <sup>22</sup>
<b>Moderator</b>	H	4.77692 10 <sup>22</sup>	4.77692 10 <sup>22</sup>
	O	2.38846 10 <sup>22</sup>	2.38846 10 <sup>22</sup>

**Table 3. Proposed macro steps for depletion calculations**

<b>Step</b>	<b>Burn-up (MWd/tHM)</b>	<b><math>\Delta(T)^\ddagger</math> (days)</b>
1	0.00	0.000
2	150.00	3.916
3	500.00	9.138
4	1 000.00	13.055
5	2 000.00	26.110
6	4 000.00	52.219
7	6 000.00	52.219
8	10 000.00	104.439
9	15 000.00	130.548
10	20 000.00	130.548
11	22 000.00	52.219
12	26 000.00	104.439
13	30 000.00	104.439
14	33 000.00	78.329
15	33 300.00	7.833
16	35 000.00	44.386
17	40 000.00	130.548
18	45 000.00	130.548
19	50 000.00	130.548

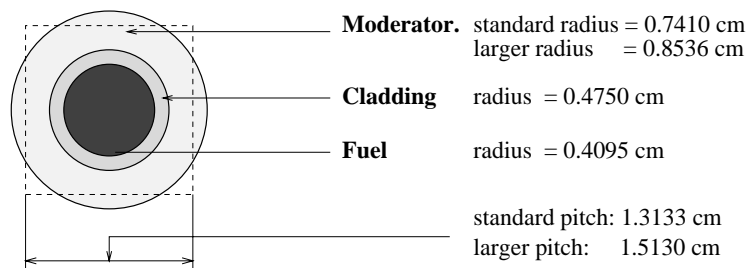
<sup>‡</sup> Power rating 183.02 W/cm.



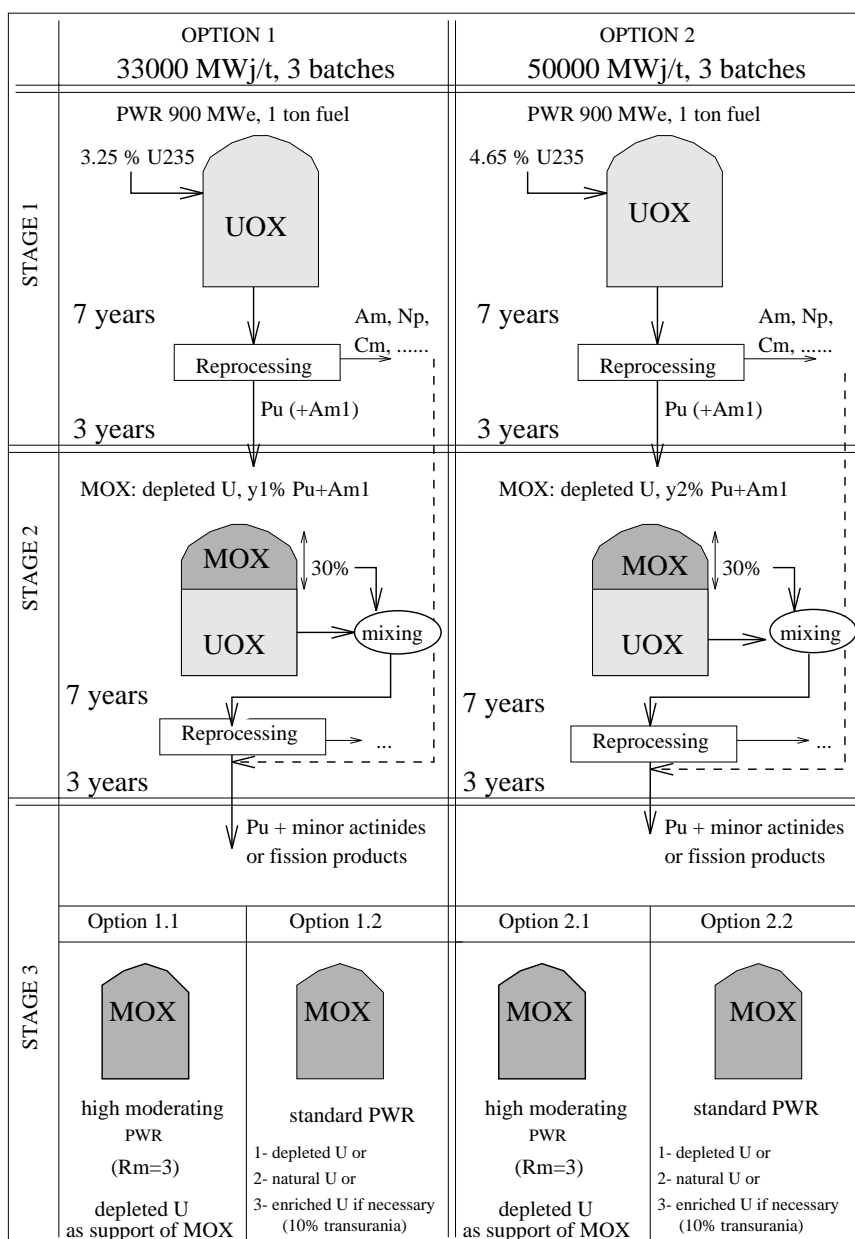
**Table 4. Stage 3 materials for PWR**

<b>Uranium</b>	
Depleted uranium	U020
Natural uranium	U070
x.yz% Enriched uranium	Uxyz
3.25% Enriched uranium fuel assemblies	U325FA
4.65% Enriched uranium fuel assemblies	U465FA
<b>Neptunium</b>	
Neptunium from Stage 1 and 33 GWd/tHM burn-up	NP33 <sub>1</sub>
Neptunium from Stage 2 and 33 GWd/tHM burn-up	NP33 <sub>2</sub>
Neptunium from Stage 1 and 50 GWd/tHM burn-up	NP50 <sub>1</sub>
Neptunium from Stage 2 and 50 GWd/tHM burn-up	NP50 <sub>2</sub>
<b>Plutonium</b>	
Plutonium from Stage 1 and 33 GWd/tHM burn-up	MOX33 <sub>1</sub>
Plutonium from Stage 2 and 33 GWd/tHM burn-up	MOX33 <sub>2</sub>
Plutonium from Stage 1 and 50 GWd/tHM burn-up	MOX50 <sub>1</sub>
Plutonium from Stage 2 and 50 GWd/tHM burn-up	MOX50 <sub>2</sub>
<b>Americium</b>	
Americium from Stage 1 and 33 GWd/tHM burn-up	AM33 <sub>1</sub>
Americium from Stage 2 and 33 GWd/tHM burn-up	AM33 <sub>2</sub>
Americium from Stage 1 and 50 GWd/tHM burn-up	AM50 <sub>1</sub>
Americium from Stage 2 and 50 GWd/tHM burn-up	AM50 <sub>2</sub>
<b>Mixed Neptunium and Americium (NPAM)</b>	
NPAM from Stage 1 and 33 GWd/tHM burn-up	NPAM33 <sub>1</sub>
NPAM from Stage 2 and 33 GWd/tHM burn-up	NPAM33 <sub>2</sub>
NPAM from Stage 1 and 50 GWd/tHM burn-up	NPAM50 <sub>1</sub>
NPAM from Stage 2 and 50 GWd/tHM burn-up	NPAM50 <sub>2</sub>
<b>Mixed Neptunium, Americium and Curium (TRU)</b>	
TRU from Stage 1 and 33 GWd/tHM burn-up	TRU33 <sub>1</sub>
TRU from Stage 2 and 33 GWd/tHM burn-up	TRU33 <sub>2</sub>
TRU from Stage 1 and 50 GWd/tHM burn-up	TRU50 <sub>1</sub>
TRU from Stage 2 and 50 GWd/tHM burn-up	TRU50 <sub>2</sub>
<b>Selected Fission Products</b>	
<sup>99</sup> Tc from Stage 1 and 33 GWd/tHM burn-up	TC33 <sub>1</sub>
<sup>99</sup> Tc from Stage 2 and 33 GWd/tHM burn-up	TC33 <sub>2</sub>
<sup>99</sup> Tc from Stage 1 and 50 GWd/tHM burn-up	TC50 <sub>1</sub>
<sup>99</sup> Tc from Stage 2 and 50 GWd/tHM burn-up	TC50 <sub>2</sub>
<sup>129</sup> I from Stage 1 and 33 GWd/tHM burn-up	I33 <sub>1</sub>
<sup>129</sup> I from Stage 2 and 33 GWd/tHM burn-up	I33 <sub>2</sub>
<sup>129</sup> I from Stage 1 and 50 GWd/tHM burn-up	I50 <sub>1</sub>
<sup>129</sup> I from Stage 2 and 50 GWd/tHM burn-up	I50 <sub>2</sub>
<sup>135</sup> Cs from Stage 1 and 33 GWd/tHM burn-up	CS33 <sub>1</sub>
<sup>135</sup> Cs from Stage 2 and 33 GWd/tHM burn-up	CS33 <sub>2</sub>
<sup>135</sup> Cs from Stage 1 and 50 GWd/tHM burn-up	CS50 <sub>1</sub>
<sup>135</sup> Cs from Stage 2 and 50 GWd/tHM burn-up	CS50 <sub>2</sub>

**Figure 1. Benchmark cell geometry for PWR, t = 20°C**



**Figure 2. Proposed benchmark calculations for PWRs**



## Appendix A.2

### Proposal for a benchmark calculation of MA transmutation in fast reactors (1 000 MWe)

**T. Wakabayashi**

Japan Nuclear Cycle Fuel Development Institute (JNC)  
4-49, Murumatsu, Tokai-mura, Naka-gun, Ibaraki, 319-1184, Japan

#### Introduction

The present proposal is made in the framework of the benchmark calculations of the Nuclear Science Committee of the NEA.

The data necessary to the neutronics calculation are given both for the subassemblies and for the core. Geometrical characteristics are given at 20°C, unless values in 5 to 7 corresponding to operating conditions.

#### Fuel subassembly

- Fissile column height: 1 000 mm.
- Subassembly lattice dimension: 179.8 mm.
- Number of pins/subassembly: 271.
- External clad diameter: 8.3 mm.
- Pellet diameter: 7.32 mm.
- Nature and density of the fuel: mixed  $\text{UO}_2\text{-PuO}_2 (= 0.48 \times \text{PR} + 5.96 + 2.5 \times \text{OM})$   
PR: Pu ratio OM: 1.98.
- Uranium isotopic composition:

	$^{235}\text{U}$	$^{238}\text{U}$
at%	0.30	99.70

- Plutonium isotopic composition: PWR  $\text{UO}_2$  fuel (50 Gwd/tHM, seven year cooling):

	$^{238}\text{Pu}$	$^{239}\text{Pu}$	$^{240}\text{Pu}$	$^{241}\text{Pu}$	$^{242}\text{Pu}$	$^{241}\text{Am}$
at %	2.76	53.74	24.24	10.63	2.76	1.65

- Pu/U + Pu ratio for inner and outer cores: 15.3%, 19.1% (wt%)(without MA: reference);
- Pu/U + Pu ratio for inner and outer cores: 15.22%, 18.96% (with 2.5% MA);
- Pu/U + Pu ratio for inner and outer cores: 15.13%, 18.84% (with 5% MA);
- Composition and density of steel (hexagonal tube and cladding): 7.97 g/cm<sup>3</sup>:

	<b>Fe</b>	<b>Cr</b>	<b>Ni</b>	<b>Mo</b>	<b>Mn</b>
<b>Mass %</b>	60.97	15.05	19.50	2.51	1.97

- Volume fraction of subassembly components:

	<b>UPuO<sub>2</sub></b>	<b>Steel</b>	<b>Sodium</b>
<b>Vol. %</b>	37.45	19.74	37.75

- Numbers of S/As in inner and outer cores: 175, 180.
- Density of sodium: 0.84867 g/cm<sup>3</sup> at 430°C.

### *Reflector subassembly*

- Volume fraction of components:

	<b>Axial</b>		<b>Radial</b>	
	<b>Steel</b>	<b>Sodium</b>	<b>Steel</b>	<b>Sodium</b>
<b>Vol. %</b>	19.74	37.52	80.0	20.0

### *Control subassembly*

- Absorber part: not calculated.
- Composition for the follower part:

	<b>Steel</b>	<b>Sodium</b>
<b>Vol. %</b>	7.622	92.378

### *Operating conditions*

- Thermal power: 2 600 MW.
- Cycle length and load factor: 365 EFPD.
- Residence time of fuel subassemblies: 1 095 EFPD.

- Core: 3 batch.
- Blanket: 4 batch.

### *Cell calculations*

- Fuel cell, cladding, tube and sodium: homogenised cells.
- Rod follower, reflectors: homogenised cells.

### *Spatial calculations*

- Reactor core map: see Figure 1.
- RZ geometry: see Figure 2.
- Mesh size: ~5cm, both R and Z.
- Broad group structure (~7 groups): see Table 1 (example).
- Boundary conditions:  $\Phi = 0$  on the outer boundary.

### *Atomic number densities*

- Atomic densities: see Table 2 (start of burn-up calculation).

### *Required calculations (RZ geometry)*

- 1)  $k_{\text{eff}}$  (In diffusion theory. Possibly: transport effects):
  - 0 EFPD (beginning of life).
  - 365 EFPD (beginning of first cycle).
  - 1 460 EFPD (beginning of fourth cycle, equilibrium cycle).
  - 1 825 EFPD (end of fourth cycle, end of life).
- 2) Critical balance components (productions, absorptions, leakage) and decomposition by isotope:
  - 0 EFPD (beginning of life).
  - 365 EFPD (beginning of first cycle).
  - 1 460 EFPD (beginning of fourth cycle, equilibrium cycle).
  - 1 825 EFPD (end of fourth cycle, end of life).

3) Spectrum indices at core centre:

$$\frac{C(^{238}\text{U})}{F(^{239}\text{Pu})} \quad \frac{F(^{238}\text{U})}{F(^{239}\text{Pu})} \quad \frac{F(^{240}\text{Pu})}{F(^{239}\text{Pu})} \quad \frac{F(^{241}\text{Pu})}{F(^{239}\text{Pu})}$$

- 0 EFPD (beginning of life).
  - 1 460 EFPD (beginning of fourth cycle, equilibrium cycle).
  - 1 825 EFPD (end of fourth cycle, end of life).
- 4) Burn-up calculation, at a thermal power of 2 600 MW, in three steps with flux calculation at each step:
- 0 EFPD (beginning of life).
  - 365 EFPD (beginning of first cycle).
  - 730 EFPD (end of first cycle).
  - 730 EFPD (beginning of second cycle).
  - 1 095 EFPD (end of second cycle).
  - 1 095 EFPD (beginning of third cycle).
  - 1 460 EFPD (end of 3rd cycle).
  - 1 460 EFPD (beginning of fourth cycle, equilibrium cycle).
  - 1 825 EFPD (end of fourth cycle, end of life).

Reactivity loss with breakdown into fission product and heavy isotope components.

- 5) Inner core and outer core isotopic compositions at the end of life (including minor actinides build-up).
- 6) Definition of transmutation rate:
- Transmutation rate =  $\frac{((\text{Loaded Mass of MA at BOC}) - (\text{Discharged Mass of MA at EOC}))}{(\text{Loaded Mass of MA at BOC})}$
- 7) Sodium void coefficient for inner core and whole core, with breakdown into components (derived from perturbation theory calculations):
- Axial leakage component.
  - Radial leakage component.
  - Scattering (spectral) component.

- Absorption component.
- Production component.

At beginning of fourth cycle (BOC) and end of fourth cycle (EOC).

8) Fuel Doppler reactivity at BOC and EOC, defined as:

$$k_{\text{eff}}^1(T = 1100^\circ\text{C}) - k_{\text{eff}}^2(T = 1600^\circ\text{C}) / k_{\text{eff}}^1 \cdot k_{\text{eff}}^2$$

Decomposition by isotope.

9) Decay heat of irradiated fuel subassembly (IC and OC) at the end of the cycle and successive cooling times  $T_c$ :  $T_c = 1$  day, 1 month, 3 months, 1 year.

10) Neutron sources and activity of irradiated fuel subassemblies.

11) Radiotoxicity of wastes at various cooling times (see appendix):

$$T_c = 0, 100 \text{ y}, 1\,000 \text{ y}, T_c = 10\,000 \text{ y}, T_c = 100\,000 \text{ y}, T_c = 1\,000\,000 \text{ y}$$

(Hypothesis on reprocessing losses: 0.3% Pu and 1% minor actinides.)

### **Radiotoxicity calculation**

The calculation of the radiotoxicity will be performed as indicated below, starting from the isotopic composition of the discharged irradiated fuel ( $T_c = 0$ ):

- Calculation of the mass of the descendants at various cooling time, for each nuclide initially present in the wastes. The nuclides to be taken into account are plutonium, neptunium, americium and curium and the fission products  $^{99}\text{Tc}$ ,  $^{129}\text{I}$  and  $^{135}\text{Cs}$ .
- Calculation of their respective activities in becquerels.
- Calculation of the corresponding radiotoxicities and summation on the whole descendance for a given initial nuclide. The radiotoxicity is obtained when multiplying the activity by the hazard factor defined in Table 3.

**Table 1. Group energetic mesh**

7G	18G	70G	Upper energy	Lower energy	Lethargy width
1	1	1	10.0000 (MeV)	7.7880 (MeV)	0.25
		2	7.7880	6.0653	0.25
	2	3	6.0653	4.7237	0.25
		4	4.7237	3.6788	0.25
2	3	5	3.6788	2.8650	0.25
		6	2.8650	2.2313	0.25
	4	7	2.2313	1.7377	0.25
		8	1.7377	1.3534	0.25
3	5	9	1.3534	1.0540	0.25
		10	1.0540	0.82085	0.25
	6	11	0.82085	0.63928	0.25
		12	0.63928	0.49787	0.25
		13	0.49787	0.38774	0.25
	7	14	0.38774	0.30197	0.25
		15	0.30197	0.23518	0.25
		16	0.23518	0.18316	0.25
	8	17	0.18316	0.14264	0.25
		18	0.14264	0.11109	0.25
		19	0.11109 (MeV)	86.517 (keV)	0.25
4	9	20	86.517 (keV)	67.379 (keV)	0.25
		21	67.379	52.475	0.25
		22	52.475	40.868	0.25
	10	23	40.868	31.828	0.25
		24	31.828	24.788	0.25
		25	24.788	19.305	0.25
	11	26	19.305	15.034	0.25
		27	15.034	11.709	0.25
		28	11.709	9.1188	0.25
5	12	29	9.1188	7.1017	0.25
		30	7.1017	5.5308	0.25
		31	5.5308	4.3074	0.25
	13	32	4.3074	3.3546	0.25
		33	3.3546	2.6126	0.25
		34	2.6126	2.0347	0.25
	14	35	2.0347	1.5846	0.25
		36	1.5846	1.2341	0.25
		37	1.2341 (keV)	0.96112 (keV)	0.25



**Table 1. Group energetic mesh (continued)**

<b>7G</b>	<b>18G</b>	<b>70G</b>	<b>Upper energy</b>	<b>Lower energy</b>	<b>Lethargy width</b>
6	15	38	961.12 (eV)	748.52 (eV)	0.25
		39	748.52	582.95	0.25
		40	582.95	454.00	0.25
	16	41	454.00	353.58	0.25
		42	353.58	275.36	0.25
		43	275.36	214.45	0.25
	17	44	214.45	167.02	0.25
		45	167.02	130.07	0.25
		46	130.07	101.30	0.25
7	18	47	101.30	78.893	0.25
		48	78.893	61.442	0.25
		49	61.442	47.851	0.25
		50	47.851	37.267	0.25
		51	37.267	29.023	0.25
		52	29.023	22.603	0.25
		53	22.603	17.603	0.25
		54	17.603	13.710	0.25
		55	13.710	10.677	0.25
		56	10.677	8.3153	0.25
		57	8.3153	6.4760	0.25
		58	6.4760	5.0435	0.25
		59	5.0435	3.9279	0.25
		60	3.9279	3.0590	0.25
		61	3.0590	2.3824	0.25
		62	2.3824	1.8554	0.25
		63	1.8554	1.4450	0.25
		64	1.4450	1.1254	0.25
		65	1.1254	0.87642	0.25
		66	0.87642	0.68256	0.25
		67	0.68256	0.53158	0.25
		68	0.53158	0.41399	0.25
		69	0.41399	0.32242	10.65
		70	0.32242 (eV)	1.00E-05 (eV)	

Table 2. Homogenised atomic density

Nuclide	Reference core		MA 2.5% core		MA 5.0% core		Axial blanket	Radial blanket	Upper shield	Radial shield	Sodium follower
	Inner core (Pu 15.4%)	Outer core (Pu 19.1%)	Inner core (Pu 15.22%)	Outer core (Pu 18.96%)	Inner core (Pu 15.13%)	Outer core (Pu 18.84%)					
<sup>238</sup> Pu	3.9035E-05	4.8493E-05	3.8605E-05	4.8156E-05	3.8376E-05	4.7861E-05					
<sup>239</sup> Pu	7.5686E-04	9.4025E-04	7.4853E-04	9.3371E-04	7.4409E-04	9.2799E-04					
<sup>240</sup> Pu	3.3997E-04	4.2234E-04	3.3622E-04	4.1940E-04	3.3423E-04	4.1683E-04					
<sup>241</sup> Pu	1.4847E-04	1.8444E-04	1.4683E-04	1.8316E-04	1.4596E-04	1.8203E-04					
<sup>242</sup> Pu	9.7084E-05	1.2061E-04	9.6015E-05	1.1977E-04	9.5446E-05	1.1903E-04					
<sup>241</sup> Am	2.3043E-05	2.8627E-05	2.2770E-05	2.8410E-05	2.2690E-05	2.8230E-05					
<sup>235</sup> U	2.3607E-05	2.2611E-05	2.2954E-05	2.1948E-05	2.2281E-05	2.1281E-05	2.8822E-05	3.8136E-05			
<sup>238</sup> U	7.7462E-03	7.4196E-03	7.5321E-03	7.2020E-03	7.3112E-03	6.9830E-03	9.4576E-03	1.2514E-02			
O	1.8165E-02	1.8190E-02	1.8162E-02	1.8187E-02	1.8159E-02	1.8184E-02	1.8973E-02	2.5104E-02			
Na	8.3436E-03	8.3436E-03	8.3436E-03	8.3436E-03	8.3436E-03	8.3436E-03	8.3436E-03	6.0635E-03	8.3453E-03	4.4484E-03	2.0547E-02
Fe	1.0343E-02	1.0343E-02	1.0343E-02	1.0343E-02	1.0343E-02	1.0343E-02	1.0343E-02	8.4772E-03	1.0344E-02	4.1922E-02	3.9941E-03
Cr	2.7421E-03	2.7421E-03	2.7421E-03	2.7421E-03	2.7421E-03	2.7421E-03	2.7421E-03	2.2475E-03	2.7425E-03	1.1115E-02	1.0589E-03
Ni	3.1476E-03	3.1476E-03	3.1476E-03	3.1476E-03	3.1476E-03	3.1476E-03	3.1476E-03	2.5799E-03	3.1482E-03	1.2759E-02	1.2156E-03
Mo	2.4785E-04	2.4785E-04	2.4785E-04	2.4785E-04	2.4785E-04	2.4785E-04	2.4785E-04	2.0315E-04	2.4791E-04	1.0047E-03	9.5721E-05
Mn	3.3971E-04	3.3971E-04	3.3971E-04	3.3971E-04	3.3971E-04	3.3971E-04	3.3971E-04	2.7844E-04	3.3977E-04	1.3770E-03	1.3119E-04
<sup>237</sup> Np			1.1586E-04	1.1605E-04	2.3172E-04	2.3210E-04					
<sup>241</sup> Am*			7.8930E-05	7.9060E-05	1.5780E-04	1.5810E-04					
<sup>242m</sup> Am			1.8071E-07	1.8101E-07	3.6141E-07	3.6200E-07					
<sup>243</sup> Am			2.5443E-05	2.5485E-05	5.0884E-05	5.0967E-05					
<sup>243</sup> Cm			1.1248E-07	1.1267E-07	2.2495E-07	2.2532E-07					
<sup>244</sup> Cm			7.4829E-06	7.4951E-06	1.4965E-05	1.4989E-05					
<sup>245</sup> Cm			4.4624E-07	4.4697E-07	8.9245E-07	8.9390E-07					

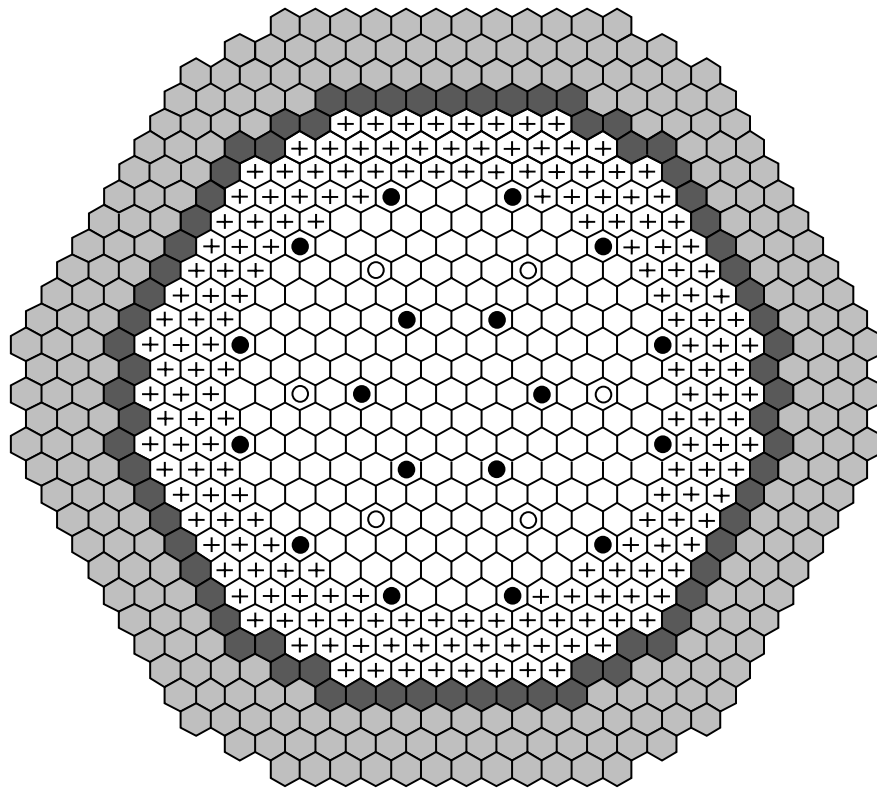
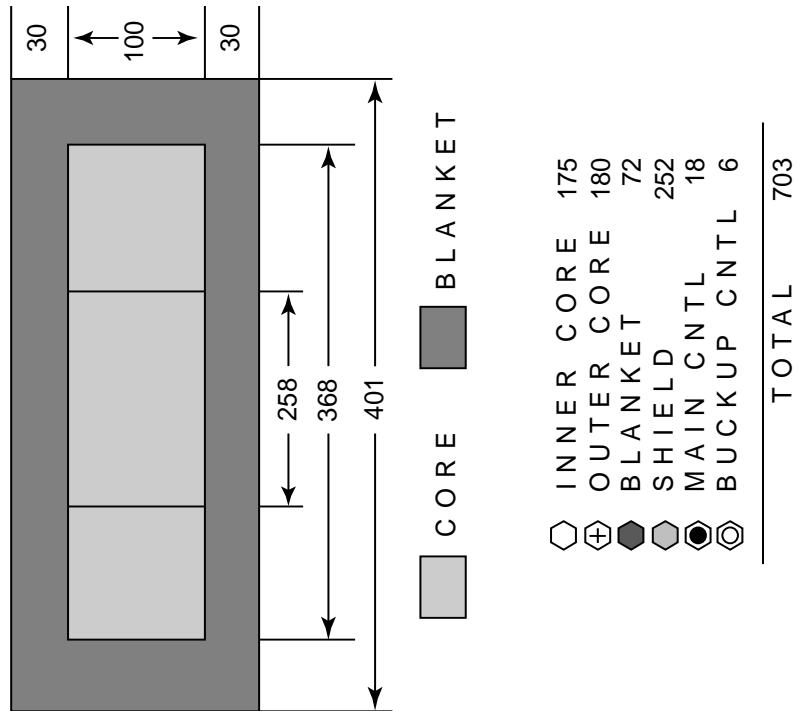
\* <sup>241</sup>Am in MA MA (Mass); MA/(MA + Pu + U)

**Table 3. Hazard ingestion factors**

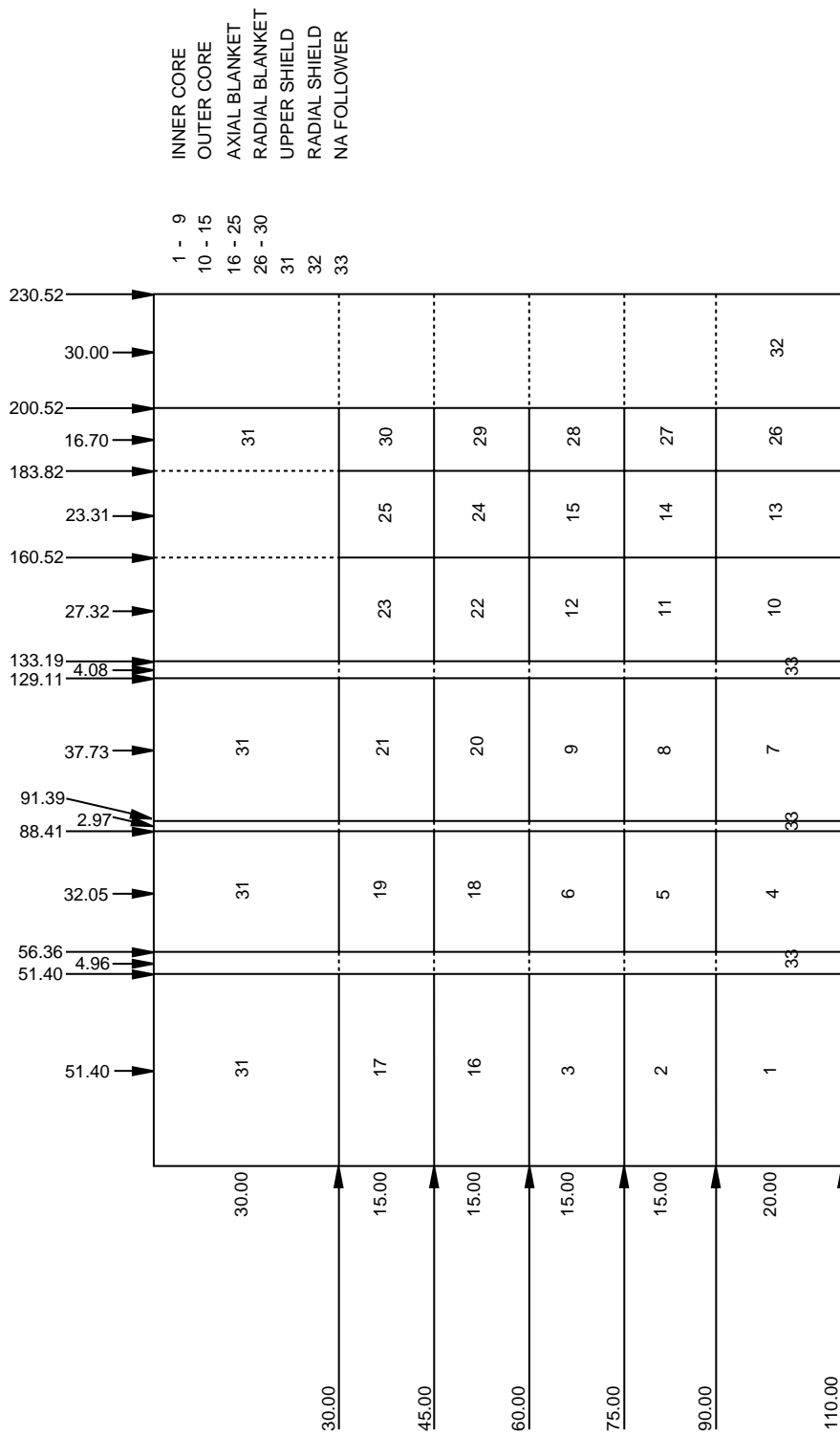
Nuclide	Hazard ingestion factor (Sv.Bq <sup>-1</sup> )	Nuclide	Hazard ingestion factor (Sv.Bq <sup>-1</sup> )
<sup>227</sup> Ac *	3.9E-6	<sup>226</sup> Ra *	3.05E-7
<sup>241</sup> Am	1.20E-6	<sup>228</sup> Ra *	3.40E-7
<sup>242m</sup> Am *	1.14E-6	<sup>228</sup> Th *	2.00E-7
<sup>243</sup> Am *	1.19E-6	<sup>229</sup> Th *	1.05E-6
<sup>242</sup> Cm	3.54E-8	<sup>230</sup> Th	1.45E-7
<sup>243</sup> Cm	7.86E-7	<sup>232</sup> Th	7.40E-7
<sup>244</sup> Cm	6.00E-7	<sup>232</sup> U	3.44E-7
<sup>245</sup> Cm	1.20E-6	<sup>233</sup> U	7.20E-8
<sup>246</sup> Cm	1.19E-6	<sup>234</sup> U	7.20E-8
<sup>247</sup> Cm *	1.11E-6	<sup>235</sup> U *	6.80E-8
<sup>248</sup> Cm	4.40E-6	<sup>236</sup> U	6.70E-8
<sup>237</sup> Np *	1.06E-6	<sup>238</sup> U *	6.70E-8
<sup>231</sup> Pa	2.89E-6	<sup>99</sup> Tc	3.4E-10
<sup>210</sup> Pb *	1.36E-6	<sup>129</sup> I	7.4E-8
<sup>236</sup> Pu	3.93E-7	<sup>135</sup> Cs	1.9E-9
<sup>238</sup> Pu	1.00E-6		
<sup>239</sup> Pu *	1.16E-6		
<sup>240</sup> Pu	1.16E-6		
<sup>241</sup> Pu *	2.36E-8		
<sup>242</sup> Pu	1.10E-6		
<sup>244</sup> Pu *	1.08E-6		

\* Indicates that the contribution of the short-life descendants is included.

Figure 1. Reference core (1 000 MWe class FBR)



**Figure 2. RZ geometry (burn-up calculation)**





### *Appendix A.3*

## **JAERI proposal of benchmark problem on method and data to calculate the nuclear characteristics in accelerator-based transmutation system with fast neutron flux**

**T. Nishida, T. Takizuka, T. Sasa**  
Transmutation System Laboratory  
Dept. of Reactor Engineering  
Japan Atomic Energy Research Institute  
Tokai-mura, Naka-gun, Ibaraki-ken, 319-11, Japan  
5 May 1995

### **Benchmark problem**

Since 1989, a conceptual design study has been carried out at JAERI on the intense proton accelerator-driven transmutation fast flux systems with solid and liquid target/core in the framework of the national research programme OMEGA on partitioning and transmutation [1,2]. JAERI's accelerator-based system aims mainly at developing a burning system for minor actinides (MA) in high level waste (HLW) discharged from the reprocessing plant of LWR spent fuel, and not the plutonium burning system. Therefore, we would like to propose an appropriate benchmark problem of code and data validation in preliminary design study for a module of a proton accelerator-driven transmutation system based on the specifications as summarised in Table 1. The dirty plutonium from HLW is mixed into MA fuel to suppress the reactivity swing at the first burn-up stage. Here plutonium and MA in HLW, obtained through partitioning after seven years cooling of products from reprocessing the fuel burned up to 33 GWd/tHM (plus three years of manufacturing time) have compositions as in Table 2 (this fuel is denoted as MOX11).

Three more fuel compositions based on Pu and MA vectors denoted as MOX21, MOX12, and MOX22 have been added to this benchmark as shown in Table 2. These extra cases are considered by the FZK (Germany), which proposes investigating the physics of different transmutation concepts in PWRs (see details in the PWR benchmark proposal). Hence, MOX21 refers to plutonium and MA compositions resulting from the reprocessing of 4.65% UO<sub>2</sub> fuel from a Stage 1 PWR burned to 50 MWd/tHM, MOX12 refers to plutonium and MA compositions resulting from the reprocessing of 4.1% MOX11 burned to 33 MWd/tHM in a Stage 2 PWR and then admixed with depleted uranium, and MOX22 refers to Pu and MA compositions resulting from the reprocessing of 6.0% MOX21 burned to 50 MWd/tHM in a Stage 2 PWR and then admixed with natural uranium. In all cases, seven years of cooling time of spent fuel before reprocessing plus three years of MOX manufacturing time is considered. The resulting accelerator fuel compositions are heavily MA dominated as required by the design constraints of the accelerator considered (sub-critical core).

Figure 1 shows the two dimensional model of our proposed accelerator-based fast flux system. This system consists of a two-region tungsten target injected by a proton beam, MA fuelled core and reflectors, each of which is cooled by sodium flow. The optimised target is a stack of tungsten discs

with two different thicknesses as shown in Figure 2(a) [6]. The MA nitride fuel pins are arranged in the core region as shown in Figure 2(b) [7]. Here the atom number densities are smeared in every region to simplify the benchmark problem, and the homogenised number densities are presented in Table 3.

### **Cross-section library**

Participants should use their own cross-section library and energy group structure and provide descriptions of both.

### **Code description [8,10]**

Code descriptions of the cascade code calculating the nuclear processes above 15 MeV energy and of the neutron transport code and the burn-up code for the energy range below 15 MeV should be provided. Specifically, the calculational method, energy group structure and the actinide chain considered in the burn-up calculations should be included in the code description.

### **Requested results**

This hybrid system is expected to be driven by a proton beam of 1 GeV energy and a current of 10 mA in the sub-critical state of  $k_{\text{eff}} = 0.9$ . The neutron transport process in target/core may be calculated as the fixed source problem based on spallation neutron distributions using transport code or diffusion code. Burn-up calculations should be made for actinides in the energy range below 15 MeV with the fixed neutron spectrum to make one-group cross-sections. Participants are requested to provide the following benchmark results that are specified in points a)-c).

- a) Spallation neutrons (energy range from 1 GeV to 15-20 MeV, initial core):
  - Number of spallation neutrons per incident proton.
  - Region averaged spallation neutron spectra in target and core.
  - Axial distribution of neutrons leaking from target at  $r = 150$  mm.
  - Maximum and average heat power densities in target region.
- b) Nuclear characteristics of transmutation target/core (energy range 15-20 MeV, initial core):
  - Effective neutron multiplication factor.
  - Sodium void reactivity effect (include sodium in target region).
  - Region averaged neutron spectra in target and core.
  - Average neutron energy in core region.
  - Axial neutron flux distributions at  $r = 75$  mm and  $r = 275$ mm.



- Average neutron flux in core region.
- Fission and capture reaction rates in whole core region.
- Maximum and average heat power density in core region.
- Amount of transmuted MA per year (only by fission).
- MA transmutation rate (only by fission).

c) Burn-up characteristics:

- Atom number densities for actinides (at the constant flux of  $1.0 \times 10^{16}$  n/cm<sup>2</sup>/s) at burn-up steps of 10, 50, 100, 150, 200 GWd/tHM.
- Time evolution of  $k_{\text{eff}}$  with burn-up.

### REFERENCES TO APPENDIX A.3

- [1] T. Takizuka, *et al.*, “A Study of Incineration Target System”, Proc. 5th Int. Conf. Emerg. Nucl. Systems, Karlsruhe (1989).
- [2] M. Mizumoto, *et al.*, “High Intensity Proton Accelerator for Nuclear Waste Transmutation”, 16th Int. Linear Accelerator Conf. LINAC-92, Ottawa (1992).
- [3] Y. Kato, *et al.*, “Accelerator Molten-Salt Target System for Transmutation of Long-Lived Nuclides”, Proc. OECD/NEA Specialists Meeting on Accelerator-Based Transmutation, PSI (1992).
- [4] H. Katsuta, *et al.*, “A Continuous Transmutation System for Long-Lived Nuclides with Accelerator-Driven Fluid Target”, Proc. 2nd Inform. Exch. Meeting, Argonne (1993).
- [5] H. Katsuta, *et al.*, “A Concept of Accelerator-Based Incineration System for Transmutation of TRU and FP with Liquid TRU-Alloy Target and Molten Salt Blanket”, Proc. ICENES’93, Makuhari (1993), pp. 424.
- [6] T. Nishida, *et al.*, “Minor Actinide Transmutation System with an Intense Proton Accelerator”, Proc. ICENES’93, Makuhari (1993), pp. 419.
- [7] T. Takizuka, *et al.*, “Conceptual Design Study of an Accelerator-Based Actinide Transmutation Plant with Sodium-Cooled Slid Target/Core”, Proc. 2nd Inform. Exch. Meeting, Argonne (1993), pp. 397.
- [8] Y. Nakahara, Tsutsui, “NMTC/JAERI – A Simulation Code System for High Energy Nuclear Reactions and Nucleon-Meson Transport Process”, JAERI-M 82-198 (1982) (in Japanese).
- [9] T. Nishida, *et al.*, “Improvement of Spallation Reaction Simulation Codes NMTC/JAERI and NUCLEUS”, 2nd Int. Symp. on Advanced Nuclear Energy Research, Mito (1990).
- [10] T. Nishhida, Y. Nakahara, JAERI-M 84-154 (1984) (in Japanese).

**Table 1. Specification of target/core transmutation system**

<b>Proton beam</b>	1.0 GeV, 10 mA
Beam radius	15 cm
Beam profile	Uniform
<b>Beam duct radius</b>	15 cm
<b>Target/core</b>	Concentric cylinders with height of 1 m
Radii	15 cm/40 cm
<b>Target</b>	Tungsten (disk layer type)
Upper region	Height 80 cm, radius 15 cm
Lower region	Height 26 cm, disk thickness 1.5 cm
<b>Fuel</b>	(90 MA-10 Pu)N (nitride pin-bundle type)
Pin outside diameter	7.3 cm
Pin pitch	9.9 cm
Pin height	80 cm
Fuel pellet diameter	6 cm
Sodium bond thickness	0.35 mm
Cladding thickness	0.3 mm (HT9 SS)
<b>Reflector</b>	Stainless steel
Inner/outer radii	40 cm/90 cm
Top thickness	30 cm
Bottom thickness	40 cm
<b>Sodium volume fraction</b>	
Target upper region	86%
Target lower region	37.2%
Core	61.7%
Reflector	41.3%

**Table 2. Actinide atom per cent fraction**

Fuel burn-up	MOX11	MOX21	MOX12	MOX22
	33 GWd/tHM	50 GWd/tHM	33 GWd/tHM	50 GWd/tHM
Nuclide atom%				
<sup>238</sup> Pu	1.5	2.7	2.6	4.1
<sup>239</sup> Pu	59.3	55.3	44.5	41.9
<sup>240</sup> Pu	23.7	23.9	31.0	30.5
<sup>241</sup> Pu	8.7	9.5	10.7	10.6
<sup>242</sup> Pu	5.5	7.1	9.5	11.3
<sup>241</sup> Am	1.3	1.5	1.7	1.7
<b>Total</b>	<b>100</b>	<b>100</b>	<b>100</b>	<b>100</b>
<sup>237</sup> Np	44.6	46.4	4.5	4.4
<sup>241</sup> Am	43.6	37.1	62.5	58.3
<sup>243</sup> Am	9.7	12.7	24.3	26.1
<sup>243</sup> Cm	0.0	0.0	0.0	0.0
<sup>244</sup> Cm	2.1	3.8	8.7	11.3
<sup>245</sup> Cm	0.0	0.0	0.0	0.0
<b>Total</b>	<b>100</b>	<b>100</b>	<b>100</b>	<b>100</b>

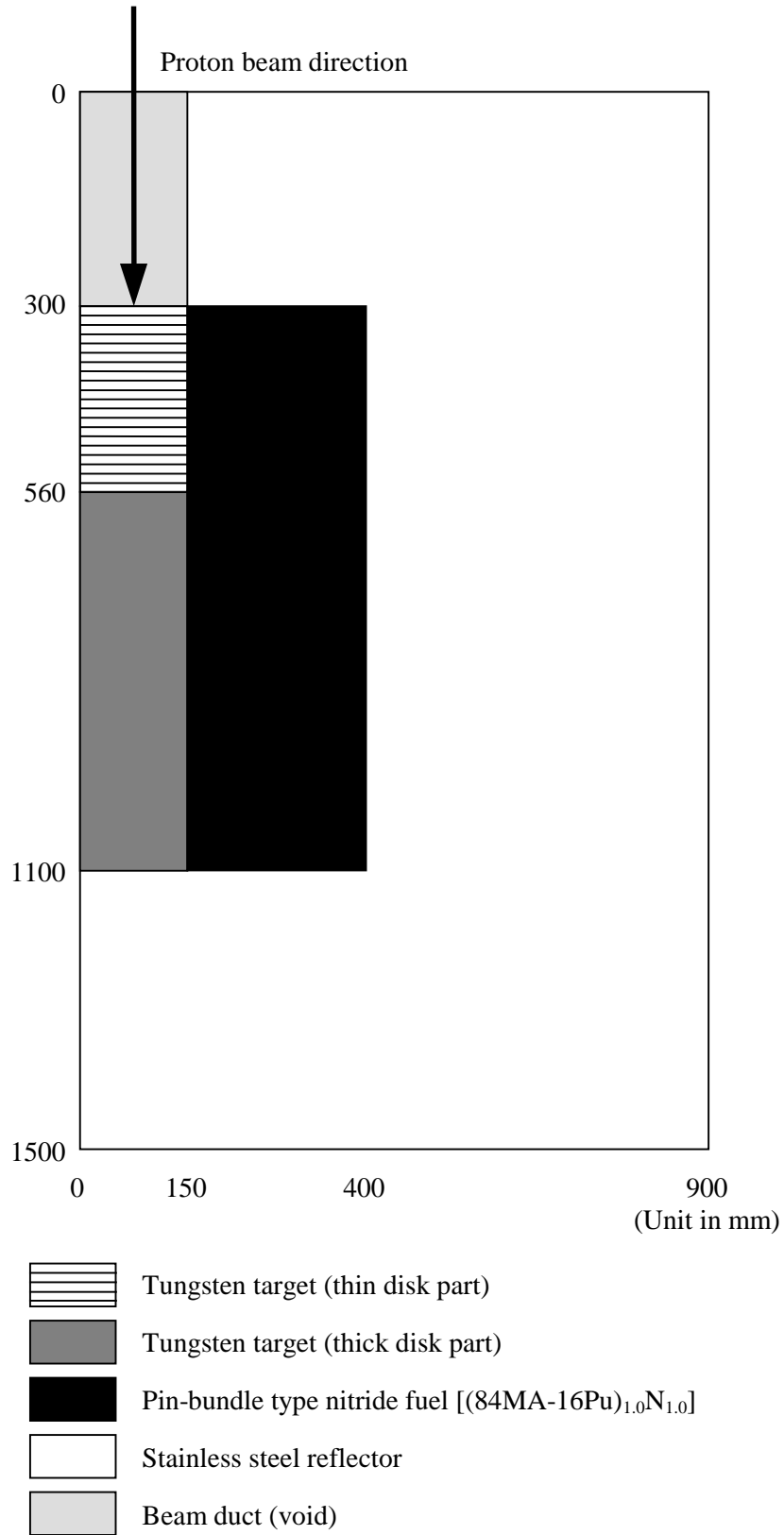
**Table 3. Homogenised atomic number densities ( $\times 10^{24}/\text{cm}^3$ )**

Nuclide	TARGET	
	Upper region	Lower region
<sup>182</sup> W	2.688E-03	1.075E-02
<sup>183</sup> W	1.453E-03	5.814E-03
<sup>184</sup> W	3.103E-03	1.241E-02
<sup>186</sup> W	2.859E-03	1.144E-02
<sup>23</sup> Na	1.821E-02	7.806E-03

Nuclide	Fuel			
	MOX11 33 GWd/tHM	MOX21 50 GWd/tHM	MOX12 33 GWd/tHM	MOX22 50 GWd/tHM
<sup>238</sup> Pu	1.251E-05	2.252E-05	2.169E-05	3.420E-05
<sup>239</sup> Pu	4.947E-04	4.613E-04	3.712E-04	3.495E-04
<sup>240</sup> Pu	1.977E-04	1.994E-04	2.586E-04	2.544E-04
<sup>241</sup> Pu	7.257E-05	7.924E-05	8.925E-05	8.842E-05
<sup>242</sup> Pu	4.588E-05	5.922E-05	7.924E-05	9.426E-05
<sup>241</sup> Am	1.084E-05	1.251E-05	1.418E-05	1.418E-05
<sup>237</sup> Np	3.353E-03	3.488E-03	3.383E-04	3.308E-04
<sup>241</sup> Am	3.278E-03	2.789E-03	4.699E-03	4.375E-03
<sup>243</sup> Am	7.293E-04	9.548E-04	1.827E-03	1.962E-03
<sup>244</sup> Cm	1.579E-04	2.857E-04	6.541E-04	8.495E-04
<sup>15</sup> N	8.352E-03			
<sup>23</sup> Na	1.296E-02			
<sup>182</sup> W	2.735E-06			
<sup>183</sup> W	1.555E-06			
<sup>184</sup> W	3.092E-06			
<sup>186</sup> W	2.868E-06			
<sup>12</sup> C	5.626E-05			
natSi	3.671E-05			
<sup>51</sup> V	2.094E-05			
natCr	8.206E-04			
<sup>55</sup> Mn	3.107E-05			
natFe	5.391E-03			
natNi	3.029E-05			
natMo	3.781E-05			

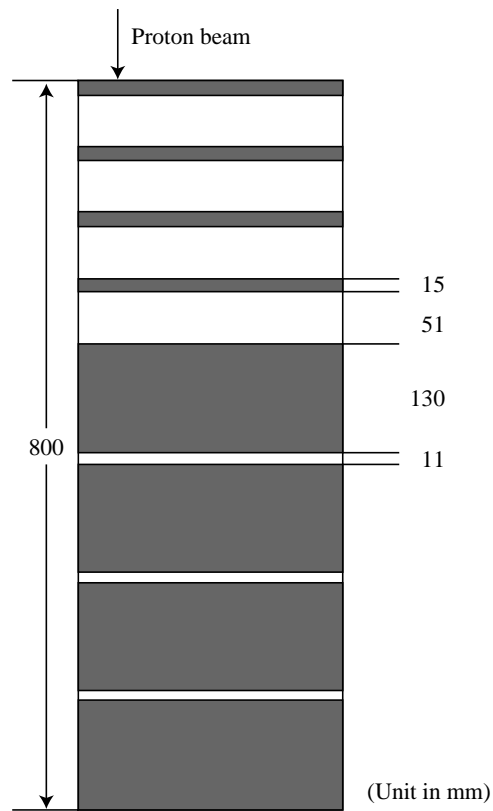
Nuclide	Reflector
<sup>23</sup> Na	8.673E-03
natCr	8.599E-03
<sup>55</sup> Mn	5.061E-04
natFe	3.424E-02
natNi	6.000E-03
natMo	1.265E-03

**Figure 4.1. Calculational model**

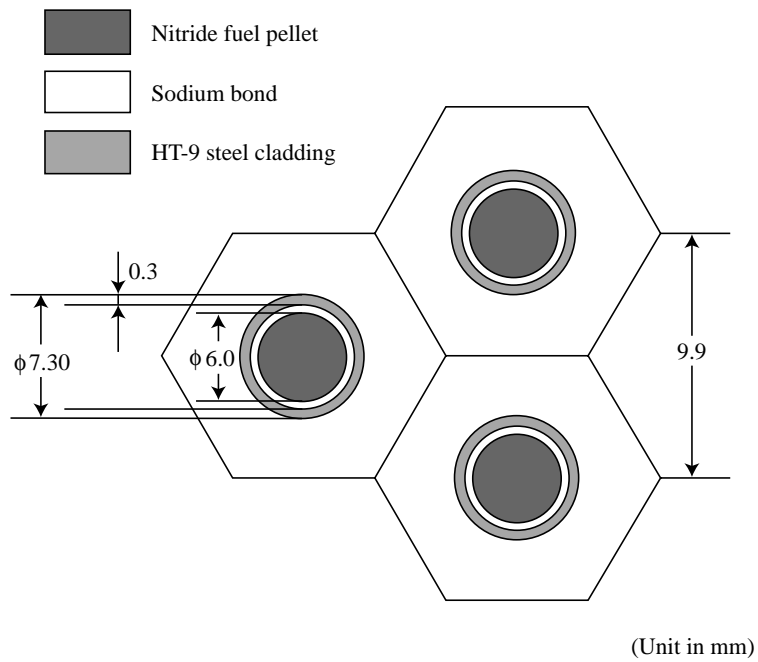


**Figure 4.2. Configurations of target and fuel**

*a) Disk-type tungsten target on which many flow holes are distributed for sodium coolant*



*b) Hexagonal arrangement of MA nitride fuel pins in the core region*



# **APPENDIX B**

## **Calculation Details Supplied by Participants**





*Appendix B.1*  
**Pressurised water reactor benchmark**

**FZK (Germany)**

**1. Name of participant:** C.H.M. Broeders

**2. Organisation:** Forschungszentrum Karlsruhe (FZK)

**3. Name of code used:** KAPROS/KARBUS

**4. Bibliographic references:**

- [1] C.H.M. Broeders, "Entwicklungsarbeiten für die neutronenphysikalische Auslegung von Fortschrittlichen Druckwasser Reaktoren (FDWR) mit kompakten Dreiecksgittern in hexagonalen Brennelementen", KfK 5072 (1992).

**5. Origin of cross-section data:**

- KEDAK4, ENDF/B-5/6, JEF-2.2

**6. Spectral calculations and data reduction method used:**

- Resonance shielding: Improved table look-up method for the self-shielding factors for all energies and all isotopes.

**7. Number of energy groups used in different phases:**

- Cell calculation: 69 group WIMS structure, upscatter cut-off 4 eV.
- Burn-up calculation: one energy group

**8. Calculations:**

- Theory used: Transport theory
- Method used: Collision probability method in cell calculations, Bateman method (ORIGEN derived) in depletion calculations

## **IKE (Germany)**

**1. Name of participant:** D. Lutz

**2. Organisation:** Institut fuer Kernenergetik und Energiesysteme  
University of Stuttgart, Germany

**3. Name of code used:** RESMOD working in the SCALE system [1]  
Reactor code system RSYST3 [2]

### **4. Bibliographic references:**

- [1] W. Bernnat, D. Lutz, J. Keinert, M. Mattes, "Erstellung und Validierung von Wirkungsquerschnittsbibliotheken im SCALE-Format auf Basis der evaluierten Dateien JEF-2 und ENDF/B-VI fuer Kritikalitaets- und Reaktorauslegungsrechnungen sowie Stoerfallanalysen, IKE 6-189 (1994).
- [2] R. Ruehle, "RSYST, an Integrated Modular System for Reactor and Shielding Calculations", Conf-730 414-12 (1973).

### **5. Origin of cross-section data:**

- JEF-2.2, processed to 292 group library N292 and 13 000 energy group library for about 40 resonance and structural nuclides [1].

### **6. Spectral calculations and data reduction method used:**

- Collapsing from 292 to 45 energy groups with a RESMOD spectrum generated applying self-shielded cross-sections (BONAMI code in the SCALE system) and an ultrafine solution of the one-dimensional slowing down equation in the energy range from 1 000 eV to 3 eV with 13 000 energy groups [1]. Mutual shielding for BOL is taken into account.
- Fission spectra are mixed corresponding to the isotopic production rates of  $^{235}\text{U}$ ,  $^{238}\text{U}$ ,  $^{239}\text{Pu}$  and  $^{241}\text{Pu}$  in the four different pin cells.
- (n,2n) reaction is included in the scattering matrices.

### **7. Number of energy groups used in different phases:**

- Spectral calculations with 292 groups.
- Cell burn-up calculations with 45 groups.

### **8. Calculations:**

- One-dimensional cell calculations with a collision probability code in RSYST [2]. Burn-up calculations for 20 actinides and 83 fission product isotopes in RSYST.

## JAERI (Japan)

**1. Name of participant:** Hideki Takano, Hiroshi Akie and Kunio Kaneko

**2. Organisation:** Japan Atomic Energy Research Institute (JAERI)

**3. Name of code used:** SRAC95

**4. Bibliographic references:**

[1] K. Tsuchihashi, *et al.*, “Revised SRAC Code System”, JAERI-1302 (1986).

[2] K. Okumure, *et al.*, “SRAC95, General Purpose Neutronics Code System”, JAERI-Data/Code 96-015 (1996), in Japanese.

**5. Origin of cross-section data:**

- JENDL-3.2.

**6. Spectral calculations and data reduction method used:**

- Resonance shielding:
  - PEACO: ultra-fine energy group calculation with collision probability method is used in the following energy range:

961.12-130.07 eV (lethargy width = 0.00025)  
130.07 eV – thermal cut-off (lethargy width = 0.0005)

(thermal cut-off energy in the benchmark = 2.3824 eV) for main resonant and fission product nuclides.

- Table look-up method: the self-shielding factors calculated by the ultra-fine group method for homogeneous system are used for the other nuclides except for those calculated with the PEACO method.
- Mutual shielding:

Mutual shielding effect is accurately treated by the PEACO method
- Weighting spectrum for scattering matrices:

Correction of the out-scatter and self-scatter cross-section is considered by elastic and elastic removal f-tables. In PEACO energy range, the out-elastic-scatter and self-elastic-scatter are calculated using ultra-fine spectrum and ultra-fine elastic cross-sections for the resonant material.

## 7. Number of energy groups used in different phases:

- Cell calculation: 107 energy groups; fast energy region is 61 groups, thermal one is 46 groups and thermal cut-off energy is 2.3824 eV.
- Burn-up calculation: One energy group.

## 8. Calculations:

- Theory used: Transport theory.
- Method used: Collision probability method is cell calculations, Bateman method in burn-up calculations.
- Calculation characteristics: Meshes (see table).

Core type	Fuel	Clad	Moderator
Standard PWR	3 $r_1 = 2.364$ mm $r_2 = 3.344$ mm $r_3 = 4.095$ mm	1 $r_4 = 4.750$ mm	3 $r_5 = 5.774$ mm $r_6 = 6.664$ mm $r_7 = 7.410$ mm
Highly moderated PWR	3 $r_1 = 2.364$ mm $r_2 = 3.344$ mm $r_3 = 4.095$ mm	1 $r_4 = 4.750$ mm	3 $r_5 = 5.712$ mm $r_6 = 6.533$ mm $r_7 = 7.262$ mm $r_8 = 7.925$ mm $r_9 = 8.536$ mm

## 9. Other assumptions and characteristics:

## 10. Comments useful for correctly interpreting the results:

The 2+1 cases following from NSC/DOC(96)10, Table A, using:

- MOX21 Pu vector with 0.0% MA – reference case for the Stage 2 fast reactor benchmark (standard PWR core).
- MOX12 Pu and MA vectors with 1% and 2.5% total MA content (standard PWR and highly moderated PWR).
- MOX22 Pu and MA vectors with 1% and 2.5% total MA content (standard PWR and highly moderated PWR).

and analysed and reported.

## Tohoku University (Japan)

1. **Name of participant:** Tomohiko Iwasaki and Daisuke Fujiwara

2. **Organisation:** Tohoku University, Japan

3. **Name of code used:** SWAT

### 4. **Bibliographies references:**

- [1] K. Suyama, T. Iwasaki and N. Hirakawa, "SWAT: Code Manual", Japan Atomic Energy Research Institute, JAERI-Data/Code 97-047 (1997).
- [2] K. Suyama, T. Iwasaki and N. Hirakawa, "Analysis of Post-Irradiation Experiments in PWR Using New Nuclear Data Libraries", *J. Nucl. Sci. Tech.*, 31 (6), 596-608 (1994).
- [3] K. Suyama, T. Iwasaki and N. Hirakawa, "Improvement of Burn-up Code System for Use in Burn-up Credit Problem", Proc. on PHYSOR'96, L-53 (1996).

### 5. **Origin of cross-section data:**

- JENDL-3.2.

### 6. **Spectral calculations and data reduction method used:**

- Resonance shielding:
  - Method 1: Direct calculation using ultra-fine energy groups.  
Energy range: 130 eV to 3.92 eV.  
Nuclides:  $^{232}\text{Th}$ ,  $^{233-236,238}\text{U}$ ,  $^{237,239}\text{Np}$ ,  $^{236,238-242}\text{Pu}$ ,  $^{241-243}\text{Am}$ ,  $^{244,245}\text{Cm}$ ,  $^{99}\text{Tc}$ ,  $^{103}\text{Rh}$ ,  $^{113}\text{In}$ ,  
 $^{131}\text{Xe}$ ,  $^{137}\text{Cs}$ ,  $^{155-158,160}\text{Gd}$ ,  $^{107,109}\text{Ag}$ ,  $^{174,176-180}\text{Hf}$ .
  - Method 2: f-table method.  
Energy range: Above 3.92 eV.  
Nuclides: Other nuclides.
- Mutual shielding: Implicitly considered by the direct calculation using ultra-fine energy groups.
- Weighting spectrum for scattering matrices:  $S(\alpha, \beta)$ .

### 7. **Number of energy groups used in the different phases:**

- Fast and epithermal:  
Energy range: 10 MeV to 3.92 eV.  
No. of groups: 59 groups.
- Thermal:  
Energy range: below 3.92 eV.  
No. of groups: 48 groups.

## **8. Calculations:**

- Theory used: Cell calculation in infinite cylinder geometry with equivalent radii.
- Method used: Collision probability method.
- Calculation characteristics:
  - Three coarse mesh for pin: Fuel, cladding, coolant.
  - Nine fine mesh for fuel.
  - One fine mesh for cladding.
  - One fine mesh for coolant.

## **9. Other assumptions and characteristics:**

Decay data: ORIGEN-2 built-in values with a few revised data based on the “Table of Isotope” (seventh edition).

FP yield: JNDC Library (1990), Fission Yield Library for 1 228 nuclides of Japan Nuclear Data Centre (1990).

## **ITEP (Russian Federation)**

**1. Names of participant:** B.P. Kochurov, A.Yu. Kwaratzheli and N.N. Selivanova

**2. Organisation:** State Scientific Centre – Institute of Theoretical and Experimental Physics  
B. Cheremushkinskaya, 25, Moscow, 117218, Russian Federation  
E-mail: Boris.Kochurov@itep.ru  
Phone/Fax: (095) 127-0543

**3. Name of code used:** TRIFON [1-3]  
(authors B.P. Kochurov, A.Yu. Kwaratzheli, V.M. Michailov)

### **4. Bibliographic references:**

- [1] B.P. Kochurov, A.Yu. Kwaratzheli, V.M. Michailov, “Computer Code TRIFON: Manual”, Pre-print ITEP 10-95, Institute of Theoretical and Experimental Physics, Moscow, 1995.
- [2] A.Yu. Kwaratzheli, B.P. Kochurov, “Computer Code TRIFON Abstract”, VANT, Ser.: PHTYAR (Russ.), 1985, N4, p. 45-47.
- [3] B.P. Kochurov, A.Yu. Kwaratzheli, A.P. Knyazev, “New Methods and Computer Codes Developments for Neutron Reactor Physics Calculations”, International Conf. on the Physics of Nuclear Science and Technology, Long Island, New York, 5-8 October 1998.
- [4] L.P. Abag'an, *et al.*, “Group Constants for Reactor and Shielding Calculations”, Moscow, Energoatomizdat, 1981.
- [5] S.F. Mughabghab, “Neutron Cross-Sections, Volume 1, Neutron Resonance Parameters and Thermal Cross-Sections”, National Nuclear Data Center, Brookhaven National Laboratory, Academic Press, 1984.
- [6] S.V. Akimushkin, B.P. Kochurov, “Effective Resonances of  $^{238}\text{U}$ ”, VANT, Ser.: PHTYAR (Russ.), 1991, N1, p. 25.
- [7] V.A. Konjshin, “Nuclear Data for Fissile Nuclides, Handbook”, Moscow, EnergoAtomizdat, 1984.
- [8] “JNDC Nuclear Data Library of Fission Products”, Second Version, JAERI 1320, Japan Atomic Energy Research Institute, September 1990.
- [9] A.D. Galanine, “Revision of Scheme of the Main Fission Products and Weak Effective Fission Products”, Pre-print ITEP 135-89, Moscow-TsniiAtomInform, 1989.

### **5. Origin of cross-section data:**

Twenty-six group system of BNAB-26 nuclear data library [4], resonance parameters [5], effective resonance parameters for  $^{238}\text{U}$  [6], cross-sections for thermal region and multi-group cross-sections for Pu isotopes [7], fission products yields [8], parameters of weak effective (lumped) fission products [9].

## 6. Spectral calculations and data reduction method used:

Fission spectrum  $\chi(E)$  in the interval of energies  $10.5 \text{ MeV} > E > 0.00465 \text{ MeV}$ , is based on the formula:

$$\chi(E) = 2\exp(-ab/4)\exp(-E/a)\text{Sh}(\text{Sqrt}(bE))/\text{Sqrt}(\pi a 3b),$$

where:  $a = 0.965(0.8+0.08\nu)$ ,  $b = 2.245/(0.8+0.08\nu)^2$ , and corresponding to  $\nu = 2.416$  was taken from [4] ( $\nu$  – number of secondary neutrons released in fission).

$K_\infty$  spectrum as the result of space-energy neutron transport solution in the cell was used for two-group microscopic cross-sections determination to simulate burn-up.

- Strong resonances of  $^{238}\text{U}$  below 215 eV and above 0.465 eV were explicitly treated with a fine non-uniform sub-division of lethargy scale into 130 groups.

Strong resonances of  $^{237}\text{Np}$ ,  $^{240}\text{Pu}$ ,  $^{242}\text{Pu}$ ,  $^{241}\text{Am}$ ,  $^{243}\text{Am}$ ,  $^{244}\text{Cm}$  were explicitly treated as well.

For  $^{238}\text{U}$  effective resonance levels [6] were used (one resonance per group in 11-16 groups of BNAB system [4]).

Self-shielding factors of  $^{235}\text{U}$ ,  $^{239}\text{Pu}$ , Zr [4] were taken into account with a mean chord (dilution cross-section) determined as the solution of inverse problem.

- Mutual shielding (overlapping of resonances).

Overlapping of strong resonances is treated automatically in the solution of space-energy problem for reactor cell.

- Weighting spectrum of scattering matrices: space-energy distribution of neutron spectrum (below 0.465 eV) was calculated as a solution of space-energy thermalisation problem with Nelkin model for  $\text{H}_2\text{O}$  and capture and fission cross-sections from [7].

## 7. Number of energy groups used in different phases:

Each of 11-16 groups having lethargy width 0.765 of BNAB system in the range of energies 215-21 500 eV was separated into 20 sub-intervals (non-uniform division) to describe resonance absorption by effective resonances of  $^{238}\text{U}$ .

One hundred thirty sub-intervals in the range 0.465-215 eV were used to describe resonance absorption by strong resonances. Ten groups were used in the interval  $0 < E < 0.465 \text{ eV}$  for thermal neutrons.

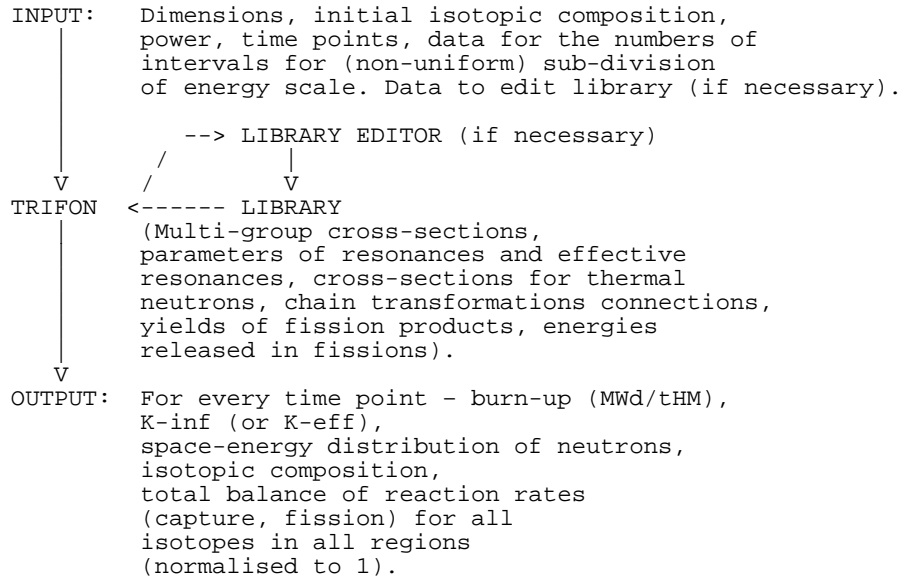
Total number of energy groups is 270.

## 8. Calculations:

- Theory used [3]: collision probability method was used for every energy group. Multi-group calculations with downscattering (above 0.465 eV) and upscattering and downscattering in the range of thermal neutrons were used.



The flow sheet of calculations by TRIFON code is presented below:



Running time for every space-energy-time burn-up simulation case was about 30-40 minutes (Pentium, CPU 200 Mhz, RAM 32).

### 9. Other assumptions and characteristics:

Simulation of burn-up was performed with space-energy re-calculations at every time point (burn-up point). Reaction rates  $R$  at every time point were presented as:

$$R = \sigma_t \phi_t + \sigma_e \phi_e$$

where:  $\sigma_t, \sigma_e$  – thermal, epithermal cross-section  
 $\phi_t, \phi_e$  – thermal, epithermal neutron flux

Epithermal flux is supposed = const; thermal flux within time interval was interpolated on the basis of dependence:

$$\sim 1/\Sigma_{at}$$

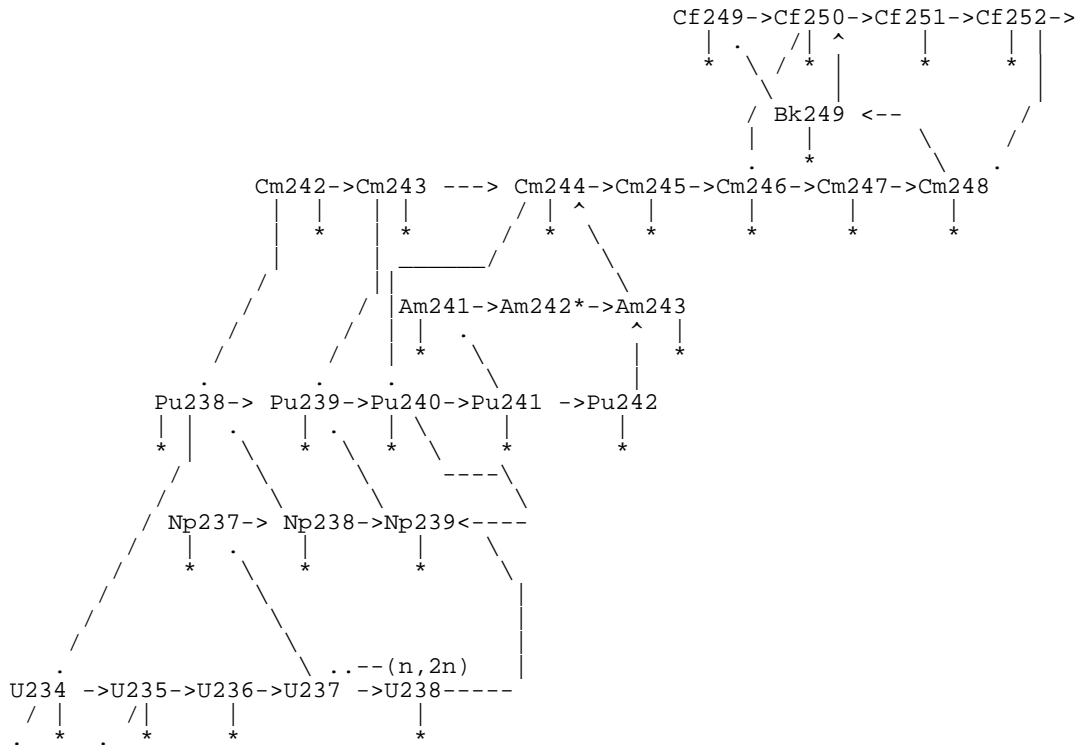
where:  $\Sigma_{at}$  – thermal macroscopic absorption cross-section

Chain transformations are presented below:

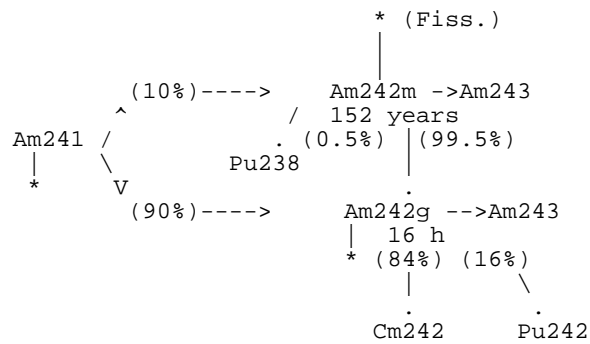
---. decay, ---\* fission, ---> (or ---) capture, -.. (n,2n) ;

Really all heavy elements are fissile materials (by fast neutrons).

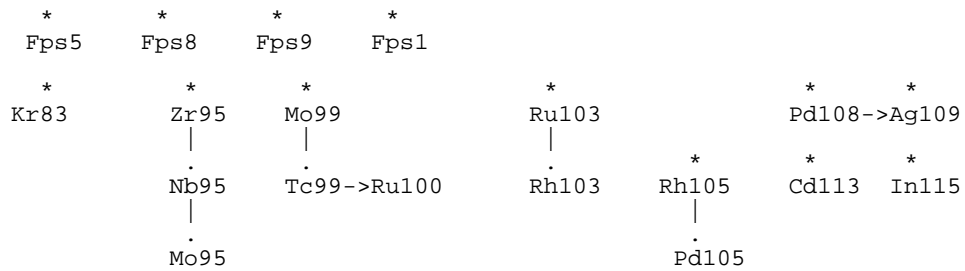
### Chain transformations for heavy nuclides

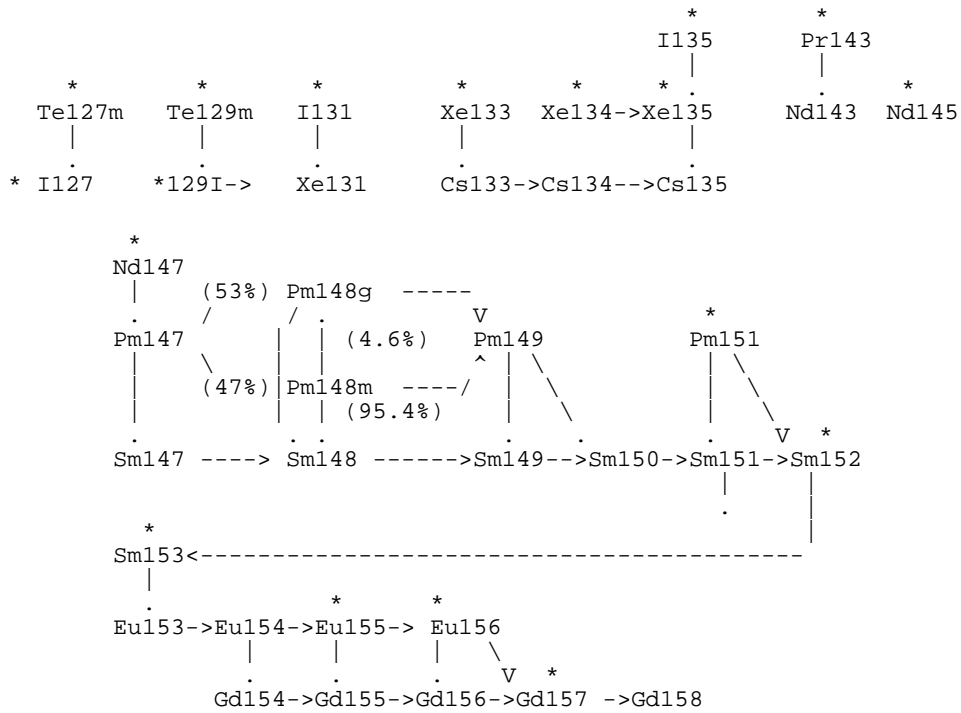


### <sup>242</sup>Am\*



### Chain transformations for fission products (\* means direct yield in fissions)





50 fission products were taken into account explicitly with the yields from [8].

Weakly absorbing fission products were presented by effective (pseudo) fission products Fps5 (for  $^{235}\text{U}$ ), etc.

### The yields of fission products [8]

	$^{235}\text{U}$	$^{236}\text{U}$	$^{238}\text{U}$	$^{237}\text{Np}$	$^{238}\text{Pu}$	$^{239}\text{Pu}$	$^{240}\text{Pu}$	$^{241}\text{Pu}$	$^{242}\text{Pu}$
Fps*	1.5200+0	1.5200+0	1.4600+0	1.4600+0	1.4600+0	1.4100+0	1.4100+0	1.3900+0	1.4100+0
$^{83}\text{Kr}$	5.3806-3	5.2213-3	3.8660-3	4.8101-3	3.9500-3	2.9500-3	3.0268-3	2.1189-3	2.3952-3
$^{95}\text{Zr}$	6.4961-2	6.4113-2	6.1068-2	6.6995-2	5.2800-2	4.8942-2	4.3965-2	4.0745-2	4.0226-2
$^{103}\text{Ru}$	3.0274-2	4.2030-2	6.2096-2	5.5831-2	6.3800-2	6.9500-2	6.7119-2	6.1440-2	5.8768-2
$^{105}\text{Rh}$	9.6384-3	2.4569-2	3.9393-2	3.1663-2	3.4800-2	5.3513-2	5.5327-2	6.1073-2	5.6422-2
$^{108}\text{Pd}$	6.6938-4	3.4485-3	5.9875-3	9.6198-3	2.9000-3	2.1685-2	3.0307-2	3.9253-2	4.2146-2
$^{109}\text{Ag}$	3.4482-4	1.4347-3	2.6844-3	4.4732-3	1.3000-3	1.8795-2	1.7948-2	2.2616-2	3.2568-2
$^{99}\text{Mo}$	6.1105-2	5.8731-2	6.1957-2	6.1558-2	6.2000-2	6.1403-2	5.9734-2	6.2334-2	5.3617-2
$^{113}\text{Cd}$	1.6075-4	3.7524-4	6.1827-4	5.0905-4	5.6000-4	6.4120-4	1.5713-3	1.4358-3	3.0292-3
$^{115}\text{In}$	1.0763-4	5.1106-4	3.3774-4	4.8796-4	4.2000-4	3.5648-4	6.6229-4	4.2137-4	1.0219-3
$^{127\text{m}}\text{Te}$	1.7335-4	3.1080-4	1.7522-4	4.9674-4	2.0000-4	6.8236-4	5.8183-4	3.1769-4	4.2208-4
$^{129\text{m}}\text{Te}$	7.1990-4	9.5532-4	9.6083-4	1.4351-3	1.5500-3	1.5672-3	1.0864-3	7.1781-4	8.0570-4
$^{129}\text{I}$	6.4586-3	8.8710-3	9.0368-3	1.2511-2	7.8100-3	1.2367-2	9.4296-3	6.6400-3	7.4240-3
$^{131}\text{I}$	2.8843-2	3.0369-2	3.2986-2	3.6977-2	3.1900-2	3.8466-2	3.5451-2	2.8463-2	3.1872-2
$^{135}\text{I}$	6.2897-2	5.6165-2	6.7830-2	6.6547-2	8.0300-2	6.4468-2	6.7436-2	7.5074-2	7.4528-2
$^{134}\text{Xe}$	7.8361-2	8.1081-2	8.0123-2	7.3936-2	6.3800-2	4.4286-2	4.7210-2	7.0544-2	6.8895-2
$^{143}\text{Pr}$	5.9388-2	6.0885-2	4.5666-2	4.7037-2	4.6800-2	4.2131-3	3.6010-3	4.7067-2	4.6800-2
$^{127}\text{I}$	1.0734-3	1.9250-3	1.0854-3	3.0743-3	1.0000-3	7.6326-2	7.0056-3	1.9676-3	2.6140-3

Fps\* – weak effective fission products (Fps5, Fps8, Fps9, Fps1) [9]

**The yields of fission products [8] (cont.)**

	<sup>235</sup> U	<sup>236</sup> U	<sup>238</sup> U	<sup>237</sup> Np	<sup>238</sup> Pu	<sup>239</sup> Pu	<sup>240</sup> Pu	<sup>241</sup> Pu	<sup>242</sup> Pu
<sup>133</sup> Xe	6.7019-2	7.0259-2	6.6065-2	6.6397-2	6.4700-2	6.9756-2	7.0510-2	6.7696-2	6.5925-2
<sup>135</sup> Xe	2.4180-3	1.5840-3	2.7900-4	8.8280-3	3.3000-3	1.1523-2	6.9840-3	2.3140-3	2.6440-3
<sup>145</sup> Nd	3.9175-2	3.6682-2	3.7559-2	3.4822-2	3.9000-2	2.9915-2	3.2772-2	3.3438-2	3.4669-2
<sup>147</sup> Nd	2.2533-2	2.3407-2	2.5298-2	2.2108-2	2.5600-2	2.0428-2	2.2329-2	2.3678-2	2.4193-2
<sup>149</sup> Pm	1.0664-2	1.3684-2	1.6076-2	1.2743-2	1.6700-2	1.2392-2	1.3692-2	1.5233-2	1.6145-2
<sup>151</sup> Pm	4.1838-3	4.2264-3	8.0064-3	7.1374-3	8.3000-3	7.7195-3	8.4315-3	9.3682-3	1.0247-2
<sup>152</sup> Sm	2.6783-3	3.8775-3	5.2075-3	4.5631-3	5.3700-3	5.8517-3	6.5758-3	7.4659-3	8.3476-3
<sup>153</sup> Sm	1.6135-3	2.5533-3	4.1095-3	3.5942-3	4.3900-3	3.6369-3	5.7967-3	5.4816-3	6.5542-3
<sup>155</sup> Eu	3.2044-4	9.2283-4	1.3266-3	1.1920-3	1.1600-3	1.6547-3	2.4760-3	2.4167-3	3.6772-3
<sup>156</sup> Eu	1.3186-4	3.3648-4	6.7481-4	9.9914-4	6.6000-4	1.1838-3	1.7543-3	1.7606-3	2.6566-3
<sup>157</sup> Gd	6.1534-5	2.3080-4	3.8719-4	3.3300-4	3.1000-4	7.4098-4	1.3040-3	1.3716-3	1.8392-3

Group cross-sections correspond to the following parameters of Fps:

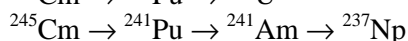
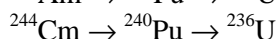
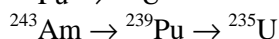
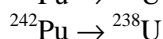
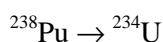
Eff. FP	Fps5	Fps8	Fps9	Fps1
From →	( <sup>235</sup> U)	( <sup>238</sup> U)	( <sup>239</sup> Pu)	( <sup>241</sup> Pu)
Yield	1.52	1.46	1.41	1.39
σ <sub>at</sub>	1.68	1.77	1.93	1.86
Ri	7.65	9.60	11.24	12.53

σ<sub>at</sub> – Capture cross-section (barn)

Ri – Resonance Integral (barn)

**10. Comments useful for correctly interpreting the results:**

The following main decay chains (→) were taken into account in calculations of radioactivity (Bk/tHM) as function of time:



**IPPE (Russian Federation)\***

- 1. Name of participant:** A.A. Tsiboulia
- 2. Organisation:** IPPE, Russian Federation
- 3. Name of code used:**
- 4. Bibliographic references:**
- 5. Origin of cross-section data:**
- 6. Spectral calculations and data reduction method used:**
- 7. Number of energy groups used in different phases:**
- 8. Calculations:**
- 9. Other assumptions and characteristics:**
- 10. Comments useful for correctly interpreting the results:**

---

\* *Calculation details have not been provided.*



*Appendix B.2*  
**Fast reactor benchmark**

**JAERI (Japan)**

**1. Name of participant:** Kazufumi Tsujimoto, Hiroyuki Oigawa and Takehiko Mukaiyama

**2. Organisation:** Japan Atomic Energy Research Institute (JAERI)

**3. Name of code used:**

- Transmutation calculation: ABC-SC code system [1], which consists of the following components:
  - Preparation of effective cross-sections: SLAROM [2].
  - Calculation of steady-state neutronics: CITATION-FBR [3].
  - Collapse of effective cross-section: ORILIB [1].
  - Calculation of burn-up and decay: ORIGEN-2 [4].
  - Management of fuel shuffling: F-CHANGE [1].
- Reactivity and reaction rate calculation: JAERI's Standard Calculation System for Fast Reactor, which consists of the following components:
  - Preparation of effective cross-sections: SLAROM [2].
  - Calculation of steady-state neutronics: CITATION-FBR [3].
  - Perturbation calculation: PERKY [5].
  - Reaction rate calculation: RADAMES [6].

**4. Bibliographic references:**

- [1] Y. Gunji, T. Mukaiyama, H. Takano and T. Takizuka, "A Computer Code System for Actinide Transmutation Calculation in Fast Reactors – ABC-SC", JAERI-M 92-032 (1992) (in Japanese).
- [2] M. Nakagawa and K. Tsuchihashi, "SLAROM: A Code for Cell Homogenisation Calculation of Fast Reactor", JAERI 1294 (1984).
- [3] S. Iijima, "CITATION-FBR", *to be published*.
- [4] A.G. Croff, "ORIGEN-2: A Revised and Updated Version of Oak Ridge Isotope Generation and Development Code", ORNL-5621 (1980).

- [5] S. Iijima, H. Yoshida and H. Sakuragi, “Calculation Program for Fast Reactor Design, 2 (Multi-Dimensional Perturbation Theory Code Based on Diffusion Approximation: PERKY)”, JAERI-M 6993 (1977) (in Japanese).
- [6] Y. Gunji and S. Iijima, “RADAMES”, private communication (1995).
- [7] H. Takano, “JFS-3-J3-2”, private communication (1995).
- [8] H. Takano, “A Study of the Group Constant Generation Method in Fast Reactor Analysis”, JAERI-M 83-075 (1983).

**5. Origin of cross-section data:**

- Steady-state neutronics calculations: JENDL-3.2.
- Burn-up calculation: JENDL-3.2 for actinides, ORIGEN-2 library for structural material and FP.

**6. Spectral calculations and data reduction method used:**

- Resonance shielding: f-table in JFS-3-J3.2 70-group set [7] was used.
- Mutual shielding: Resonance overlapping of  $^{238}\text{U}$  was taken into account [8].
- Weighting spectrum: Neutron spectrum of Japanese prototype fast reactor was used.

**7. Number of energy groups used in different phases:**

- Steady-state neutronics calculation: 70-group.
- Burn-up calculation: 1 group.

**8. Calculations:**

- SLAROM: Cell calculation code using collision probability method. Only homogeneous cells were, however, used in the present calculation. Hence, this code was used to prepare effective cross-sections by f-table method.
- CITATION-FBR: Diffusion code using finite difference method. Mesh size: about 5 cm for both R and Z directions;  $D = 1/(3\sigma_{tr})$ .
- ORIGEN-2: One point one-group burn-up calculation code.

**9. Other assumptions and characteristics:**

- Figure 1 shows the calculation scheme.
- Inner core was divided into nine regions as indicated in the instruction. Each of the regions has three different compositions because of their different burn-up states. Hence total 27 ( $= 9 \times 3$ ) compositions were dealt with.

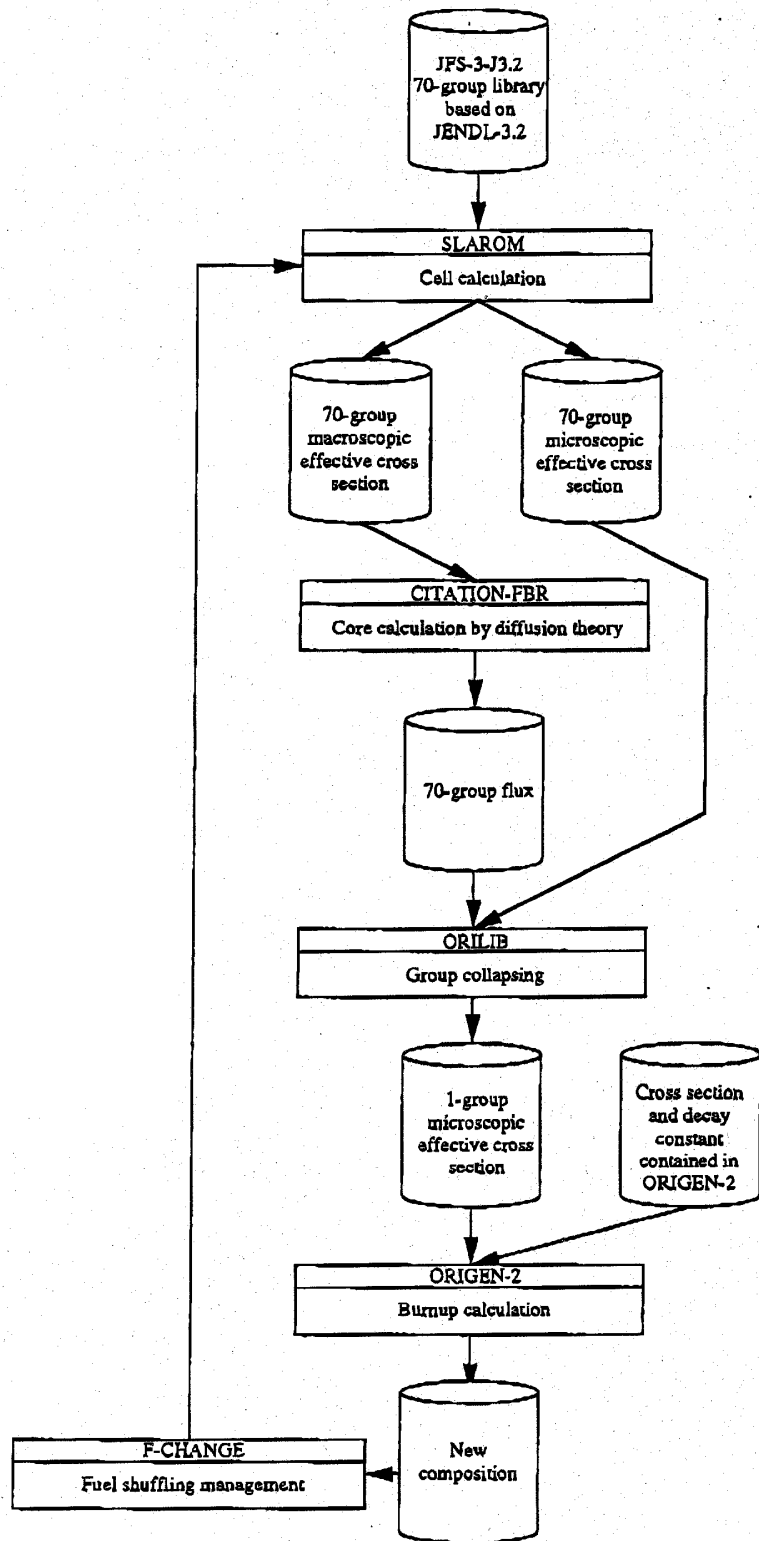


- Outer core was divided into six regions as indicated in the instruction. Each of the regions has three different compositions because of their different burn-up states. Hence total 18 ( $= 6 \times 3$ ) compositions were dealt with.
- Axial blanket was divided into two regions; one is located above and below the inner core and the other is for the outer core. Each of the regions has three different compositions because of their different burn-up states. Hence total 6 ( $= 2 \times 3$ ) compositions were dealt with.
- Radial blanket was combined into one region, which has four different compositions because of their different burn-up states. Hence total 4 ( $= 1 \times 4$ ) compositions were dealt with.
- A total of 55 compositions were, therefore, dealt with in this problem.
- The codes SLAROM, ORILIB and ORIGEN-2 were executed 55 times per each burn-up step, respectively, to obtain effective cross-sections and compositions of each region.
- CITATION-FBR calculated  $k_{\text{eff}}$  and 70-group flux of each region, which was then used for collapsing cross-sections in ORILIB.
- The thermal power output was normalised at 2 600 MW. The energy release per fission was assumed at 202.6 MeV for all nuclei.
- ORILIB collapsed microscopic effective cross-section from 70-group to one-group. This one-group cross-section was used in ORIGEN-2 to update the actinide effective cross-section.
- Burn-up calculation in ORIGEN-2 was based on constant flux approximation. The flux values were taken from the CITATION-FBR results.
- No cooling time was assumed between burn-up states.
- No cooling time was assumed before the reprocessing.
- Two burn-up calculations and three  $k_{\text{eff}}$  calculations were performed in one cycle (365 EFPD).

#### 10. Comments useful for correctly interpreting the results:

- Table 5: Reactivity losses:  
The calculation method for  $k_{\text{eff}}$  was not the same as that in Table 1. The 55 compositions were mixed into 18 regions before the SLAROM calculation for Table 5, though this procedure was performed after the SLAROM calculation for Table 1. The difference in burn-up reactivity was less than 0.01%.
- Table 9: Doppler reactivity worth:  
 $^{238}\text{Pu}$ ,  $^{242\text{M}}\text{Am}$  and  $^{243}\text{Cm}$  do not have temperature dependent f-tables in JFS-3-J3.2. Hence, there is no Doppler effect in these nuclei.
- Table 11: Number densities of wastes:  
Average values for inner core, outer core and axial blanket.

Figure 1. Calculation scheme of ABC-SC code system



## CEA (France)

1. **Name of participant:** Jean Tommasi

2. **Organisation:** Commissariat à l'Energie Atomique (CEA, France)

3. **Name of code used:** ERANOS (European Reactor Analysis Optimised System)

4. **Bibliographic references:**

5. **Origin of cross-section data:**

CARNAVAL-IV library + JEF-1 additions (the following isotopes come from JEF-1 and are neither self-shielded nor described in temperature dependent form:  $^{237}\text{Np}$ ,  $^{238}\text{Pu}$ ,  $^{241}\text{Am}$ ,  $^{242\text{m}}\text{Am}$ ,  $^{243}\text{Am}$ ,  $^{242}\text{Cm}$ ,  $^{243}\text{Cm}$ ,  $^{244}\text{Cm}$ ,  $^{245}\text{Cm}$ ).

6. **Spectral calculations and data reduction method used:**

7. **Number of energy groups used in different phases:**

8. **Calculations:**

Diffusion theory, finite difference method, RZ geometry,  $\approx 5$  cm R and Z meshes.

9. **Other assumptions and characteristics:**

10. **Comments useful for correctly interpreting the results:**

- No cooling time is assumed between each cycle, thus there is no decay of  $^{239}\text{Np}$  and  $^{242}\text{Cm}$  during intercycles for example.
- The sodium void calculations have been performed by voiding inner and outer core at the same time; a perturbation analysis yielded then the inner core and (inner + outer) core decompositions.
- *Number densities* of waste, in atoms/(b.cm), were requested for Table 11 and computed using:

$$\mathbf{n}_i = \frac{\sum_i \sum_j n_{ij} V_j}{\sum_j V_j}$$

where  $n_i$  is the number density of atom  $i$  in waste, to be reported in Table 11,  $n_{ij}$  the number of density of atom  $i$  in region  $j$ , and  $V_j$  the volume of region  $j$ . I used only the compositions of the discharged subassemblies, i.e. for fuel the subassemblies having undergone three irradiation cycles ( $3 \times 365$  EFPD), for radial blanket those having undergone four irradiation cycles ( $4 \times 365$  EFPD). The waste is then defined as 0.3% of the discharged U + Pu and 1% of the discharged minor actinides (Np + Am + Cm).

## **JNC (Japan)**

- 1. Name of participant:** Toshio Wakabayashi
- 2. Organisation:** Power Reactor and Nuclear Fuel Development Corporation, Japan
- 3. Name of code used:** SLAROM, CITATION, PERKY, ORIGEN-2
- 4. Bibliographic references:**
- 5. Origin of cross-section data:**
  - JENDL-3.2.
- 6. Spectral calculations and data reduction method used:**
  - See Figure 1.
- 7. Number of energy groups used in different phases:**
  - Burn-up calculation: 7-group.
  - Reactivity coefficient calculations: 70-group.
- 8. Calculations:**
  - Theory used: Diffusion.
  - Method used: Finite difference.
  - Calculation characteristics:
- 9. Other assumptions and characteristics:**
  - Decay chain: See Figures 2 and 3.
- 10. Comments useful for correctly interpreting the results:**

Figure 1. Code and output table

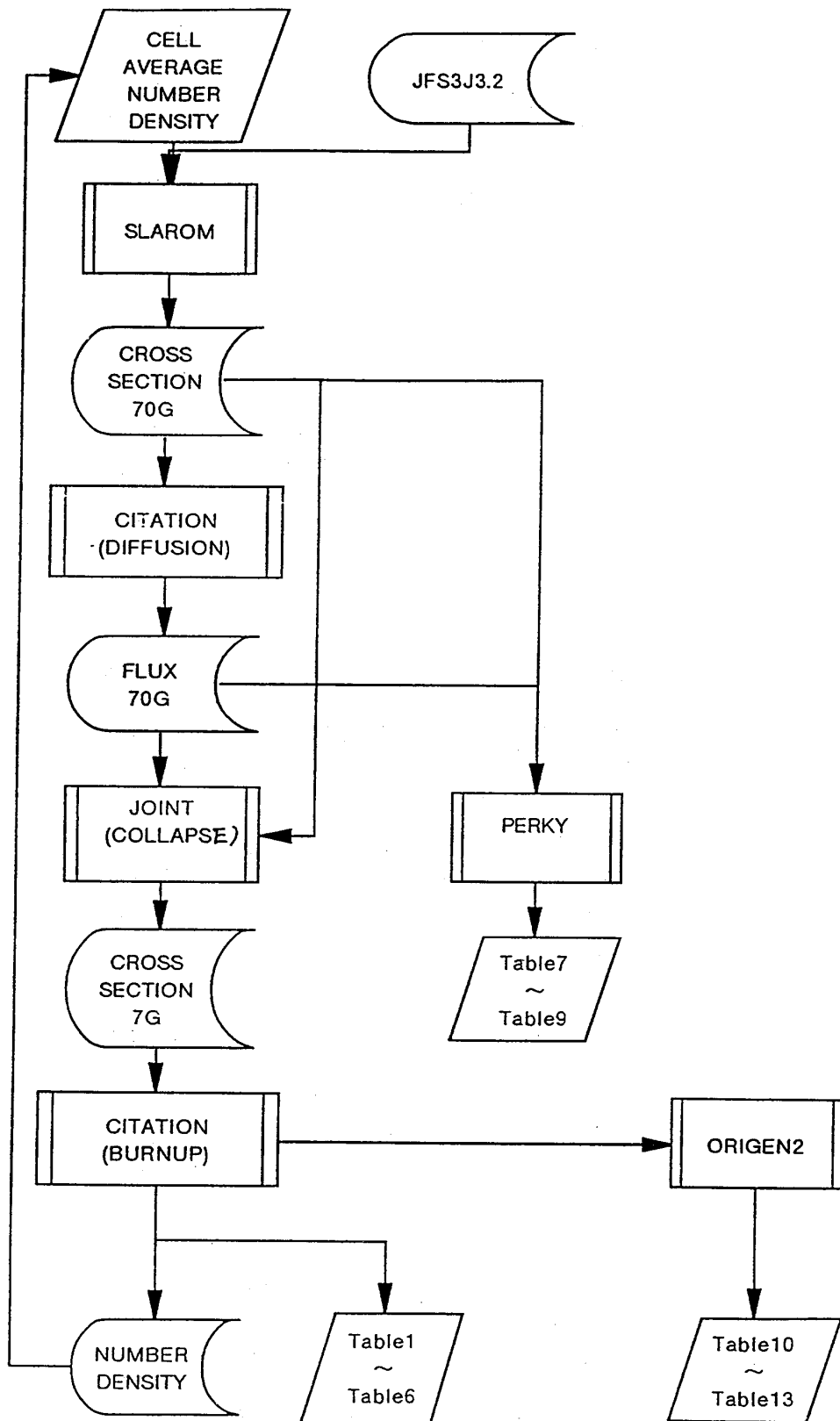


Figure 2. Decay base chain

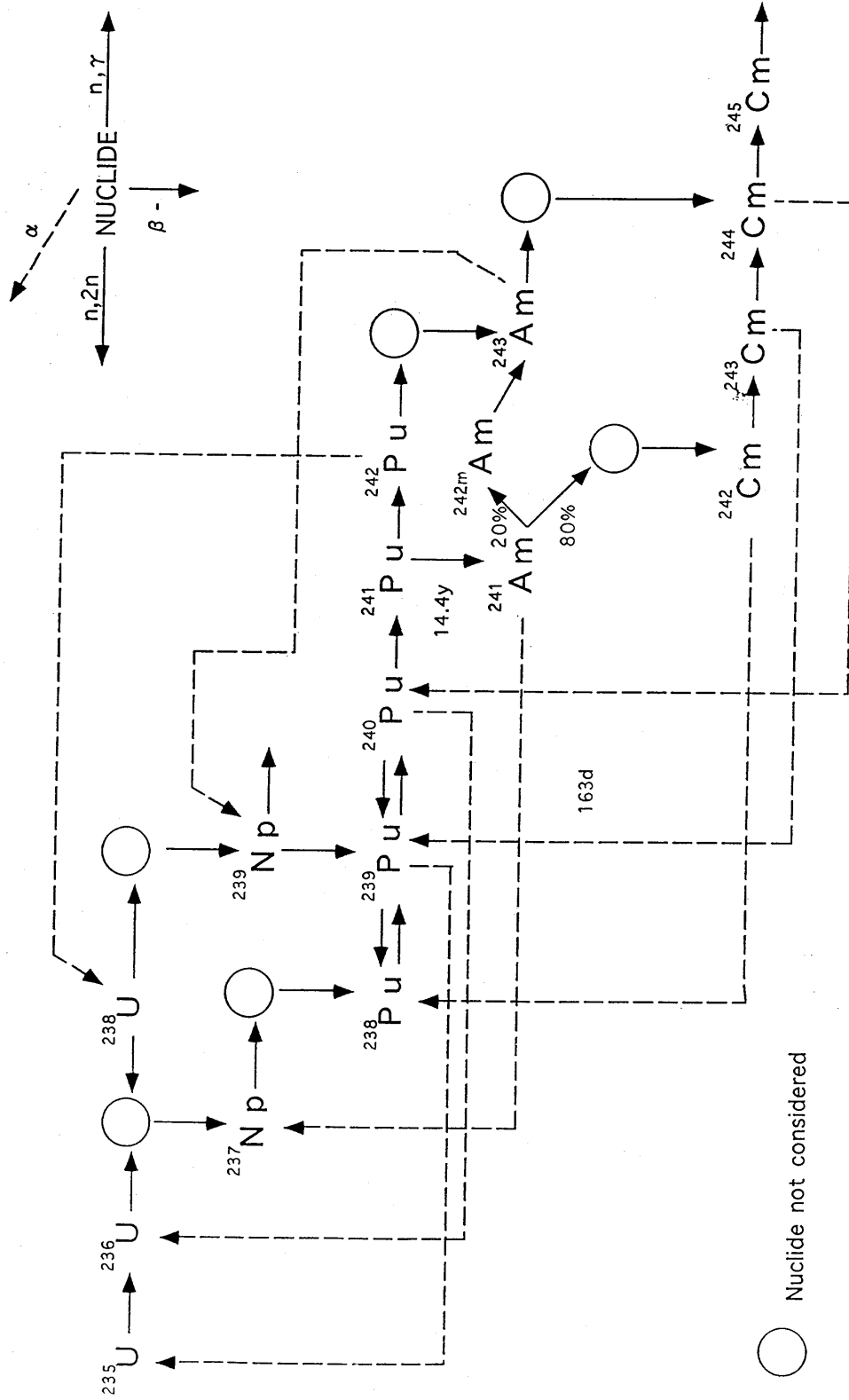
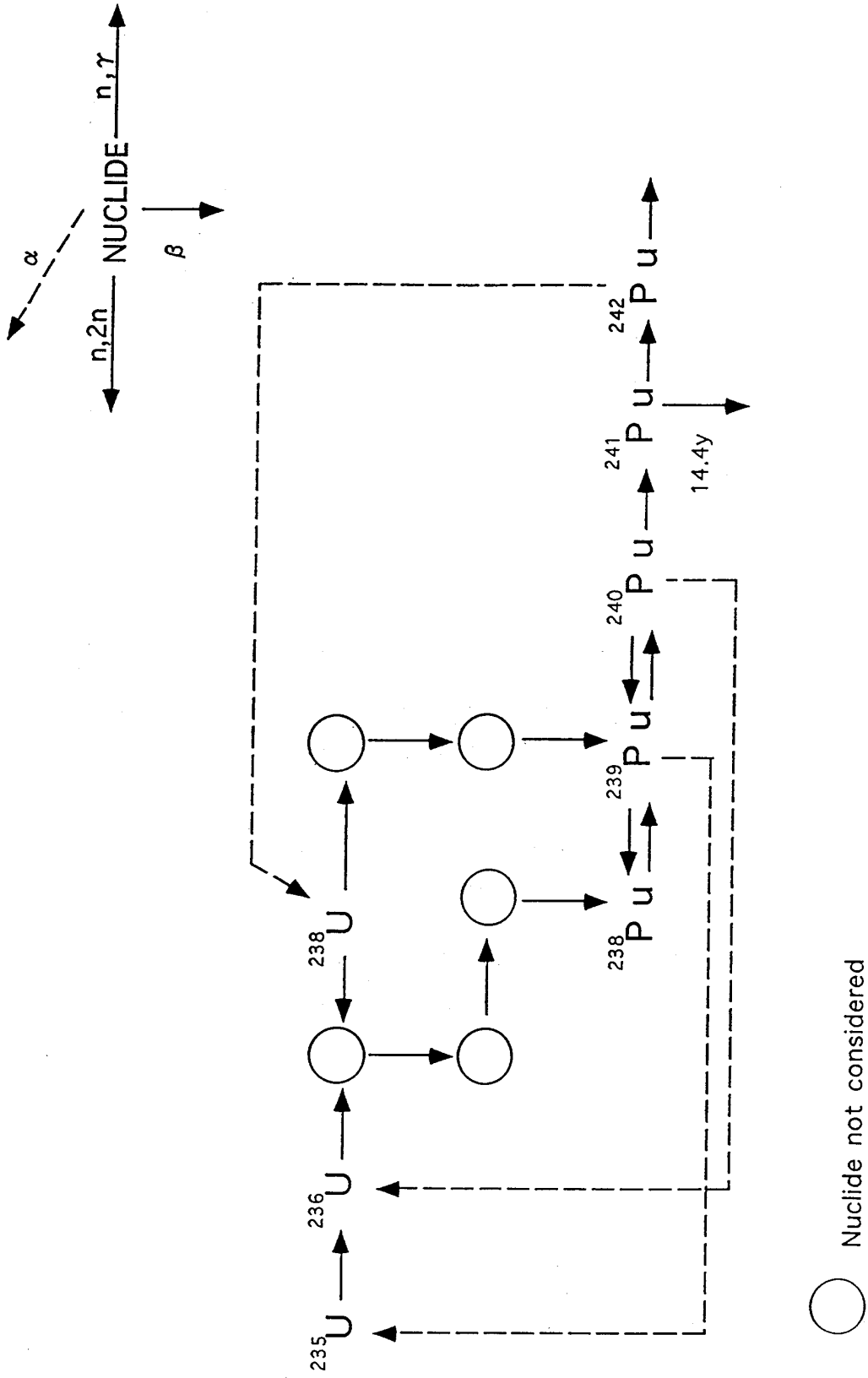


Figure 3. U, Pu decay chain

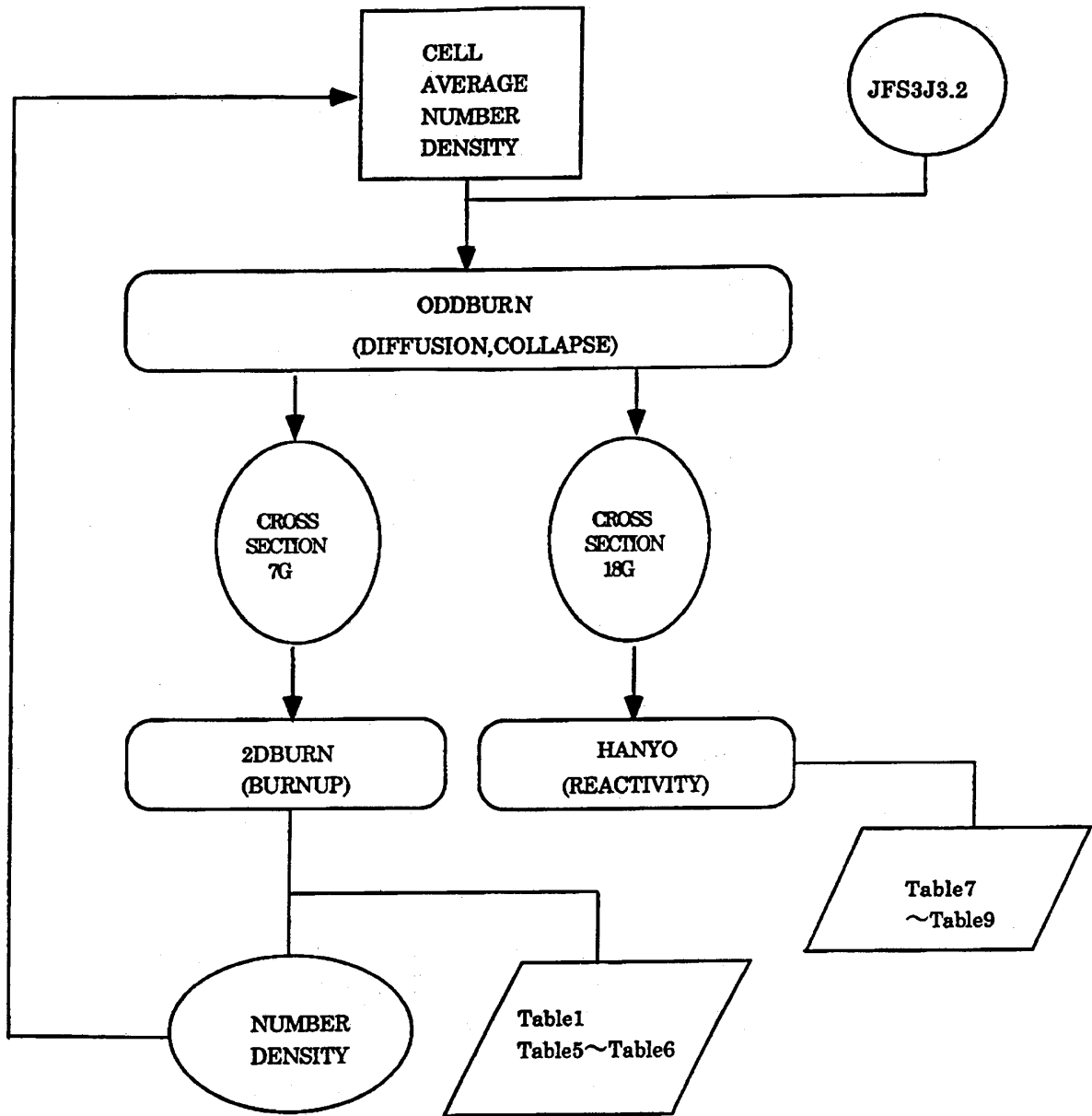


## **mitsubishi (Japan)**

- 1. Name of participant:** Mari Yano
- 2. Organisation:** Mitsubishi Heavy Industries, Ltd.
- 3. Name of code used:** ODDBURN, 2DBURN, HANYO
- 4. Bibliographic references:**
  - None.
- 5. Origin of cross-section data:**
  - JENDL-3.2.
- 6. Spectral calculations and data reduction method used:**
  - See Figure 1.
- 7. Number of energy groups used in different phases:**
  - Burn-up calculation: 7-group.
  - Reactivity coefficient calculations: 18-group.
- 8. Calculations:**
  - Diffusion.
  - Finite difference.
  - –
- 9. Other assumptions and characteristics:**
  - Decay chain: See Figure 2.
- 10. Comments useful for correctly interpreting the results:**



Figure 1. Code and output table





## **TOSHIBA (Japan)**

- 1. Name of participant:** Masatoshi Kawashima and M. Yamaoka
- 2. Organisation:** Nuclear Engineering Laboratory, Toshiba Corporation
- 3. Name of code used:** STANBRE-V3 (private code)
- 4. Bibliographic references:**

- None.

This code uses conventional multi-group diffusion theory with the “corner mesh” scheme in two-dimensional RZ geometry. Simplified burn-up chains are available using analytic expressions involving several approximations.

- 5. Origin of cross-section data:**

- 70-group group constants JFS-3-J3.2 processed from JENDL-3.2 by JAERI.

- 6. Spectral calculations and data reduction method used:**

- Please refer to the JFS-3-J3.2 document (or see Dr. Wakabayashi’s paper).
- Mutual shielding: Ignored.
- Weighting spectrum for scattering matrices: No special treatment. The region-wise 70-group spectra are calculated using one-dimensional R-model. RZ burn-up model for each burn-up step specified by the user. The 70-group microscopic cross-sections are determined for the averaged burn-up compositions in every step defined by the user (if necessary).

- 7. Number of energy groups used in different phases:**

The burn-up calculations were done with the specified 7-group structure. Seventy-group diffusion calculations are done for the Doppler and sodium void worth in the core region.

- 8. Calculations:**

- Diffusion.
- Finite difference with flux definition by “corner-mesh”.
- Calculation characteristics: Basically specified meshes and groups are used.

- 9. Other assumptions and characteristics:**

Three lumped FP cross-sections are used as follows:

- LFP(<sup>235</sup>U): <sup>235</sup>U.
- LFP(<sup>238</sup>U): <sup>236</sup>U, <sup>238</sup>U, <sup>238</sup>Pu, <sup>240</sup>Pu, <sup>242</sup>Pu, MAs.
- LFP(<sup>239</sup>Pu): <sup>239</sup>Pu, <sup>241</sup>Pu.

The original constant set includes several types of lumped FP cross-sections. The FP cross-sections used correspond to 547.5 days burn-FP composition under the FP gas non-release assumption from fuels to gas plenum region. The recent group constant set has lumped cross-sections for  $^{241}\text{Pu}$ -FP, but the present model uses the above substitution.

#### **10. Comments useful for correctly interpreting the results:**

The mesh-size effect on  $k_{\text{eff}}$  is different than for the “volume centre” mesh codes.

A cycle length is divided into five steps for the initial and the equilibrium cycles. Neutron spectra for group reductions are calculated for every step. The self-shielding factors are determined by the average compositions obtained by burn-up calculations at the beginning, middle and end of cycles.

**IPPE (Russian Federation)\***

- 1. Name of participant:** M. Semenov and A.A. Tsiboulia
- 2. Organisation:** IPPE, Russian Federation
- 3. Name of code used:**
- 4. Bibliographic references:**
- 5. Origin of cross-section data:**
- 6. Spectral calculations and data reduction method used:**
- 7. Number of energy groups used in different phases:**
- 8. Calculations:**
- 9. Other assumptions and characteristics:**
- 10. Comments useful for correctly interpreting the results:**

---

\* *Calculation details have not been provided.*



*Appendix B.3*  
**Accelerator-driven system benchmark**

**JAERI (Japan)**

**1. Name of participant:** T. Nishida, T. Takizuka and T. Sasa

**2. Organisation:** Japan Atomic Energy Research Institute  
Tokai Mura, Naka-gun, Ibaraki-ken 319-11, Japan  
Transmutation System Laboratory, Department of Reactor Engineering

**3. Name of code used:**

- Spallation cascade code: MNTC/JAERI94 (Monte Carlo) (> 20 MeV).
- Neutron transport code: TWODANT ( $S_n$  method) (< 20 MeV) – using 73 group cross-sections.
- Burn-up code: BURNER
- Data processing code: SCALE

**4. Bibliographic references:**

**5. Origin of cross-section data:**

- JENDL-3.2.

**6. Spectral calculations and data reduction method used:**

**7. Number of energy groups used in different phases:**

**8. Calculations:**

**9. Other assumptions and characteristics:**

**10. Comments useful for correctly interpreting the results:**

## PSI and CEA (Switzerland and France)

**1. Name of participant:** G. Youinou<sup>1,2</sup>, S. Pelloni<sup>1</sup> and P. Wydler<sup>1</sup>

**2. Organisation:** <sup>1</sup>Paul Scherrer Institut, CH-5232 Villigen PSI, Switzerland  
<sup>2</sup>CEA, CE Cadarache, F-13108 Saint-Paul-lez-Durance, France

**3. Name of code used:**

- For energies larger than 15 MeV: HETC (PSI version).
- For energies smaller than 15 MeV: NJOY (Version 89.62), MICROR (Ed. 2), MICROX-2 (Ed. 14), 2DTB, HETC-to-2DTB neutron source reformatting code.

**4. Bibliographic references:**

- For HETC: F. Atchison, PSI Proceedings 92-02, (1992) 440.
- For NJOY: R.E. MacFarlane and D.W. Muir, LA-12740-M, (1994).
- For MICROR: D.R. Mathews, J. Stepanek, S. Pelloni, C.E. Higgs, EIR Report 539 (1984).
- For MICROX-2: D. Mathews, PSI-97-11, (1997).
- For TWODANT: R.E. Alcouffe, R.S. Baker, F.W. Brinkley, D.R. Marr, R.D. O'Dell and W.F. Walters, LA-12969-M (1995).
- For 2DB: W.W. Little, Jr. and R.W. Hardie, BNWL-831, Rev. 1 (1968).
- For 2DTB: S. Pelloni, Y. Kadi and H.U. Wenger, "Present Methods for Physics Calculations of Hybrid Fast Systems at PSI", Proc. Specialists Mtg. on Intermediate Energy Nuclear Data: Models and Codes, Vol. 1, pp. 342-348, Issy-les-Moulineaux (1994).

**5. Origin of cross-section data:**

- JEF-2.2.

**6. Spectral calculations and data reduction method used:**

For energies smaller than 15 MeV:

- Pointwise cross-sections and P<sub>0</sub>-P<sub>3</sub> fine group cross-sections in 92 epithermal neutron groups between 15 MeV and 2.38 eV were generated using NJOY (Version 89.62). The fine group cross-sections were produced applying the standard Bondarenko method. A typical fast reactor flux spectrum (IWT = 7 in the NJOY terminology) was employed.
- The interface program MICROR (Ed. 2) was applied to generate the following code-specific libraries for use in conjunction with the cell code MICROX-2:
  - A multi-group data library, consisting of the computed  $\sigma_0$  dependent, P<sub>0</sub>-P<sub>3</sub> cross-sections and fission spectra.



- A pointwise data library, consisting of additional cross-sections below 8 keV. In total, the cross-sections were given in about 24 000 energy points equally spaced in velocity.
- The two-region MICROX-2 code was employed to generate shielded, microscopic broad group cross-sections, as well as the global fission spectrum, for later use in detailed core and burn-up calculations with the code 2DTB:
  - The consistent diagonal transport correction was used to produce P<sub>0</sub>-P<sub>2</sub> cross-sections.
  - The broad energy structure chosen (33 groups) is equally spaced in lethargy ( $\Delta u = 0.5$ ).

For energies above 8 keV, the broad group cross-sections were computed from those available in the fast data library. The  $\sigma_0$  dependent cross-sections (also in the unresolved energy range) were interpolated in the two regions, using a two-point, semi-logarithmic algorithm. The required energy dependent  $\sigma_0$ s were calculated using the background cross-section method.

For energies below 8 keV, the broad group cross-sections were derived from those available in the pointwise data library, thereby accounting for resonance overlap. The required fluxes for energy collapsing were obtained from a resonance calculation in two regions. For the fuel cells, B1 neutron slowing-down balance equations were solved, in which appropriate sources, obtained from cross-sections available in the fast data library, were used. For non fuel cells, the same sources were used, but the buckling was not searched for.

- In the core calculations (with the external neutron source), 2 cm meshes in the radial direction and 2.5 cm meshes in the axial direction, as well as P<sub>2</sub>-S<sub>8</sub> approximations, were used.

2DTB is a PSI code based upon the General Atomic code 2DB (for the diffusion option) and TWODANT (for the transport option). For the burn-up calculations, six fission product yield sets were used, describing the fission of <sup>237</sup>Np, <sup>238</sup>Pu, <sup>239</sup>Pu, <sup>242</sup>Pu, <sup>241</sup>Am and <sup>244</sup>Cm. For each of these actinides, 71 explicit fission products were used together with “pseudo fission products” to compensate for missing absorption. For the latter, cross-sections were generated using the PSI code PSD.

## 7. Number of energy groups used in different phases:

- Cell calculations: 93 neutron groups in conjunction with about 24 000 energy points below 8 keV.
- Core calculations: 33 neutron groups.

## 8. Calculations:

- Transport theory.
- P<sub>2</sub>-S<sub>8</sub>, finite difference.
- 2 cm meshes in the radial direction, 2.5 cm meshes in the axial direction.

## **9. Other assumptions and characteristics:**

Each region was associated with a burn-up zone. Fission yields of actinides others than  $^{237}\text{Np}$ ,  $^{238}\text{Pu}$ ,  $^{239}\text{Pu}$ ,  $^{242}\text{Pu}$  and  $^{241}\text{Am}$  were approximated with those available. The burn-up calculations did not include the contributions from energies higher than 15 MeV.

## **10. Comments useful for correctly interpreting the results:**

## **IPPE (Russian Federation)**

**1. Name of participant:** T.T. Ivanova, V.F. Batyaev and A.A. Tsiboulia

**2. Organisation:** IPPE, Russian Federation

**3. Name of codes used:**

- > 20 MeV – HETC.
- < 20 MeV – CONSYST2 – preparation of group cross-sections.  
TWODANT-SYS – neutron transport.  
CARE – burn-up calculation.

**4. Bibliographic references:**

- [1] Radiation Shielding Information Centre, “HETC Monte Carlo High-Energy Nucleon-Meson Transport Code”, Report CCC-178, Oak Ridge National Laboratory (August 1977).
- [2] RSICC DLC-182 “ABBN-90: Multi-Group Constant Set for Calculation of Neutron and Photon Radiation Fields and Functionals, Including the CONSYST2 Program.”
- [3] RSICC CCC-547, “TWODANT-SYS: One- and Two-Dimensional, Multi-Group, Discrete Ordinates Transport Code System.”
- [4] A.L. Kochetkov, “CARE – Isotope Generation and Depletion Code”, IPPE-2431, 1995.

**5. Origin of cross-section data:**

- FOND-2 data library.

**6. Spectral calculations and data reduction methods used:**

- Resonance shielding: Resonance self-shielding effects are taken into account by using Bondarenko self-shielding factors.
- Mutual shielding: See resonance shielding (above).
- Weighting spectrum for scattering matrices: 0-dimensional 299 groups spectrum calculation.

**7. Number of energy groups used in the different phases:**

- > 20 MeV – continuous energy.
- < 20 MeV – 28 neutron groups.

## 8. Calculations:

- Theory used: 2-D transport theory.
- Method used: > 20 MeV – Monte Carlo.  
< 20 MeV – DSN 16.
- Calculation characteristics: > 20 MeV – 1 000 000 histories, continuous energy.  
< 20 MeV – total amount of meshes – 2 925.

## LIST OF CONTRIBUTORS

### Problem specification

<i>PWR</i>	<i>FR</i>	<i>ADS</i>
C. Broeders, FZK (Germany)	T. Wakabayashi, JNC (Japan)	T. Nishida, JAERI (Japan)
H. Küsters, FZK (Germany)		T. Takizuka, JAERI (Japan)
L. Payen, FZK (Germany)		T. Sasa, JAERI (Japan)
J. Vergnes, EDF (France)		

### Summary and analysis of results

<i>PWR</i>	<i>FR</i>	<i>ADS</i>
T. Iwasaki Tohoku University (Japan)	T. Wakabayashi JNC (Japan)	T. Sasa JAERI (Japan)

### Secretariat

B.C. Na, OECD/NEA
-------------------

### Benchmark participants

<i>PWR</i>	<i>FR</i>	<i>ADS</i>
C. Broeders, FZK (DE)	K. Tsujimoto, JAERI (JP)	T. Nishida, JAERI (JP)
D. Lutz, IKE (DE)	H. Oigawa, JAERI (JP)	T. Takizuka, JAERI (JP)
H. Takano, JAERI (JP)	T. Mukaiyama, JAERI (JP)	T. Sasa, JAERI (JP)
H. Akie, JAERI (JP)	J. Tommasi, CEA (FR)	G. Youinou, PSI (CH)
K. Kaneko, JAERI (JP)	T. Wakabayashi, JNC (JP)	S. Pelloni, PSI (CH)
T. Iwasaki, Tohoku Univ. (JP)	M. Yano, Mitsubishi (JP)	P. Wydler, PSI (CH)
D. Fujiwara, Tohoku Univ. (JP)	M. Kawashima, Toshiba (JP)	T.T. Ivanova, IPPE (RU)
B. Kochurov, ITEP (RU)	M. Yamaoka, Toshiba (JP)	V.F. Batyaev, IPPE (RU)
A. Kwaratzheli, ITEP (RU)	M. Semenov, IPPE (RU)	A.A. Tsiboulia, IPPE (RU)
N. Selivanova, ITEP (RU)	A. Tsiboulia, IPPE (RU)	
A. Tsiboulia, IPPE (RU)		

FR = France, DE = Germany, JP = Japan, RU = Russian Federation, CH = Switzerland

